MONTHLY WEATHER REVIEW

VOLUME 82 NUMBER 2

FEBRUARY 1954

CONTENTS

U. S. DEPARTMENT OF COMMERCE • WEATHER BUREAU

PUBLICATIONS OF THE U. S. WEATHER BUREAU

As the national meteorological service for the United States, the Weather Bureau issues several periodicals, serials, and miscellaneous publications on weather, climate, and meteorological science as required to carry out its public service functions. The principal periodicals and serials are described on this page and on the inside of the back cover. A more complete listing of Weather Bureau publications is available upon request to Chief, U. S. Weather Bureau, Washington 25, D. C.

Orders for publications should be addressed to the Superintendent of Documents, Government Printing Office, Washington 25, D. C.

MONTHLY WEATHER REVIEW

First published in 1872, the Monthly Weather Review serves as a medium of publication for technical contributions in the field of meteorology, principally in the branches of synoptic and applied meteorology. In addition each issue contains an article descriptive of the atmospheric circulation during the month over the Northern Hemisphere with particular reference to the effect on weather in the United States. A second article deals with some noteworthy feature of the month's weather. Illustrated. Annual subscription: Domestic, $3.50; Foreign, $4.50; 30¢ per copy. Subscription to the *Review* does not include the *Supplements* which have been issued irregularly and are for sale separately.

CLIMATOLOGICAL DATA—NATIONAL SUMMARY

This monthly publication contains climatological data such as pressure, temperature, winds, rainfall, snowfall, severe storms, floods, etc., for the United States as a whole. A short article describing the weather of the month over the United States, tables of the observational data, and a description of flood conditions are supplemented by 15 charts. An annual issue summarizes weather conditions in the United States for the year. More detailed local data are provided in the Climatological Data (by sections) for 45 sections representing each State or a group of States, and Hawaii, Alaska, and the West Indies. Subscription price for either the National Summary or for a Section: $1.50 per year (including annual issue), 15¢ per copy.

(Continued on inside back cover)

The Weather Bureau desires that the *Monthly Weather Review* serve as a medium of publication for original contributions within its field, but the publication of a contribution is not to be construed as official approval of the views expressed.

The issue for each month is published as promptly as monthly data can be assembled for preparation of the review of the weather of the month. In order to maintain the schedule with the Public Printer, no proofs will be sent to authors outside of Washington, D. C.

The printing of this publication has been approved by the Director of the Bureau of the Budget, February 11, 1952

DEPARTMENT OF COMMERCE
SINCLAIR WEEKS, Secretary

WEATHER BUREAU
F. W. REICHELDERFER, Chief

MONTHLY WEATHER REVIEW

Editor, JAMES E. CASKEY, JR.

Volume 82
Number 2

FEBRUARY 1954

Closed April 15, 1954
Issued May 15, 1954

METHODS OF CALCULATING SOLAR RADIATION VALUES AT BLUE HILL OBSERVATORY, MILTON, MASSACHUSETTS

I. F. HAND

U. S. Weather Bureau, Blue Hill Observatory, Milton, Mass.[1]

[Manuscript received June 10, 1953; revision received October 5, 1953]

ABSTRACT

Methods of calculating direct solar radiation received at normal incidence and the total solar and sky radiation received on a horizontal surface, applicable with accuracies within ±2.5 percent at Blue Hill Observatory, are presented. As many workers in radiation are content with accuracies within 10 or 15 percent, the same methods might be used with a lesser degree of accuracy in many other areas where atmospheric conditions approximate those at Blue Hill. With data of total solar and sky radiation received on a horizontal surface now available from more than 80 stations in continental United States, Canada, Alaska, and outlying islands, but with few values of normal incidence radiation in the same solar network, it is suggested that these methods can be used to estimate normal incidence for many new regions.

INTRODUCTION

The primary purpose of this paper is to show methods of using the numerous available values of total solar and sky radiation received on a horizontal surface to calculate the amount of solar radiation received at normal incidence. A method also is shown whereby normal incidence data may be used to calculate the total solar radiation received on a horizontal surface; calculated values of diffuse radiation on a horizontal surface may be obtained as a by-product. These methods are developed from radiation records at Blue Hill Observatory for January 1950 through April 1952. A brief review of instrumental equipment furnishing radiation records is made before developing the methods to give the reader an indication of the type and accuracy of available data.

INSTRUMENTAL EQUIPMENT

Records of total solar and sky radiation received on a horizontal surface at numerous stations in the United States, Canada, Alaska, and outlying islands are furnished by the e. m. f. generated by Eppley 180° pyrheliometers [1, 2] and suitable potentiometers. At all the normal incidence stations in this network, with the exception of Table Mountain, Calif., values are obtained by means of Eppley normal incidence pyrheliometers [3, 4] and suitable recording potentiometers. At Table Mountain, the Smithsonian Institution uses silver-disk pyrheliometers to measure the solar constant, while at Blue Hill this type of instrument is used for standardization purposes. Although recording instruments suffice for most climatological purposes, this method of obtaining normal incidence values with a secondary instrument lacks sufficient accuracy to warrant its use in this study. It was necessary to use the recordings of total solar and sky radiation obtained instrumentally, but values of normal incidence radiation measured with the eye-read silver-disk pyrheliometer at Blue Hill were used exclusively in these calculations. Experienced observers can and do read these instruments with an accuracy within one-fourth of one percent [5]. Obvious errors occur in recorded values unless the instrumental equipment is maintained in almost perfect condition, that is, the pyrheliometer compared frequently with a standard and the potentiometer calibrated so that it reads correctly at all points. At Blue Hill, the 180° pyrheliometer is compared periodically with a standard and the potentiometer is checked frequently. That this apparatus is in good condition seems apparent from the results presented in this

[1] Present address: Box 115, Afton, N. Y. Mr. Hand retired from the Weather Bureau in September 1953.

282889—54——1

paper. Diffuse radiation on a horizontal surface is measured by means of an occulting ring which continuously shades the diffuse pyrheliometer from the direct rays of the sun, but permits the diffuse or sky radiation to impinge upon the receiving surface at all times [6]. Some of the instrumental sources of errors are listed in the terminal section of the present study.

DEFINITIONS OF SYMBOLS

The following symbols will be used:

I_{hm} is the measured total solar and sky radiation received on a horizontal surface, expressed in langleys/minute [1, 2]. In order to avoid such a cumbersome expression, hereafter it will be termed "total horizontal radiation".

I_{nm} is the measured direct normal incidence radiation, expressed in langleys/minute [3, 4].

D_{hm} is the measured diffuse radiation on a horizontal surface, expressed in langleys/minute [6].

Z is the solar zenith distance expressed in degrees.

I_{nc} is the calculated direct solar radiation received on a surface normal to the sun and expressed in langleys/minute.

I_{hc} is the calculated total solar and diffuse radiation received on a horizontal surface expressed in langleys/minute.

D_{hc} is the calculated diffuse radiation on a horizontal surface expressed in langleys/minute.

CALCULATION METHODS

The calculation methods are to be developed through use of the ratio

$$F=\frac{I_{nm}\cos Z}{I_{hm}} \tag{1}$$

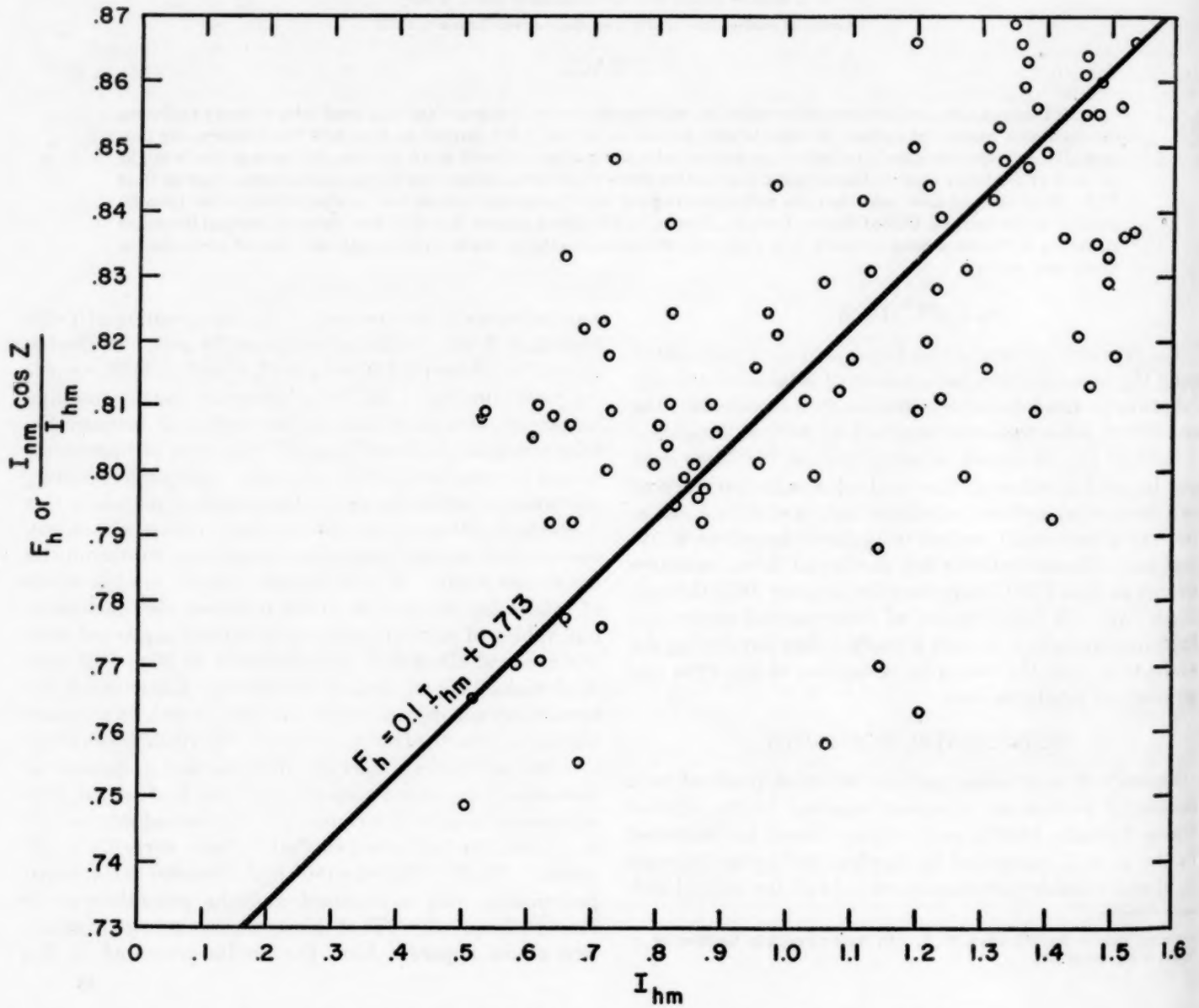

FIGURE 1.—Plot of the ratio $(I_{nm}\cos Z)/I_{hm}$ against I_{hm}. The straight line, fitted by eye, gives equation (4).

Kimball [7] has evaluated this ratio as a function of solar altitude, but for the present purposes we shall first designate it as F_h and empirically evaluate it as a linear function of I_{hm} to be used in computing I_{hc}. Next, we shall designate the ratio as F_n and evaluate it as a linear function of I_{nm} to be used in computing I_{hc}. Thus, the factors F_h and F_n are the critical quantities for the calculation methods. In terms of F_h and F_n, the calculated values I_{nc} and I_{hc} are given respectively by

$$I_{nc}=I_{hm}F_h/\cos Z \tag{2}$$

and

$$I_{hc}=(I_{nm}\cos Z)/F_n \tag{3}$$

To obtain F_h for use in (2) we plot the ratio $(I_{nm}\cos Z)/I_{hm}$ against the measured total horizontal radiation I_{hm} (see fig. 1). Drawing a line of best fit as determined visually we obtain a linear equation,

$$F_h=0.1I_{hm}+0.713 \tag{4}$$

having substituted F_h for $(I_{nm}\cos Z)/I_{hm}$ in accordance with (1).

In a similar manner we obtain F_n for use in (3) by plotting the same ratio against measured normal incidence radiation I_{nm} (fig. 2). Drawing a line of best fit as determined by eye, we find [1]

$$F_n=0.275I_{nm}+0.4475 \tag{5}$$

Finally, by definition of terms, D_{hc} may be calculated from

$$D_{hc}=I_{hm}-I_{nm}\cos Z \tag{6}$$

RESULTS

The Blue Hill data from which figures 1 and 2 and equations (4) and (5) were derived are presented in table 1. The results of computations of I_{nc}, I_{hc}, and D_{hc} are also given in table 1 and are compared with the measured values I_{nm}, I_{hm}, and D_{hm}, respectively. As an example to illustrate the methods described in the preceding section, the computations for January 17, 1950 are given step by step at the foot of table 1.

While the percentage differences between the measured and calculated diffuse radiation are rather large, the average difference in langleys/minute is relatively small, being of the order of 0.07 ly./min. In every case, the calculated value is larger than the measured.

The results for I_{nc} and I_{hc} show promise as evidenced by the small probable errors of the values of calculated from measured which average less than ±2.5 percent based on the formula

$$p.e.=0.6745\sqrt{\frac{v^2}{n-1}}$$

Obviously the chief cause of the close relationship between the ratios of the two types of radiation values is the secant-effect. Nevertheless, when used with caution we believe this method should prove useful for rough determinations. However, discretion should be exercised in applying these methods to other areas for unless at-

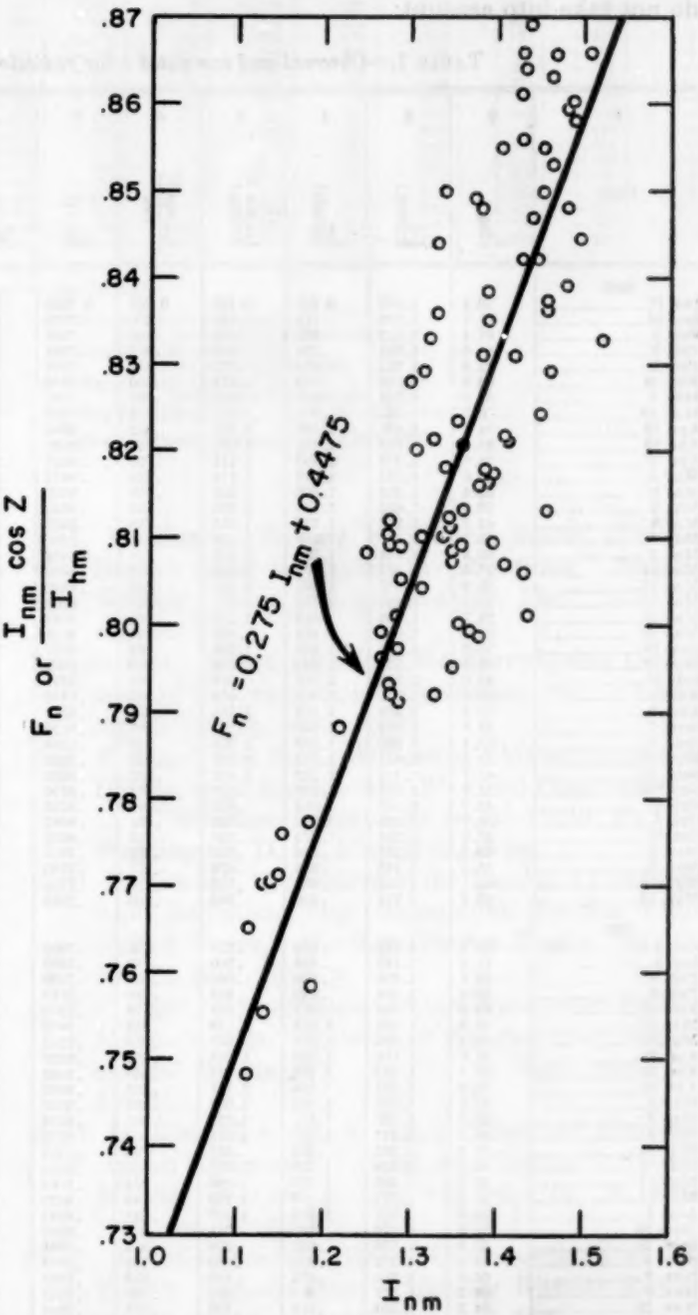

FIGURE 2.—Plot of the ratio $(I_{nm}\cos Z)/I_{hm}$ against I_{nm}. The straight line, fitted by eye, gives equation (5).

[1] EDITORIAL NOTE: It is apparent that equations (4) and (5), with F_h and F_n replaced by $(I_{nm}\cos Z)/I_{hm}$, are not strictly compatible. This inconsistency may be avoided by constructing a single scatter diagram on which values of I_{hm} are plotted against the coordinate values I_{nm} and $\cos Z$. Equally-spaced straight isopleths can then be fitted to the field of I_{hm}, and the resulting chart used to determine either I_{hc} or I_{nc} with an accuracy on the Blue Hill developmental data comparable to that obtained by Hand.

mospheric conditions approximate those at Blue Hill, serious errors will result. In particular, no attempt should be made to use these methods over large industrial areas as the diffuse radiation then is too large a percentage of the total radiation [8].

SOURCES OF ERROR

In the interpretation of the results for Blue Hill or in the application of the methods to data from other stations, the following sources of instrumental and observational errors should be kept in mind in addition to errors resulting from changes in atmospheric conditions that the methods do not take into account:

(1) The occulting ring cuts off approximately 5 percent of the sky radiation in addition to shading the instrument from the direct rays of the sun [6].

(2) The area adjacent to the sun is the brightest portion of the sky [9].

(3) Errors of Eppley pyrheliometers, while not of great magnitude, include internal reflections from the inner portion of the hemispherical bulb, caustics and striae caused by the glass cover, and variations in efficiency of the thermopile with fluctuations in temperature [10]. And obviously the shaded diffuse pyrheliometer remains cooler than a freely exposed instrument when the sun is shining.

TABLE 1.—*Observed and computed solar radiation values at Blue Hill Observatory, Milton, Mass.*

1 Date	2 Z (deg.)	3 I_{n_o} (ly/min)	4 I_{h_o} (ly/min)	5 $I_{n_o}\cos Z$ (ly/min)	6 $\frac{I_{n_o}\cos Z}{I_{h_o}}$	7 F_h (Eq. 4)	8 $I_{h'}$ (Eq. 2) (ly/min)	9 $I_{h'}-I_{h_o}$ (ly/min)	10 $\frac{I_{h'}-I_{h_o}}{I_{h_o}}\times 100\%$	11 $D_{h'}$ (Eq. 6) (ly/min)	12 D_{h_o} (ly/min)	13 F_s (Eq. 5)	14 $I_{h'}$ (Eq. 3) (ly/min)	15 $I_{h'}-I_{h_o}$ (ly/min)	16 $\frac{I_{h'}-I_{h_o}}{I_{h_o}}\times 100\%$
1950															
Jan. 17	70.1	1.249	0.526	0.425	0.808	0.7656	1.183	−0.066	−5	0.101	0.064	0.7910	0.537	+.011	+2
Jan. 26	61.1	1.150	.716	.556	.776	.7846	1.162	+.012	+1	.160	.108	.7638	.728	+.012	+2
Feb. 3	61.4	1.432	.856	.685	.800	.7986	1.428	−.004	0	.171	.112	.8413	.815	−.041	−5
Feb. 3	64.6	1.381	.724	.592	.818	.7854	1.326	−.055	−4	.132	.104	.8273	.716	−.008	−1
Feb. 3	73.0	1.272	.458	.372	.812	.7588	1.189	−.083	−7	.086	.064	.7973	.466	+.008	+2
Feb. 20	60.6	1.368	.840	.672	.800	.7970	1.364	−.004	0	.168	.145	.8237	.815	−.025	−3
Mar. 6	67.8	1.324	.632	.500	.791	.7762	1.298	−.027	−2	.132	.112	.8116	.616	−.016	−3
Mar. 19	60.7	1.345	.828	.658	.795	.7958	1.346	+.001	0	.170	.107	.8174	.805	−.023	−3
Apr. 10	34.8	1.451	1.466	1.191	.812	.8596	1.535	+.084	+6	.275	.210	.8465	1.408	−.058	−4
Apr. 10	35.1	1.518	1.491	1.242	.833	.8621	1.571	+.053	+3	.249	.210	.8650	1.436	−.055	−4
Apr. 27	28.6	1.272	1.408	1.117	.793	.8538	1.369	+.097	+8	.291	.200	.7973	1.401	−.007	0
May 8	40.0	1.454	1.310	1.114	.850	.8440	1.443	−.012	−1	.196	.085	.8474	1.315	+.005	0
May 8	32.4	1.483	1.460	1.252	.858	.8590	1.485	+.002	0	.208	.104	.8553	1.464	+.004	0
May 8	29.4	1.462	1.514	1.265	.836	.8644	1.502	+.050	+3	.249	.115	.8468	1.494	−.020	−1
May 8	42.3	1.374	1.272	1.016	.799	.8402	1.445	+.071	+5	.256	.116	.8254	1.231	−.041	−3
May 9	36.3	1.437	1.368	1.158	.846	.8498	1.442	+.005	0	.210	.104	.8427	1.374	+.006	0
May 9	39.8	1.395	1.304	1.064	.816	.8434	1.432	+.047	+3	.240	.123	.8284	1.284	−.020	−2
May 14	27.6	1.387	1.472	1.229	.835	.8602	1.429	+.042	+3	.243	.115	.8289	1.483	+.011	+1
May 17	23.2	1.337	1.502	1.229	.818	.8632	1.411	+.074	+6	.273	.178	.8152	1.507	+.005	0
May 22	27.9	1.451	1.532	1.282	.837	.8662	1.502	+.051	+4	.250	.098	.8465	1.515	−.017	−1
May 22	24.7	1.424	1.512	1.294	.856	.8642	1.438	+.014	+1	.218	.100	.8391	1.542	+.030	+2
May 22	52.3	1.321	.984	.808	.821	.8114	1.306	−.015	−1	.176	.105	.8108	.996	+.012	+1
June 18	28.0	1.427	1.458	1.260	.864	.8588	1.418	−.009	−1	.198	.100	.8399	1.500	+.042	+3
June 18	19.8	1.434	1.552	1.349	.869	.8682	1.432	−.002	0	.203	.113	.8419	1.603	+.051	+3
July 27	37.0	1.150	1.204	.918	.762	.8334	1.256	+.106	+9	.286	.232	.7638	1.202	−.002	0
Aug. 8	40.2	1.301	1.212	.994	.820	.8342	1.324	+.023	+2	.218	.118	.8052	1.234	+.022	+2
Aug. 8	25.6	1.324	1.428	1.194	.836	.8558	1.355	+.031	+2	.234	.116	.8116	1.471	+.043	+3
Sept. 7	48.8	1.262	1.040	.831	.799	.8170	1.290	+.028	+2	.209	.116	.7946	1.046	+.006	0
Sept. 7	38.4	1.299	1.230	1.018	.828	.8360	1.312	+.013	+1	.212	.114	.8047	1.265	+.035	+3
Sept. 17	39.7	1.445	1.320	1.112	.842	.8450	1.450	+.005	0	.208	.075	.8449	1.316	−.004	0
Sept. 17	41.7	1.416	1.272	1.057	.831	.8402	1.431	+.015	+1	.215	.087	.8369	1.263	−.009	−1
Sept. 17	51.7	1.343	1.026	.832	.811	.8156	1.350	+.007	+1	.194	.070	.8168	1.019	−.007	−1
Oct. 5	49.7	1.358	1.080	.878	.813	.8210	1.371	+.013	+1	.202	.127	.8210	1.070	−.010	−1
Oct. 5	53.7	1.288	.952	.763	.801	.8082	1.300	+.012	+1	.189	.138	.8017	.951	−.001	0
Oct. 31	57.3	1.284	.870	.694	.798	.8000	1.288	+.004	0	.176	M	.8006	.866	−.004	0
Nov. 6	60.3	1.283	.794	.636	.801	.7924	1.270	−.013	−1	.158	.102	.8003	.794	0	0
Nov. 6	65.4	1.148	.620	.478	.771	.7750	1.154	+.009	+1	.142	.102	.7632	.626	+.006	+1
Nov. 13	63.1	1.135	.680	.514	.756	.7810	1.174	+.039	+3	.166	M	.7596	.676	−.004	−1
Nov. 13	69.2	1.112	.516	.395	.766	.7646	1.111	−.001	0	.121	M	.7533	.524	+.008	+2
1951															
Jan. 9	65.6	1.284	.670	.530	.791	.7800	1.265	−.019	−1	.140	.129	.8006	.663	−.007	−1
Jan. 9	71.6	1.142	.468	.360	.769	.7598	1.127	−.015	−1	.108	.098	.7616	.473	+.005	+1
Feb. 9	62.7	1.408	.800	.646	.807	.7930	1.383	−.025	−2	.154	.101	.8347	.774	−.026	−3
Feb. 9	56.4	1.494	.980	.827	.844	.8110	1.436	−.058	−4	.153	.106	.8584	.963	−.016	−2
Feb. 16	60.2	1.334	.818	.663	.810	.7948	1.308	−.026	−2	.155	.113	.8144	.814	−.004	0
Mar. 27	40.0	1.475	1.333	1.130	.848	.8463	1.473	−.002	0	.203	.105	.8531	1.324	−.009	−1
Mar. 27	49.4	1.393	1.110	.907	.817	.8240	1.405	+.012	+1	.203	.107	.8306	1.092	−.018	−2
Apr. 23	31.9	1.455	1.490	1.235	.829	.8620	1.512	+.057	+4	.255	.162	.8476	1.457	+.033	+2
Apr. 30	36.6	1.462	1.356	1.174	.866	.8486	1.433	−.029	−2	.182	.120	.8496	1.382	+.026	+2
Apr. 30	35.6	1.452	1.368	1.181	.863	.8498	1.430	−.022	−2	.187	.110	.8468	1.394	+.026	+2
May 3	41.1	1.376	1.236	1.037	.839	.8366	1.454	+.078	+6	.199	.118	.8259	1.255	+.019	+2
May 3	28.2	1.421	1.454	1.252	.861	.8584	1.416	−.005	0	.202	.130	.8383	1.494	+.040	+3
May 9	40.5	1.332	1.192	1.013	.850	.8322	1.305	−.027	−2	.179	.133	.8138	1.245	+.053	+4
May 13	57.2	1.206	.862	.686	.796	.7992	1.272	+.006	0	.176	.111	.7956	.862	0	0
May 14	39.1	1.324	1.218	1.027	.843	.8348	1.310	−.014	−1	.191	.143	.8116	1.266	+.048	+4
May 14	25.8	1.400	1.475	1.260	.854	.8605	1.410	+.010	+1	.215	.152	.8325	1.514	+.039	+3
May 14	30.1	1.373	1.399	1.188	.849	.8529	1.379	+.006	0	.211	.152	.8251	1.440	+.041	+3
Aug. 2	38.8	1.421	1.315	1.107	.842	.8445	1.425	+.004	0	.208	M	.8383	1.321	+.006	0
Sept. 25	55.8	1.270	.881	.714	.810	.8011	1.256	−.014	−1	.167	M	.7968	.896	+.015	+2
Sept. 26	55.9	1.385	.951	.776	.816	.8081	1.371	−.014	−1	.175	.128	.8284	.937	−.014	−1
Nov. 4	57.2	1.272	.870	.689	.792	.8000	1.285	+.013	+1	.181	.112	.7973	.884	−.006	−1
Nov. 9	65.5	1.316	.655	.546	.833	.7785	1.230	−.086	−7	.109	.085	.8094	.674	+.019	+3
Nov. 9	60.2	1.377	.817	.684	.837	.7947	1.307	−.071	−5	.133	.087	.8262	.828	+.011	+1
Nov. 25	64.2	1.350	.714	.588	.823	.7844	1.287	−.063	−5	.126	.081	.8188	.718	+.004	+1
Nov. 27	63.1	1.372	.732	.621	.848	.7862	1.272	−.100	−7	.111	.085	.8248	.753	+.021	+3
Nov. 27	67.4	1.345	.640	.517	.808	.7770	1.297	−.048	−4	.123	.080	.8174	.632	−.008	−1
Dec. 4	64.3	1.183	.660	.513	.777	.7790	1.186	+.003	0	.147	.102	.7728	.664	+.004	+1
Dec. 11	67.6	1.285	.608	.490	.806	.7738	1.235	−.050	−4	.118	.077	.8009	.611	+.003	0
Dec. 27	65.4	1.358	.688	.565	.821	.7818	1.292	−.066	−5	.123	.110	.8210	.689	+.001	0

TABLE 1.—*Observed and computed solar radiation values at Blue Hill Observatory, Milton, Mass.*—Continued

1 Date	2 Z (deg.)	3 I_{ss} (ly/min)	4 I_{ds} (ly/min)	5 $I_{ss}\cos Z$ (ly/min)	6 $\frac{I_{ss}\cos Z}{I_{ds}}$	7 F_s (Eq. 4)	8 I_{ss} (Eq. 2) (ly/min)	9 $I_{ss}-I_{ss}$ (ly/min)	10 $\frac{I_{ss}-I_{ss}}{I_{ss}}\times 100\%$	11 D_{ds} (Eq. 6) (ly/min)	12 D_{ds} (ly/min)	13 F_s (Eq. 6)	14 I_{ds} (Eq. 3) (ly/min)	15 $I_{ds}-I_{ds}$ (ly/min)	16 $\frac{I_{ds}-I_{ds}}{I_{ds}}\times 100\%$
1953															
Jan. 4	70.2	1.112	.504	.377	.748	.7634	1.136	+.024	+2	.127	.096	.7533	.500	−.004	−1
Jan. 4	66.8	1.136	.582	.448	.770	.7712	1.139	+.003	0	.134	.113	.7599	.589	+.007	+1
Jan. 11	70.2	1.275	.534	.432	.809	.7764	1.208	−.067	−5	.102	.073	.7981	.541	+.007	+1
Jan. 11	64.9	1.393	.730	.591	.809	.7860	1.353	−.040	−3	.139	.087	.8306	.711	−.019	−3
Jan. 11	64.7	1.352	.722	.578	.800	.7852	1.327	−.025	−2	.144	.083	.8193	.705	−.017	−2
Feb. 12	67.6	1.310	.616	.499	.810	.7746	1.252	−.058	−4	.117	.079	.8078	.618	+.002	0
Feb. 12	61.3	1.409	.824	.677	.821	.7954	1.365	−.044	−3	.147	.087	.8350	.810	−.014	−2
Feb. 12	56.5	1.449	.970	.800	.824	.8100	1.423	−.026	−2	.170	.091	.8460	.945	−.025	−3
Feb. 12	59.7	1.428	.894	.720	.806	.8024	1.422	−.006	0	.174	.091	.8402	.857	−.037	−4
Feb. 12	66.4	1.346	.668	.539	.807	.7798	1.301	−.045	−3	.129	.087	.8177	.659	−.009	−1
Feb. 13	60.1	1.309	.812	.653	.804	.7942	1.294	−.015	−1	.159	.112	.8075	.808	−.004	0
Apr. 4	42.2	1.215	1.142	.900	.788	.8272	1.275	+.060	+5	.242	.172	.7816	1.152	+.010	+1
Apr. 16	47.1	1.380	1.130	.939	.831	.8260	1.371	−.009	−1	.191	.092	.8270	1.136	+.006	+1
Apr. 17	48.0	1.310	1.058	.877	.829	.8188	1.295	−.015	−1	.181	.179	.8078	1.085	+.027	+3
Apr. 17	41.5	1.340	1.238	1.004	.811	.8368	1.383	+.043	+3	.234	.124	.8160	1.230	−.008	−1
Apr. 17	34.7	1.358	1.380	1.116	.809	.8510	1.428	+.070	+5	.264	.154	.8210	1.360	−.020	−2
Apr. 18	46.9	1.181	1.064	.807	.758	.8194	1.276	+.095	+8	.257	.121	.7723	1.045	−.019	−2
Apr. 18	40.5	1.277	1.200	.971	.809	.8330	1.315	+.038	+3	.229	.124	.7987	1.216	+.016	+1
Apr. 24	35.9	1.450	1.372	1.175	.856	.8502	1.440	−.010	−1	.197	.122	.8463	1.388	+.016	+1
Apr. 30	43.4	1.429	1.199	1.038	.866	.8329	1.374	−.055	−4	.161	.106	.8405	1.235	+.036	+3
Apr. 30	39.1	1.460	1.328	1.133	.853	.8458	1.447	−.013	−1	.195	.112	.8490	1.335	+.007	+1
Apr. 30	30.8	1.482	1.480	1.273	.860	.8610	1.484	+.002	0	.207	.125	.8551	1.489	+.009	+1
Apr. 30	27.9	1.501	1.532	1.327	.866	.8662	1.502	+.001	0	.205	.095	.8603	1.542	+.010	+1
Apr. 30	32.3	1.408	1.449	1.190	.821	.8579	1.471	+.063	+4	.259	.094	.8347	1.426	−.023	−2
Apr. 30	37.7	1.477	1.360	1.169	.859	.8490	1.459	−.018	−1	.191	.090	.8537	1.369	+.009	+1

Sample computation for Jan. 17, 1950

Given: $Z=70.1°$, $\cos Z=0.34038$
$I_{ss}=1.249$ ly/min
$I_{ds}=0.526$ ly/min
$D_{ds}=0.064$ ly/min

Step 1: From equation (4),
$F_s=0.1(0.526)+0.713=.7656$

Step 2: From equation (2),
$I_{ss}=(0.526)(.7656)/0.34038=1.183$

Step 3: Difference $=I_{ss}-I_{ss}=1.183-1.249=-0.066$

Step 4: Percent difference $=\frac{-0.066}{1.249}\times 100\%=-5\%$

Step 5: From equation (6),
$D_{ds}=0.526-(1.249)(0.34038)=0.101$

Step 6: From equation (5),
$F_s=0.275(1.249)+0.4475=0.7910$

Step 7: From equation (3),
$I_{ds}=(1.249)(0.34038)/0.7910=0.537$

Step 8: Difference $=I_{ds}-I_{ds}=0.537-0.526=0.011$

Step 9: Percent difference $=\frac{0.011}{0.526}\times 100\%=2\%$

(4) Errors arising from instrumental recording. In this particular case, the recording pyrheliometer used for diffuse radiation lacks the accuracy of the recorder for measuring total horizontal radiation. Differences in the same direction and of approximately the same magnitude were found by Dr. C. F. Brooks and Miss S. H. Wollaston in an unpublished study.

(5) The human error ordinarily is an important factor, but in this case we have attempted to minimize this effect by double-checking integration of records and the various calculations.

REFERENCES

1. I. F. Hand, *Pyrheliometers and Pyrheliometric Measurements*, U. S. Weather Bureau, Washington, D. C., 1946, 55 pp.
2. H. H. Kimball and H. E. Hobbs, "A New Form of Thermoelectric Recording Pyrheliometer," *Monthly Weather Review*, vol. 51, No. 5, May 1923, pp. 239–242.
3. H. H. Kimball, "Turbidity and Water Vapor Determinations from Solar Radiation Measurements at Blue Hill and Relations to Air-Mass Types," *Monthly Weather Review*, vol. 62, No. 9, Sept. 1934, pp. 330–333.
4. I. F. Hand, "Review of United States Weather Bureau Solar Radiation Investigations," *Monthly Weather Review*, vol. 65, No. 12, Dec. 1937, pp. 415–441.
5. Charles G. Abbot, *Annals of the Astrophysical Observatory* of the Smithsonian Institution, vol. 5, Washington 1932, p. 136.
6. I. F. Hand and F. A. Wollaston, "Measurements of Diffuse Solar Radiation at Blue Hill Observatory," U. S. Weather Bureau, *Technical Paper* No. 18, Washington, D. C., May 1952, 19 pp.
7. H. H. Kimball, "Variations in the Total and Luminous Solar Radiations with Geographical Position in the United States," *Monthly Weather Review*, vol. 47, No. 11, Nov. 1919, p. 777.
8. I. F. Hand, "Atmospheric Contamination over Boston, Massachusetts," *Bulletin of the American Meteorological Society*, vol. 30, No. 7, Sept. 1949, pp. 252–254.
9. H. H. Kimball and I. F. Hand, "Daylight Illumination on Horizontal, Vertical, and Sloping Surfaces," *Monthly Weather Review*, vol. 50, No. 12, Dec. 1922, pp. 615–628.
10. T. H. MacDonald, "Some Characteristics of the Eppley Pyrheliometer," *Monthly Weather Review*, vol. 79, No. 8, Aug. 1951, pp. 153–159.

BIBLIOGRAPY OF SCIENTIFIC PAPERS BY I. F. HAND

The preceding is the last paper prepared for the *Monthly Weather Review* by Mr. I. F. Hand in his capacity as head of the Weather Bureau Solar Radiation Field Testing Station located at Blue Hill. Mr. Hand retired on September 30, 1953 after 41½ years with the Weather Bureau, spent mainly in the field of solar radiation. Because his many articles are of continuing interest to other workers in the field of solar radiation, we are printing the following bibliography of Mr. Hand's principal articles published to date. In addition several miscellaneous articles have appeared in *Scientific American, American Motorist, New Mexico, Miniature Camera*, etc.

Sept. 1920 "Distribution of Weather Forecasts, Warnings, and Information by Radio," *Monthly Weather Review*, vol. 48, No. 9, pp. 532–533.

Sept. 1921 "Sky Brightness and Daylight Illumination Measurements," with H. H. Kimball, *Monthly Weather Review*, vol. 49, No. 9, pp. 481–488.

Dec. 1922 "Daylight Illumination on Horizontal, Vertical, and Sloping Surfaces," with H. H. Kimball, *Monthly Weather Review*, vol. 50, No. 12, pp. 615–628.

June 1923 "An Examination of the Dust Content of the Atmosphere," *Bulletin of the American Meteorological Society*, vol. 4, No. 6–7, pp. 92–93.

Mar. 1924 "Investigation of Dust Content of the Atmosphere," with H. H. Kimball, *Monthly Weather Review*, vol. 52, No. 3, pp. 133–139.

April 1924 "Clouds and Other Observations from Airplanes," *Tycos-Rochester*, vol. XIV, No. 2, pp. 7, 23.

May 1924 "Destruction of an Aerial During a Thunderstorm," *Monthly Weather Review*, vol. 52, No. 5, pp. 270–271.

May 1924 "Investigation of the Dust Content of the Atmosphere," with H. H. Kimball, *Bulletin of the American Meteorological Society*, vol. 5, No. 5, pp. 67–69 (authors' summary and discussion).

April 1925 "Effect of Local Smoke on Visibility and Solar Radiation Intensities," *Monthly Weather Review*, vol. 53, No. 4, pp. 147–148.

June 1925 "Investigation of the Dust Content of the Atmosphere," with H. H. Kimball, *Monthly Weather Review*, vol. 53, No. 6, pp. 243–246.

Jan. 1926 "A Study of the Smoke Cloud over Washington, D. C. on January 16, 1926," *Monthly Weather Review*, vol. 54, No. 1, pp. 19–20.

May 1927 "Blue Sky Measurements," *Monthly Weather Review*, vol. 55, No. 5, pp. 235–236.

1927 "Bleaching of Methylene-Blue-Acetone-Water Solution by Ultra-Violet Radiation", with H. H. Kimball, *Bulletin of the National Research Council*, No. 61, pp. 123–125, Washington, D. C., 1927. (*Transactions of the American Geophysical Union*, 8th Annual Meeting 1927, pp. 123–125.)

June 1928 "Blue Sky Measurements at Washington, D. C.," *Monthly Weather Review*, vol. 56, No. 6, pp. 225–226.

Jan. 1929 "A Dense Smoke Cloud on January 3, 1929 at Washington, D. C.," *Monthly Weather Review*, vol. 57, No. 1, pp. 18–19.

July 1929 "Reflectivity of Different Kinds of Surfaces," with H. H. Kimball, *Monthly Weather Review*, vol. 57, No. 7, pp. 291–295.

Nov. 1929 "Utilization of Fixed Searchlights in Measuring Cloud Heights," *Monthly Weather Review*, vol. 57, No. 11, pp. 471–472.

July 1930 "Reflectivity of Different Kinds of Surfaces," with H. H. Kimball, *Monthly Weather Review*, vol. 58, No. 7, pp. 280–282.

Jan. 1931 "What Was the Highest Temperature Today?," *Tycos-Rochester*, vol. XXI, No. 1, p. 15.

Sept. 1931 "Investigation of the Dust Content of the Atmosphere," with H. H. Kimball, *Monthly Weather Review*, vol. 59, No. 9, pp. 349–352.

Jan. 1933 "The Magnitude of the Error in Measurements of the Solar Radiation Received on a Horizontal Surface Arising from the Assumption that the Ratio Between Radiant Energy Received and Electrical Energy Recorded is a Constant," with H. H. Kimball, *Monthly Weather Review*, vol. 61, No. 1, p. 4.

Mar. 1933 "The Use of Glass Color Screens in the Study of Atmospheric Depletion of Solar Radiation," with H. H. Kimball, *Monthly Weather Review*, vol. 61, No. 3, pp. 80–83.

June 1933 "Mountain and Valley Atmospheric-Dust Measurements," *Monthly Weather Review*, vol. 61, No. 6, p. 169.

Oct. 1933 "An Aid in Locating and Studying Clouds," *Monthly Weather Review*, vol. 61, No. 10, pp. 302–303.

May 1934 "The Character and Magnitude of the Dense Dust-Cloud which Passed over Washington,

D. C., May 11, 1934," *Monthly Weather Review*, vol. 62, No. 5, pp. 156–157.

Sept. 1935 "Lightning Does Strike Twice in the Same Place," *Taylor-Tycos-Rochester*, vol. XXV, No. 3, p. 84.

1936 "The Intensity of Solar Radiation as Received at the Surface of the Earth and Its Variations with Latitude, Altitude, the Season of the Year and the Time of Day," with H. H. Kimball, Chapter V of *Biological Effects of Radiation*, McGraw-Hill Book Co., New York, 1936, pp. 211–226.

Dec. 1937 "Review of the U. S. Weather Bureau Solar Radiation Investigations," *Monthly Weather Review*, vol. 65, No. 12, pp. 415–441.

Sept. 1939 "Methods and Results of Ozone Meaurements over Mt. Evans, Colo.," with Ralph Stair, *Monthly Weather Review*, vol. 67, No. 9, pp. 331–338.

Sept. 1939 "Variation in Solar Radiation Intensities at the Surface of the Earth in the United States," *Monthly Weather Review*, vol. 67, No. 9, pp. 338–340.

1939 "Preliminary Measurements of Ozone over Mt. Evans, Colo.," with R. Stair, *Transactions of the American Geophysical Union*, Part III, 1939, pp. 338–340.

April 1940 "An Instrument for the Spectroscopic Determination of Precipitable Atmospheric Water Vapor, and its Calibration," *Monthly Weather Review*, vol. 68, No. 4, pp. 95–98.

Aug. 1940 "A Balanced Direct Current Amplifier for Alternating Current Use," with R. Stair, *Review of Scientific Instruments*, vol. 11, No. 8, pp. 257–259.

Dec. 1940 "The Variability of the Thermoelectric Pyrheliometer Factor," *Monthly Weather Review*, vol. 68, No. 12, pp. 339–344.

Apr. 1941 "A Summary of Total Solar and Sky Radiation Measurements in the United States," *Monthly Weather Review*, vol. 69, No. 4, pp. 95–125.

May 1941 "The Characteristics of the Eppley Pyrheliometer," with B. S. Woertz, *Monthly Weather Review*, vol. 69, No. 5, pp. 146–148.

June 1941 "A Stable Photoelectric Amplifier and Its Application in Ultraviolet and Ozone Studies," with R. Stair, *Bulletin of the American Meteorological Society*, vol. 22, No. 6, pp. 259–265.

Sept. 1941 "Recalibration of Instrumental Equipment at Solar Radiation Stations," with Helen F. Cullinane, *Monthly Weather Review*, vol. 69, No. 9, pp. 262–264.

1941 "Preliminary Study of Radiation Penetration Through Snow," with R. E. Lundquist, *Proceedings, Central Snow Conference Dec. 11–12, 1941*, vol. 1, Michigan State College, East Lansing, 1941, pp. 42–44.

Feb. 1942 "Observations of Radiation Penetration Through Snow," with R. E. Lundquist, *Monthly Weather Review*, vol. 70, No. 2, pp. 23–25.

Mar. 1943 "A Plastic Snow-Tube," *Bulletin of the American Meteorological Society*, vol. 24, No. 3, p. 111.

May 1943 "Simultaneous Pyrheliometric Measurements at Different Heights at Mt. Washington, N. H.," with J. H. Conover and W. A. Boland, *Monthly Weather Review*, vol. 71, No. 5, pp. 65–69.

May 1943 "Transmission of the Total and the Infrared Component of Solar Radiation Through a Smoky Atmosphere," *Bulletin of the American Meteorological Society*, vol. 24, No. 5, pp. 201–204.

Feb. 1944 "Neighbors to the Sun," *New Mexico*, Feb. 1944, pp. 9, 33–35.

May 1945 "Herbert Harvey Kimball (1862–1944)" [Obituary and bibliography of papers published] *Bulletin of the American Meteorological Society*, vol. 26, No. 5, pp. 188–191.

Sept. 1946 "Solar Energy Received on a Vertical Surface Facing South," *Bulletin of the American Meteorological Society*, vol. 27, No. 7, p. 416.

Nov. 1946 *Pyrheliometers and Pyrheliometric Measurements*, U. S. Weather Bureau, Washington, D. C., 1946, 55 pp.

Oct. 1947 "Preliminary Measurements of Solar Energy Received on Vertical Surfaces," *Transactions of the American Geophysical Union*, vol. 28, No. 5, pp. 705–712.

Dec. 1947 "Solar Energy for House Heating," *Heating and Ventilating*, vol. 44, No. 12, pp. 80–94.

1947 "Sunshine," *Encyclopedia Britannica*, 1947 ed.

Sept. 1949 "Atmospheric Contamination over Boston Massachusetts," *Bulletin of the American Meteorological Society*, vol. 30, No. 7, pp. 252–254.

1949 "Weekly Mean Values of Daily Total Solar and Sky Radiation," U. S. Weather Bureau *Technical Paper* No. 11, Washington, D. C. 1949, 17 pp.

Jan. 1950 "Insolation on Clear Days at the Times of Solstices and Equinoxes for Latitude 42° N.," *Heating and Ventilating*, vol. 47, No. 1, pp. 92–94.

1952 "Measurements of Diffuse Solar Radiation at Blue Hill Observatory," with Frances A. Wollaston, U. S. Weather Bureau *Technical Paper* No. 18, Washington, D. C., 1952, 19 pp.

July 1953 "Distribution of Solar Energy over the United States", *Heating and Ventilating*, vol. 50 No. 7, pp. 73–75

Feb. 1954 "Methods of Calculating Solar Radiation Values at Blue Hill Observatory, Milton, Mass.," *Monthly Weather Review*, vol. 82, No. 2, pp. 43–48.

1954 "Methods of Calculating the Amount of Solar Energy Impinging upon a Vertical Surface Facing South," (to be published).

THE WORLD-RECORD 42-MINUTE HOLT, MISSOURI, RAINSTORM

GEORGE A. LOTT

Division of Hydrologic Services, U. S. Weather Bureau,* Washington, D. C.

(Manuscript received September 21, 1953; revision received December 18, 1953)

INTRODUCTION

The Holt, Mo., storm of June 22, 1947, is the outstanding example of a very intense, small-area rainstorm. The point-rainfall value of 12 inches in 42 minutes is a world record [1]. Figure 1 includes an isohyetal map showing the results of a Corps of Engineers bucket survey conducted shortly after the storm. The totals represent rainfall during the afternoon and/or evening of the 22d only. Figure 2 shows the average depth of storm rainfall over areas up to 4,000 square miles in the Holt center during the storm period.

This report will concern itself mainly with presenting the meteorological data available in this most unusual storm and suggesting a possible rain-producing mechanism.

June 1947 was the wettest June of record (1888–1947) in northern Missouri. The Holt storm itself caused major local floods which, in turn, added to the already swollen Missouri River. A disastrous flood at St. Louis on July 2, exceeded up to that time only by the flood of 1844, was the result of this June rainfall.

The Holt storm occurred as a local intensification in a long, narrow, warm sector convective system (the leading edge of which may be interpreted as an instability line) a short distance ahead of a surface cold front. This elongated convective system deposited rainfall totals of ½ to 2½ inches in eastern Kansas and Nebraska before the intensification took place. The heavy burst of rain in the Holt storm lasted about 45 minutes at a given point, but light showers continued until after the cold front passage several hours later.

SURFACE SYNOPTIC SITUATION

Figure 3 illustrates the large-scale synoptic conditions about 6 hours before the Holt storm. The extensive air mass in the eastern part of the country was unusually cold for the season. The front separating the eastern cold air mass from the warm air over southwestern Missouri was diffuse. The tropical air in the warm sector had a very high moisture content; e. g., the surface dewpoint of 76° F. at Little Rock, Ark., is exceeded only about 1½ percent of the hours in an average June [2].

Figures 4 and 5 are detailed weather maps of the region of greatest interest. They were selected from a series of

*In cooperation with the Corps of Engineers, Department of the Army.

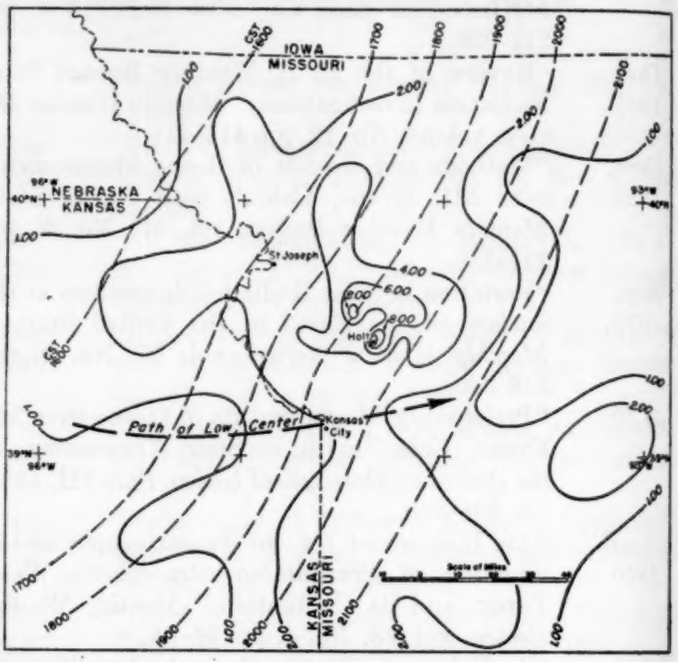

FIGURE 1.—Isohyetal map of storm rainfall in Holt, Mo. region, June 22, 1947. Precipitation amounts are in inches. Isochrones show hourly positions of the forward edge of the convective system.

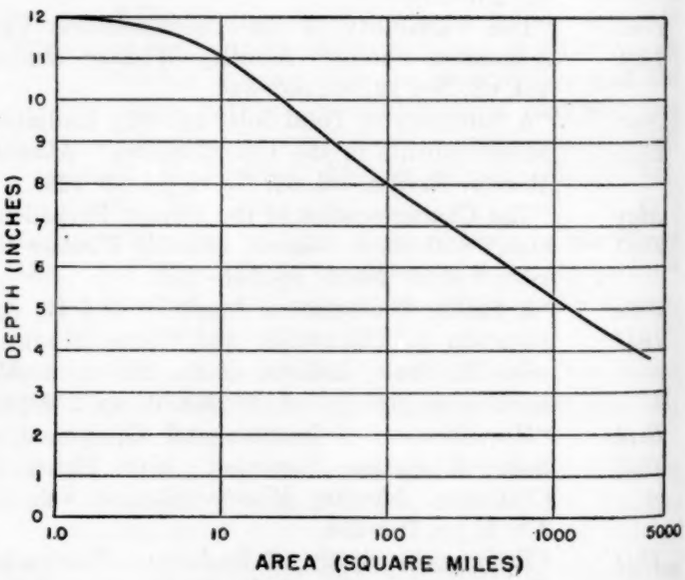

FIGURE 2.—Average amount of storm rainfall June 22, 1947 over areas up to 4000 square miles.

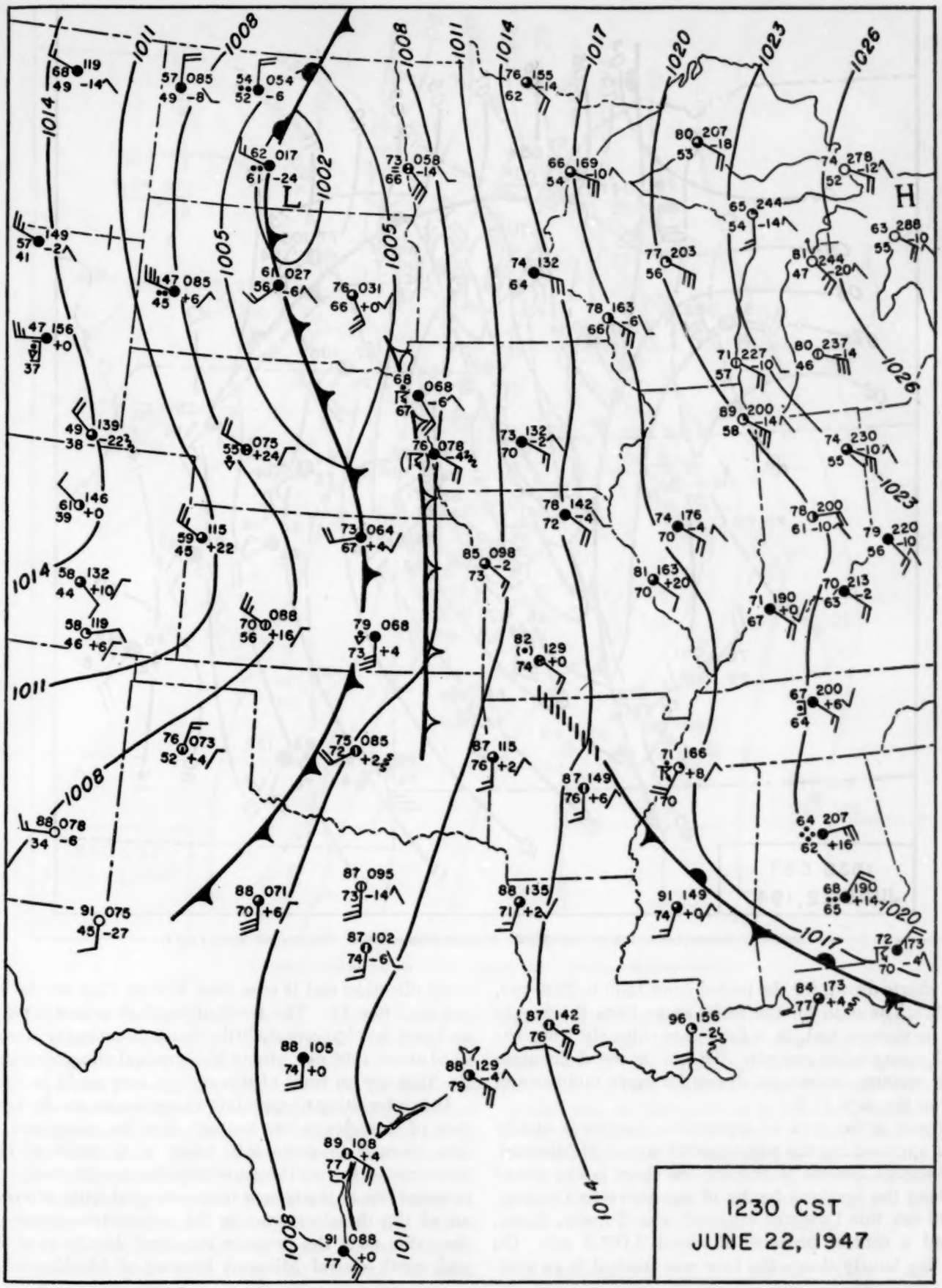

FIGURE 3.—Surface chart for 1230 CST, June 22, 1947 about 6 hours before the Holt storm. Note the high dewpoints in the warm sector. (After WBAN Analysis Center.)

292389—54——2

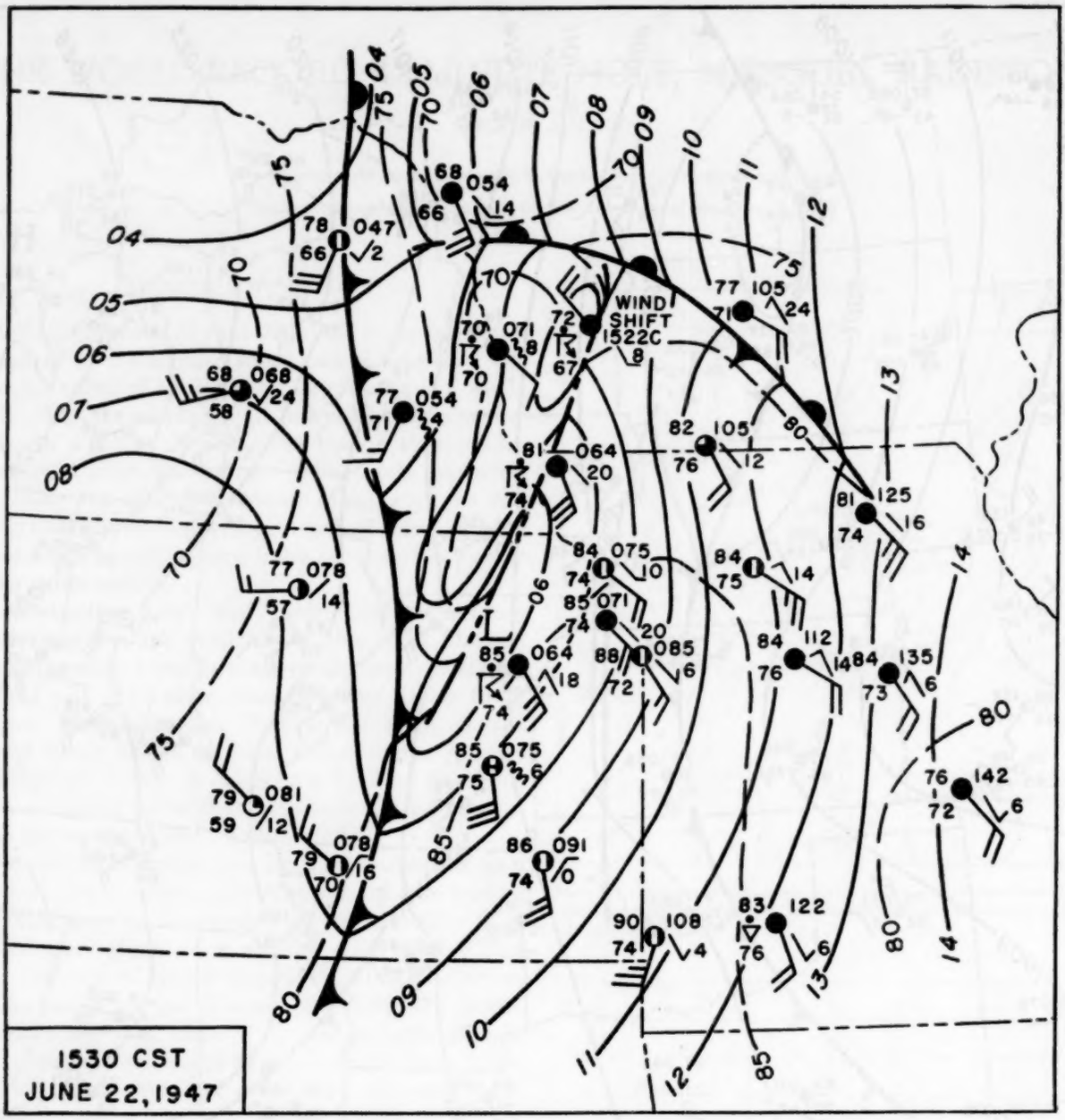

FIGURE 4.—Surface chart for 1530 CST June 22, 1947. Note closed central isobar. Compare with figures 3 and 5.

hourly charts drawn for the period from 1530 to 2130 CST, June 22. The data for the series came from the hourly airway sequences and, in a few cases, directly from the original autographic records. To aid in the delineation of weak systems, isobars are drawn for every millibar and isotherms for each 5° F.

On figure 4 the area of convective showers is clearly evident approaching the northwestern corner of Missouri. A noteworthy feature of the surface chart is the closed Low along the southern border of the convective system. At 1630 CST this Low was centered near Topeka, Kans., and had a central pressure of about 1,005.5 mb. On succeeding hourly charts the Low was tracked in an eastward direction and is seen near Kansas City on the 1830 CST map (fig. 5). The track of the Low center is plotted on figure 1. Apparently little change in intensity occurred until about 1900 CST, after which gradual filling took place. By 2130 CST no trace of this surface Low could be found.

It is interesting to speculate about the reason for formation of this closed low center. For the most part, the Low seemed to come into being as a result of rising pressures to the northwest within the trough itself. The pressure rise in the trough was associated with rain-cooled air of the thunderstorms in the convective system. At the same time the pressure remained steady over Iowa and north-central Missouri because of blocking of the

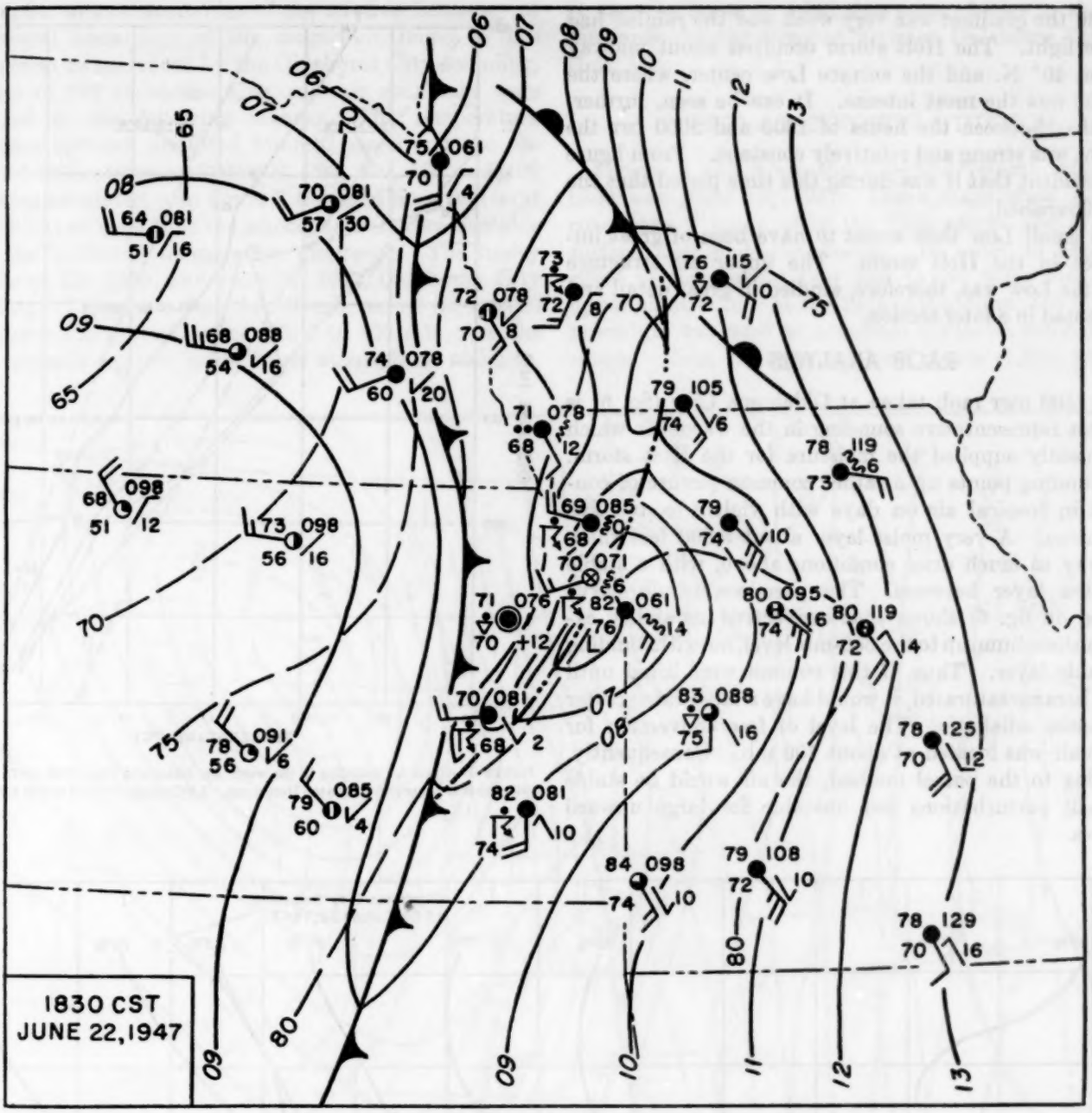

FIGURE 5.—Surface chart for 1830 CST, June 22, 1947. Compare with figures 3 and 4.

large High over the northeast (fig. 3). The effect was to leave a small system of low pressure cut off from the parent trough in the warm sector.

Figure 1 also shows hourly positions of the forward edge of the convective system. The positions were determined by the beginning of heavy rain which coincided very closely with the wind-shift line. Records from the Weather Bureau First-Order Airport Stations and about 50 Cooperative Observers in the area were available for analysis. The position of the rainfall center, relative to the surface Low, is of interest. A reference to figure 1 shows that the rainfall was relatively light along and south of the track of the Low. North of the path the rainfall increased rapidly to about latitude 39°30′ N. and then declined. In an west-east direction the most intense rainfall fell at about 94°20′ W. Although the central pressure of the Low did not vary much between 1600 and 1900 CST, the rainfall rate to the north of it increased constantly with time. An element that seems to have been associated with the intensity of rainfall was the pressure gradient north of the Low. The following table gives the gradient as measured from the Low center along the line of the eastern edge of the convective system.

Map time (CST)	1730	1830	1930	2030
Gradient (mb./mi.)	.025	.040	.038	.020

By 2130 the gradient was very weak and the rainfall had become light. The Holt storm occurred about midway between 40° N. and the surface Low center, where the gradient was the most intense. It can be seen, furthermore that between the hours of 1800 and 2000 CST the gradient was strong and relatively constant. From figure 1 it is evident that it was during this time period that the storm flourished.

This small Low then seems to have been of great importance in the Holt storm. The upper air structure above the Low was, therefore, studied in great detail and is presented in a later section.

RAOB ANALYSIS

The 1500 GMT raob taken at Oklahoma City (fig. 6) is the most representative sounding in the warm air which subsequently supplied the moisture for the Holt storm. The sounding points up a rather common picture of conditions in tropical air on days with violent convective phenomena. A very moist layer about 5,000 feet thick gave way to much drier conditions above, with a stable transition layer between. The pseudo-wet-bulb curve (plotted on fig. 6) shows that convective instability existed in the column up to the 660-mb. level, notwithstanding the stable layer. Thus, if this column were lifted until the air became saturated, it would have a lapse rate greater than moist adiabatic. The level of free convection for surface air was located at about 700 mb. Consequently, according to the parcel method, the air would be stable for small perturbations but unstable for large upward impulses.

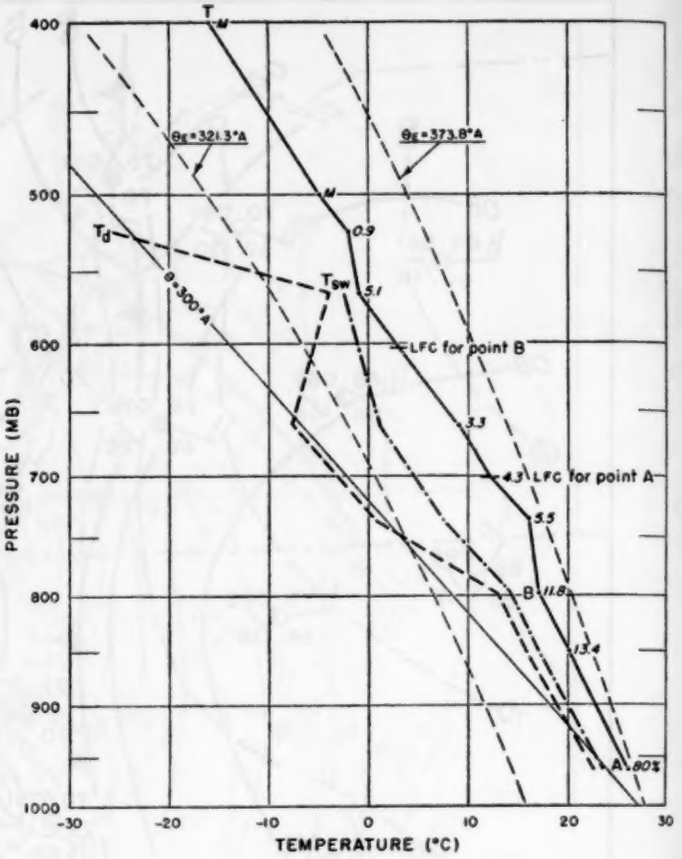

FIGURE 6.—Upper air sounding in the warm air, Oklahoma City, 1500 GMT, June 22, 1947, about 10 hours previous to the Holt storm. LFC stands for level of free convection.

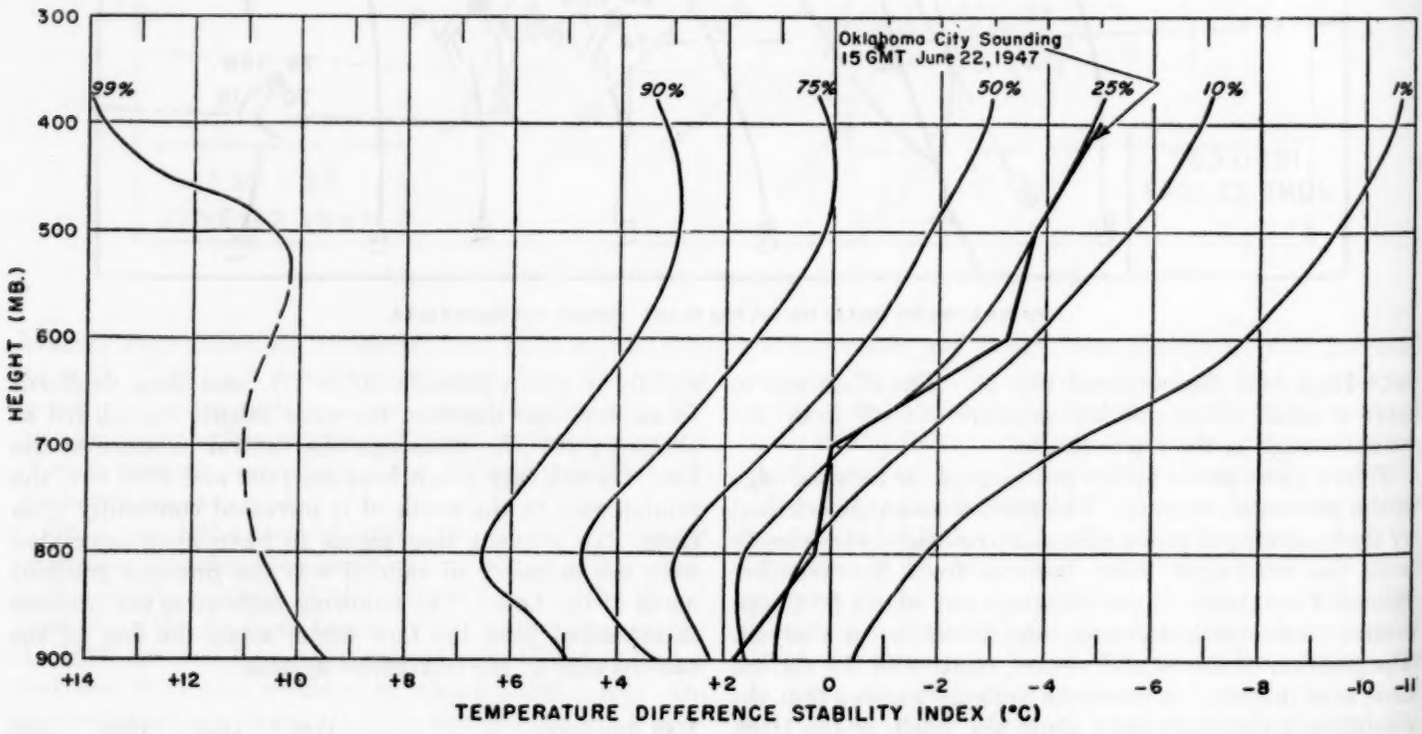

FIGURE 7.—Diagram comparing conditional instability of the Oklahoma City 1500 GMT sounding (heavy line) with average instability as measured by temperature difference computed from 282 Oklahoma City summer soundings. Light lines represent percent of time atmosphere is more unstable than the indicated temperature difference.

In order to gain some idea of the relative frequency of conditional instability of the magnitude found in the Holt storm as measured by the Oklahoma City sounding, a series of 282 Oklahoma City summer soundings were analyzed in the following manner. The temperature difference between the lifted 950-mb. parcel and the observed temperatures at 900, 800, 700, 600, 500 and 400 mb. were tabulated. In figure 7 the light lines represent the percent of time that the atmosphere is more unstable than the indicated temperature difference. The heavy line shows the 1500 GMT June 22, 1947, Oklahoma City sounding. It appears that the 950-mb. parcel (about 700 feet above the ground) when lifted to 800 mb., was the most unstable relative to the usual atmospheric stability. It must be borne in mind that some change in the lapse rate undoubtedly occurred between Oklahoma City and Holt, Mo.

UPPER AIR SYNOPTIC SITUATION

Figures 8 and 9 are the 850- and 700-mb. charts for 0300 GMT June 23, 1947. These maps show observed conditions 3 hours after the Holt storm and after the surface Low had disappeared. In order to assess the effect of the surface Low and to get some idea of the upper air structure at the time of the storm, the following procedure was used to construct synthetic constant-level charts. First, the constant-level charts (1,000, 850, 700,

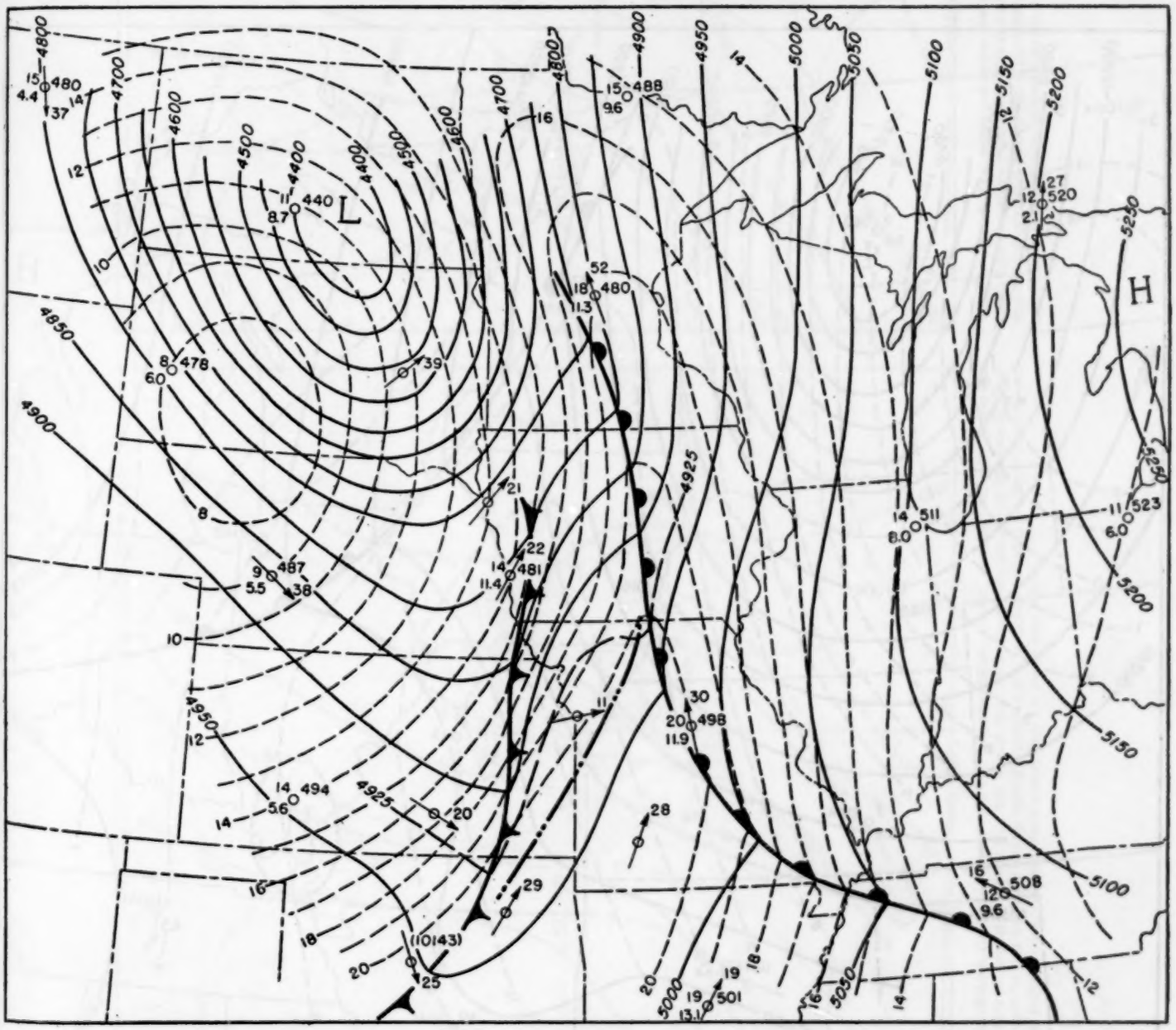

FIGURE 8.—850-mb. chart for 0300 GMT, June 23, 1947, three hours after the Holt storm. Contours are in feet (solid lines), isotherms in °C. (dashed lines).

500, and 300 mb.), for 1500 GMT of the 22d and 0300 GMT of the 23d were carefully analyzed, using small intervals of temperature and height. Thickness charts were then constructed for the 1,000–850, 850–700, 700–500, and 500–300-mb. layers for both 1500 GMT and 0300 GMT. Since the 1900 CST isochrone (see fig. 1) approximately bisects the Holt storm area, this time was chosen to illustrate the flow aloft at the time of the great storm. Thickness lines were then interpolated between the map times for 1900 CST. For the most part, objective linear interpolation of thickness lines was possible, but in some sections judgment was necessary, especially in local areas where a confused change in pattern was evident.

Figures 10–13 show the resultant 850-, 700-, 500-, and 300-mb. charts. In each case 50-ft. contours are used, and the thickness lines (proportional to the mean virtual temperature of the respective column) are also included. The edge of the convection area for 1900 CST and the total storm isohyetal pattern appear in each of these figures (the shaded portion of the isohyetal pattern is the area of intense rain, i. e., greater than about 6 in./hr. at map time).

A glance at the maps shows that the surface Low was reflected in the flow aloft up to at least the 500-mb. level, although the closed circulation seems to have been confined to the 850-mb. level only.

At the 850-mb. level (fig. 10) the Low was still very marked. An inflow from the east almost at right angles

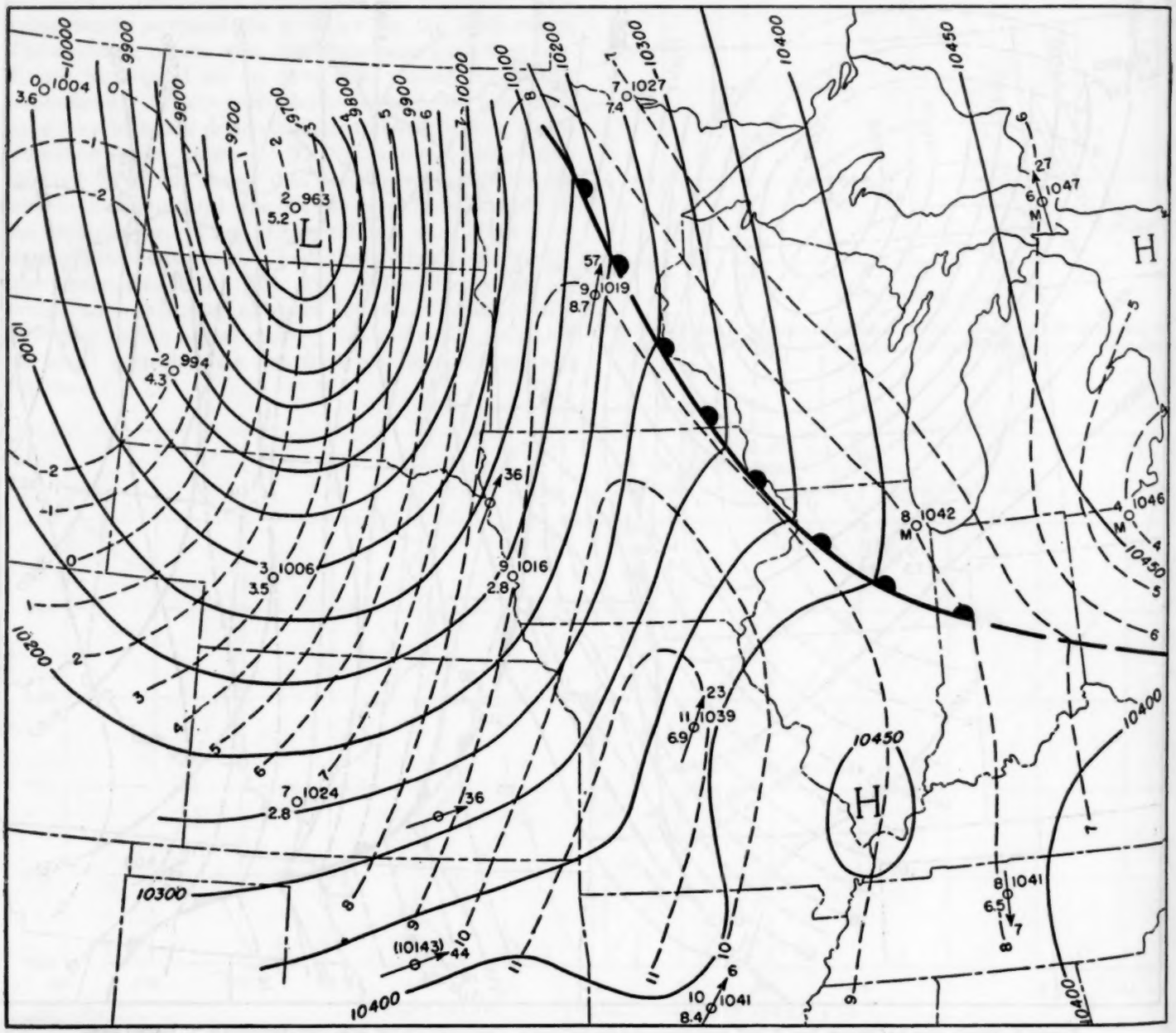

FIGURE 9.—700-mb. chart for 0300 GMT, June 23, 1947, three hours after the Holt storm. Contours are in feet (solid lines), isotherms in °C. (dashed lines).

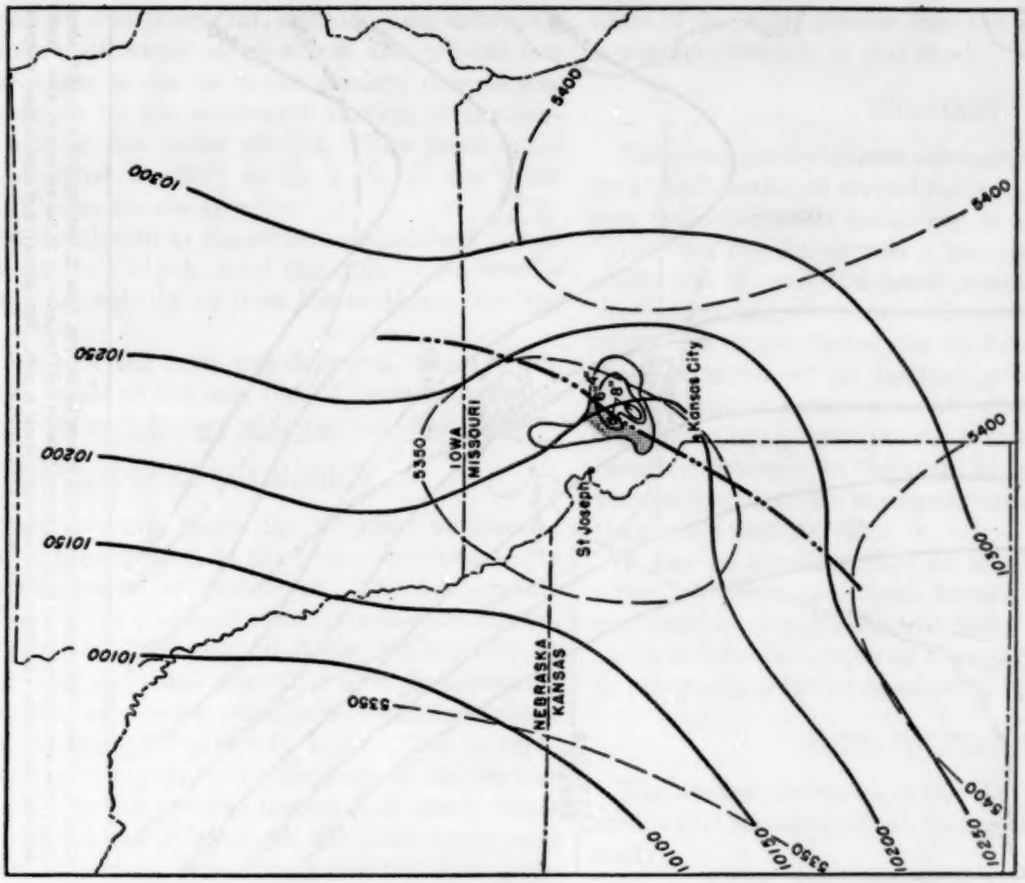

FIGURE 11.—700-mb. chart constructed as described in text for 1900 CST, June 22, 1947, the time of the Holt storm. Heavy lines are pressure contours (ft.); thin dashed lines are thickness contours (ft.) of 850-700-mb. layer. Heavy dash-dot line represents leading edge of convection area at surface. Shaded portion of superimposed isohyetal pattern indicates rainfall rate of greater than 6 in./hr. at map time.

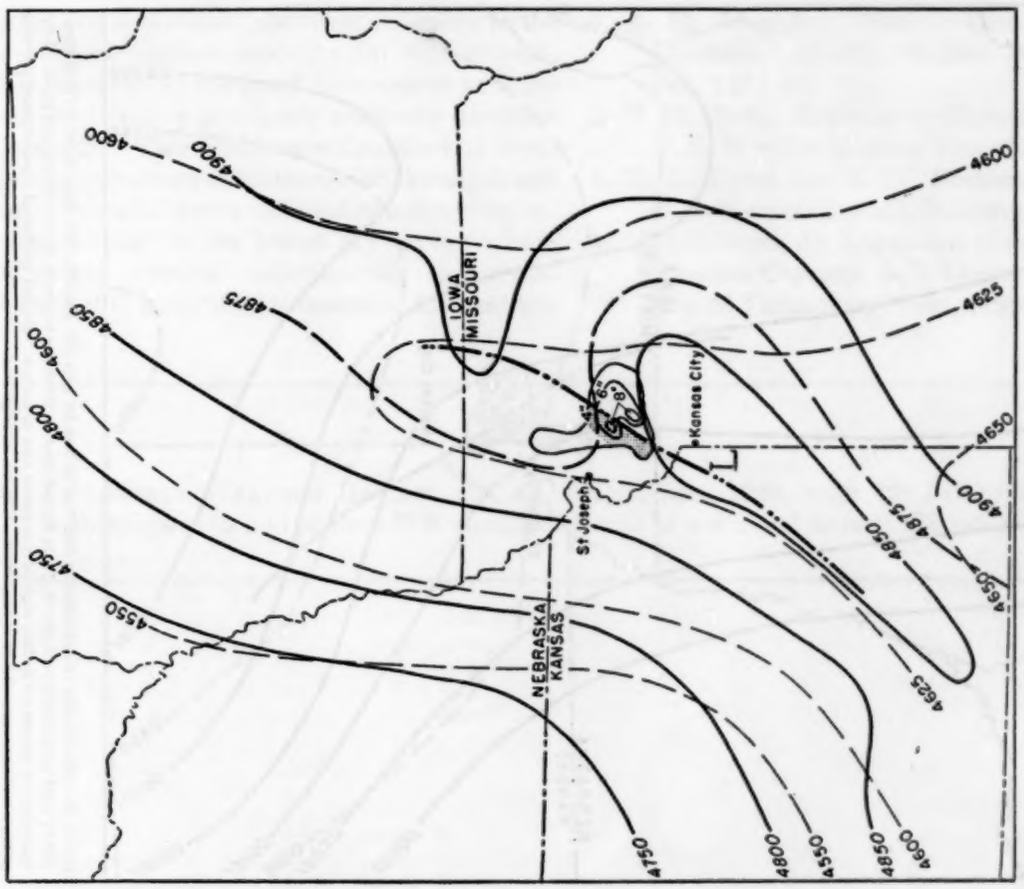

FIGURE 10.—850-mb. chart constructed as described in text for 1900 CST, June 22, 1947, the time of the Holt storm. Heavy lines are pressure contours (ft.); thin dashed lines are thickness contours (ft.) of 1000-850-mb. layer. Heavy dash-dot line represents leading edge of convection area at surface. Shaded portion of superimposed isohyetal pattern indicates rainfall rate of greater than 6 in./hr. at map time.

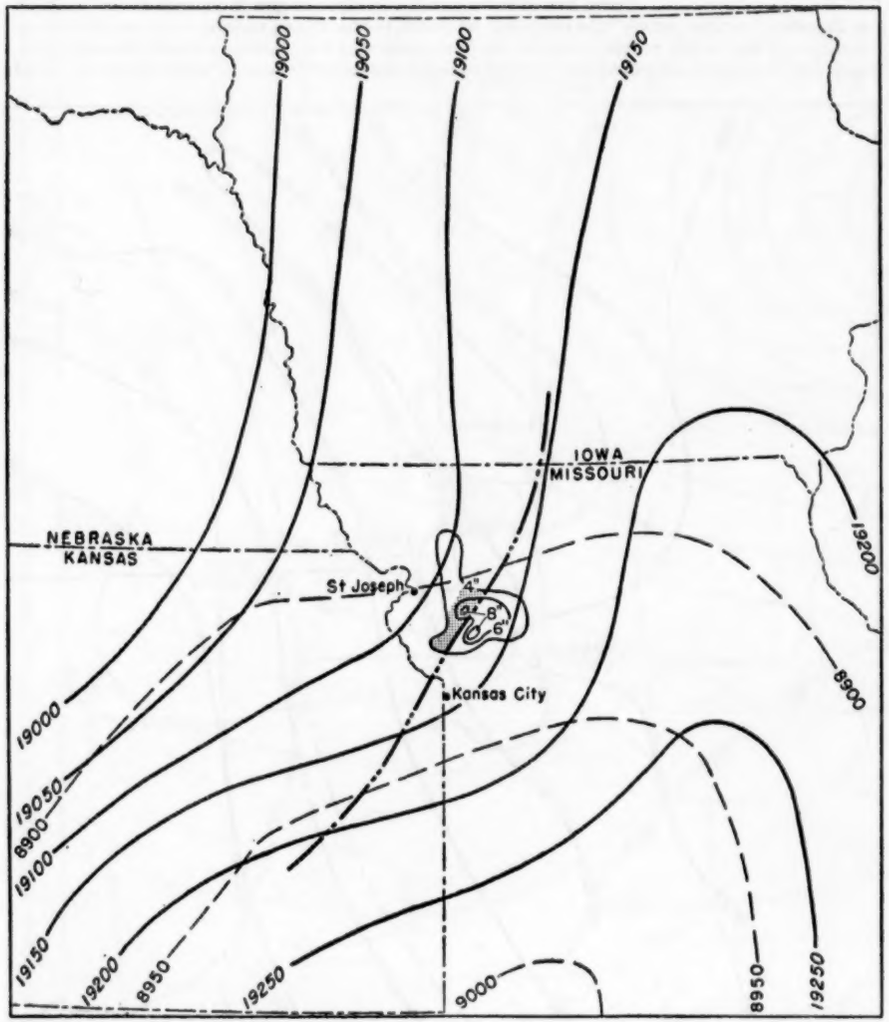

FIGURE 12.—500-mb. chart constructed as described in text for 1900 CST, June 22, 1947, the time of the Holt storm. Heavy lines are pressure contours (ft.); thin dashed lines are thickness contours, (ft.) of 700-500-mb. layer. Heavy dash-dot line represents leading edge of convection area at surface. Shaded portion of superimposed isohyetal pattern indicates rainfall rate of greater than 6 in./hr. at map time.

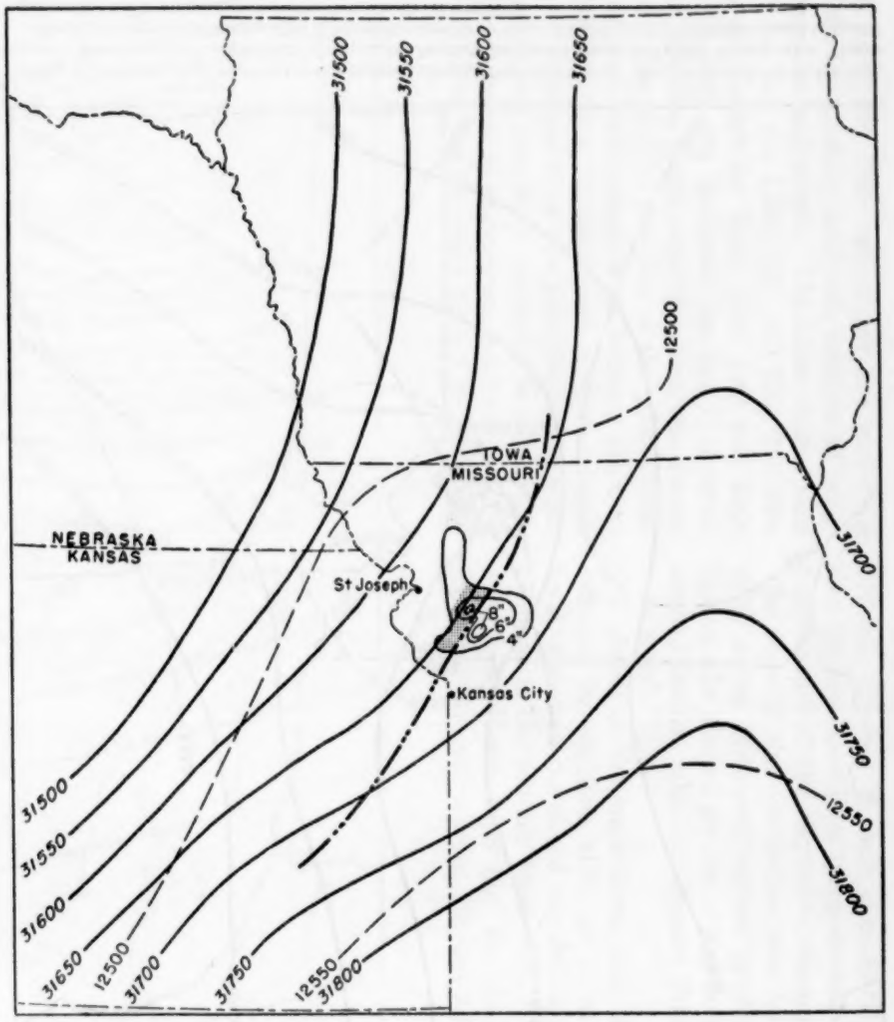

FIGURE 13.—300-mb. chart constructed as described in text for 1900 CST, June 22, 1947, the time of the Holt storm. Heavy lines are pressure contours (ft.); thin dashed lines are thickness contours (ft.) of 500-300-mb. layer. Heavy dash-dot line represents leading edge of convection area at surface. Shaded portion of superimposed isohyetal pattern indicates rainfall rate of greater than 6 in./hr. at map time.

to the convective area is evident, indicating an extremely favorable inflow of warm moist air in the critical low levels. The origin of the air in this easterly current was tropical as shown by the southward turning of the contour lines only a few miles upwind. The geostrophic wind was measured at 080°, 48 m. p. h. at the point of contact with the shower area.

The closed circulation at the surface and 850-mb. levels disappeared at the 700-mb. level (fig. 11). Cyclonically curved isobars brought in air from the southeast into the convective system.

The influence of the Low was fading at the 500-mb. level (fig. 12), while at 300 mb. (fig. 13) there appears to have been almost no influence of the surface system.

PROPOSED MECHANISM

The 1900 CST 850-mb. chart (fig. 10) must be thought of as a first approximation to the true conditions above the Holt storm center at that level. The temperature field in the convective area is, of course, the main unknown. Byers and Braham [3] suggest that the temperature at the 850-mb. level decreases somewhat in a thunderstorm rain area and that a very considerable cooling (about 5° C.) occurs in the 2,000–4,000 ft. layer. The 850-mb. cooling occurs about 3 miles to the rear of the surface wind shift line (in the average mature cell case). Since the cooling in the lower layers in the Holt storm was evaporational in nature, rather than frontal, it is probable that the horizontal temperature gradient at the 2,000–4,000 ft. level was only of the order of 2 miles to the rear of the surface outflow cooling. On the 850-mb. chart (fig. 10) the effect of the small Low was to turn the winds at that level from a previously southerly direction to a strong easterly. This could have the effect of forming a cross isotherm pattern of extraordinary strength and concentration. Areas of warm differential advection, especially if concentrated in the lowest layers, have been linked with strong vertical velocities [4]. A certain amount of conditional instability is favorable for continuation of the lifting process once the level of free convection is pierced (700 mb. in this case).

SUMMARY

This remarkably intense rainstorm was probably caused by a combination of several factors. Of great importance was the conditional instability in the tropical air mass. While the instability was a necessary condition for the storm and favored the development of warm sector convective systems, it was not sufficient to cause this explosive storm. A unique factor was the tightening of the pressure gradient north of an instability-line Low, causing an extraordinarily strong low-level flow of unstable air into the pre-existing convective system. The Holt storm occurred precisely at the point of injection into the convective system of the strongest winds in the layer between the surface and 850 mb.

It can be surmised that an area of strong differential advection could have been formed by the action of the combination of a pre-existent sharp temperature gradient and a sudden formation of a strong wind at right angles to this gradient by the uncommon pressure distribution.

ACKNOWLEDGMENT

The author desires to thank Dr. C. S. Gilman for his advice and encouragement during all phases of the storm study.

REFERENCES

1. A. H. Jennings, "World's Greatest Observed Point Rainfalls," *Monthly Weather Review*, vol. 78, No. 1, Jan. 1950, pp. 4–5.
2. H. K. Gold, Dewpoints—Durations and Frequencies, U. S. Weather Bureau, (unpublished).
3. H. R. Byers and R. D. Braham, *The Thunderstorm*, U. S. Weather Bureau, Washington, D. C., June 1949.
4. C. S. Gilman, An Expansion of the Thermal Theory of Pressure Changes, ScD Thesis, Massachusetts Institute of Technology, 1949, (unpublished).

CORRECTION

MONTHLY WEATHER REVIEW, vol. 82, No. 1, Jan. 1954, page 19: In the legends within figures 9a and 9b lines WW should be keyed as x x x and lines WWW as ● ● ● .

THE WEATHER AND CIRCULATION OF FEBRUARY 1954[1]

The Warmest February on Record for the United States

ARTHUR F. KRUEGER

Extended Forecast Section, U. S. Weather Bureau, Washington, D. C.

TEMPERATURE AND CIRCULATION

The month of February 1954 was characterized by extreme warmth over most of the United States, particularly in the North where average temperatures ranged as high as 20° F. above normal in the Dakotas and 10° above in Maine (Chart I–B). This was the warmest February on record for many parts of the Northern Plains, the Northeast, and the Great Lakes region and the warmest since 1930 for much of the Central and Southern Plains. For the country as a whole the weighted temperature average was higher than for any pervious February in the 61-year period of record. Furthermore, many stations reported record high daily temperatures during the month. In parts of Texas temperatures of 90° F. or greater occurred on two or three afternoons with extremes of 96° F. at Corpus Christi, 94° at Brownsville, and 93° at Austin.

This abnormal warmth was related to the fact that monthly mean 700-mb. heights were above normal over all the United States except the extreme Southeast (fig. 1). The largest departures for the country (+280 ft.) were observed in the Great Basin in the vicinity of a well developed 700-mb. ridge and an abnormally strong Basin High at the surface (Chart XI and inset). On the other hand, in Alaska, northwestern Canada, and the adjacent Arctic Ocean, subnormal 700-mb. heights and sea level pressures occurred accompanied by a greatly weakened surface polar anticyclone. In fact, in the Arctic Ocean north of Alaska a closed low center replaced the normal ridge, with the resulting anomalies (−550 ft. at 700 mb., −18 mb. at surface) being the lowest that have ever been noted for this region during the years of available data. The presence of negative height anomalies in northwestern Canada is concomitant with warmth over much of the United States, as emphasized by Martin [1].

In the eastern Pacific below normal heights were associated with a trough extending from Alaska southward to the Hawaiian Islands. East of this trough stronger than normal southwesterly flow carried warm Pacific air across the coasts of Washington and British Columbia, after which it was further heated during descent over the eastern slopes of the Rockies. The average speeds in this current were about 14–16 m/sec. and were as much as 8 m/sec. above normal (fig. 2 A and B). The unusually fast flow across Canada left little opportunity for this Pacific air to be transformed into polar continental air; thus the mean polar High was weak (Chart XI) and there were few cold-air outbreaks penetrating the United States. In the Northeast above normal temperatures were enhanced by anomalous flow from the southeast to the rear of an abnormally strong ridge in mid-Atlantic (anomaly of +430 ft. at 700 mb. and +12 mb. at sea level).[2]

The strength of the westerlies over Canada and the corresponding weakness of the polar anticyclone may be related to the circulation upstream. To the east of an abnormally strong ridge in northeastern Siberia (fig. 1) cold air was swept southward into the central Pacific where it interacted with warmer air forming a confluence zone [2]. Numerous cyclonic disturbances originated in this frontogenetical region and moved rapidly eastward to the Canadian coast (Chart X). Many of these storms either crossed the mountains or induced cyclogenesis on the lee side; as a result cyclonic activity was greater than normal in most of Canada. These storms traveled, for the most part, to the left of the axis of strongest winds at 700 mb. in the region of cyclonic shear.

PRECIPITATION

Subnormal precipitation over most of the country (Chart III) was associated with a ridge over the Basin, fast westerlies in Canada, and a trough along the east coast (fig. 1). The resulting anomalous flow from the Rockies eastward to the Atlantic Coast was from the north and because of subsidence and low humidities within this current, little precipitation occurred. Especially noticeable was the lack of any measurable precipitation in western and southern Texas, while much of the remainder of the State reported less than 10 percent of the normal amount, as did also parts of Colorado, Wyoming, Nebraska, and Kansas. This month was the driest February since 1901 at Brownsville, Tex., the driest

[1] See Charts I–XV following p. 72 for analyzed climatological data for the month.

[2] The anomalous flow is simply the vector deviation of the monthly mean geostrophic wind from the monthly normal and is represented by the isopleths of the departure from normal height field (dashed lines in fig. 1).

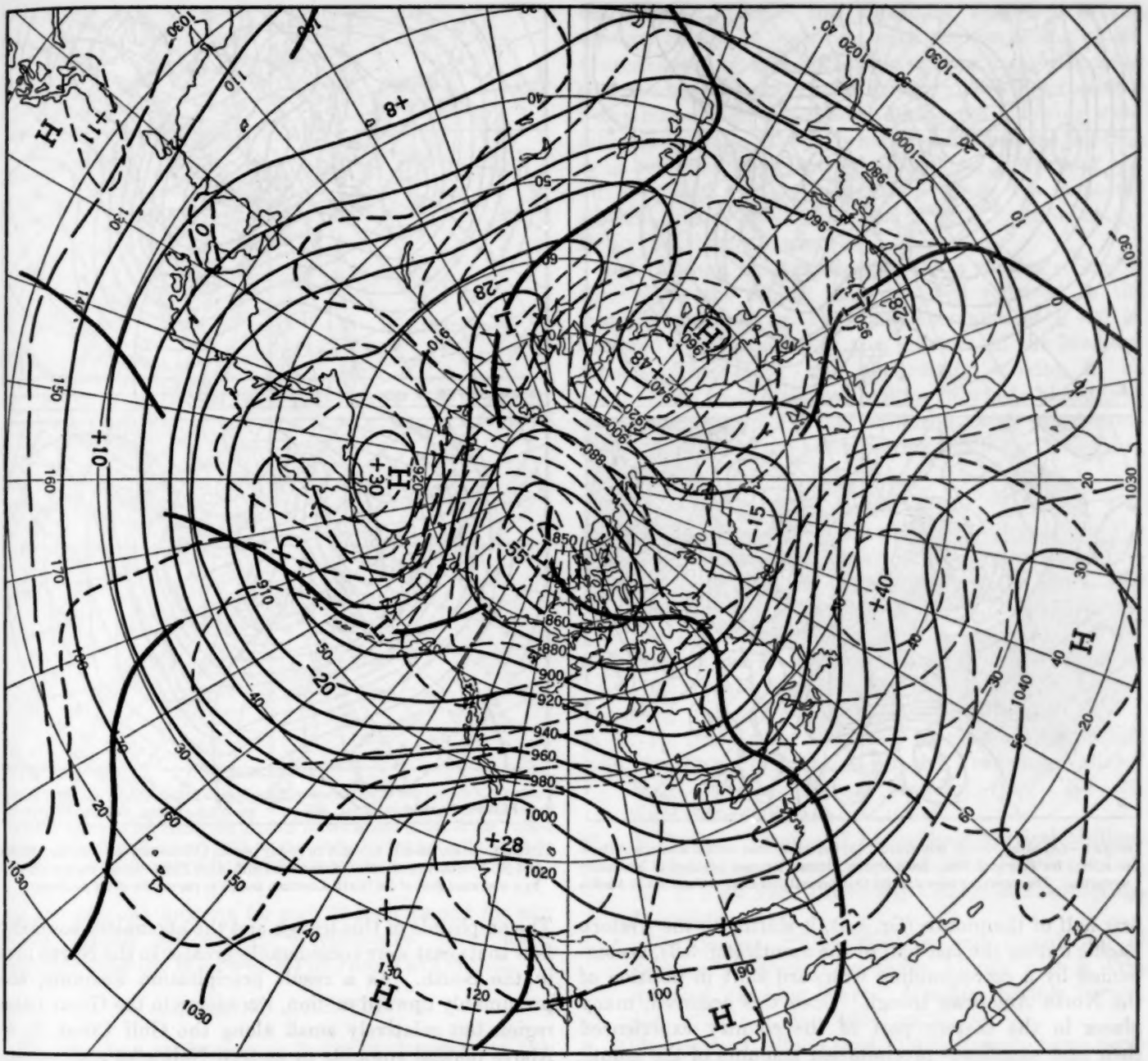

FIGURE 1.—Mean 700-mb. height contours and departures from normal (both in tens of feet) for January 30-February 28, 1954. Heights were below normal in Alaska, northwest Canada, and the adjacent Arctic Ocean, but were above normal over most of the United States.

since 1916 at San Antonio, and the second driest February on record at Corpus Christi. By the end of the month, 11 weeks had elapsed without substantial precipitation for much of the Central and Southern Plains, and the resulting drought situation was further aggravated by unseasonably warm temperatures and high winds which evaporated much of the soil moisture. In addition, the high winds caused considerable soil-blowing and even duststorms reminiscent of the 1930's.

Precipitation in significant amounts took place primarily in parts of the Central Plains, the Great Lakes region, the Northeast, the Pacific Northwest, and southern Florida. The amounts in the Northeast were associated with a strong anomalous flow of warm moist air just to the east of the mean trough. In the Pacific Northwest excess precipitation occurred as strong southwesterlies were forced over the coastal ranges, while in southern Florida heavy rains may be attributed to cyclonic curvature and resulting convergence in a deeper than normal trough.

Not as easily explained from figure 1 are the large precipitation amounts occurring in the Central Plains and Great Lakes region. These amounts, however, were the result of a change in the circulation during the latter half of the month, as illustrated in figure 3. While the mean trough was found in the central Pacific during the

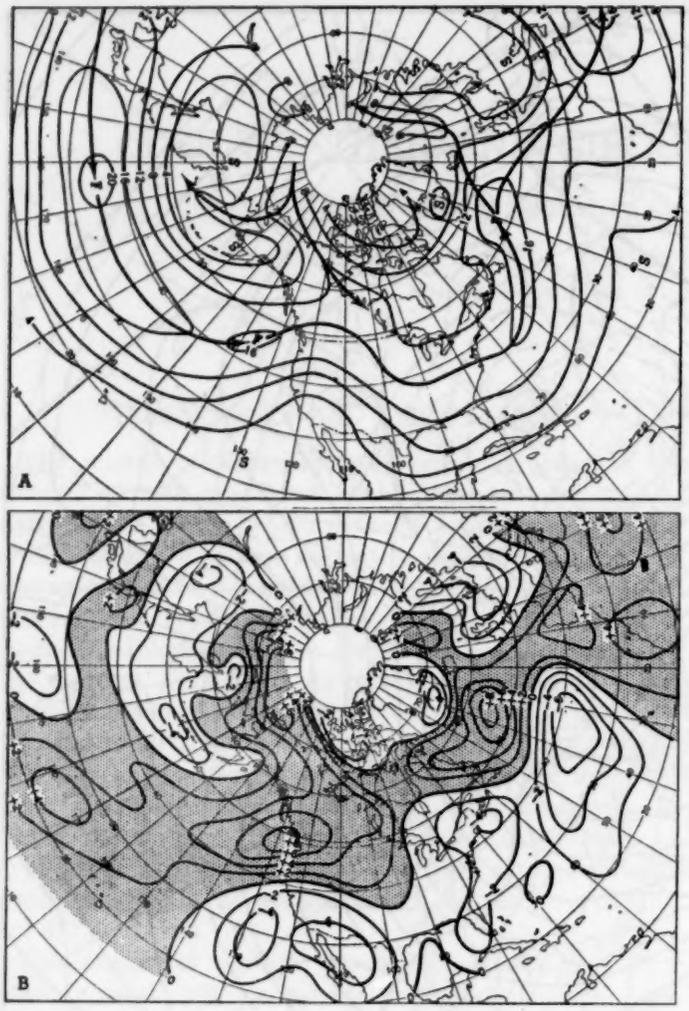

FIGURE 2.—(A) Mean 700-mb. isotachs and (B) departure from normal wind speed (both in m/sec.) for February 1954. Solid arrows indicate average position of maximum westerlies. The westerlies were stronger than normal over most of Canada and Alaska.

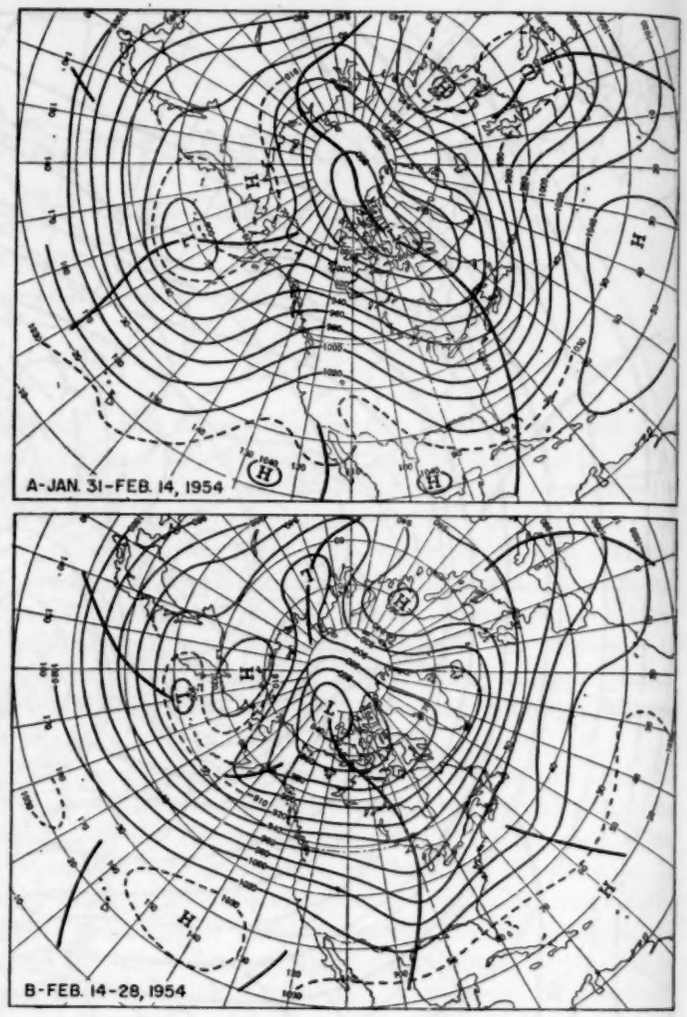

FIGURE 3.—Mean 700-mb. contours for 15-day periods (A) January 31—February 14, 1954 and (B) February 14–28, 1954. A westward shift of the Pacific trough was accompanied by a westward shift of the North American trough to the middle of the continent.

first half of the month (fig. 3*A*), it shifted to the western Pacific during the last half of the month (fig. 3*B*), accompanied by a corresponding westward shift in position of the North American trough. Once this occurred, many places in the eastern part of the country experienced their first significant precipitation amounts of the month as moist Gulf air was carried northward ahead of the trough [3] in the central United States. Anomalous flow from the south, responsible for this precipitation, is indicated in figure 4*B*, which is the departure from normal of the 15-day mean 700-mb. heights shown in figure 3*B*. A striking contrast is provided by figure 4*A*, the departure from normal of the 700-mb. heights in figure 3*A*, where the anomalous flow is strongly from the north.

Table 1 compares the precipitation during the last half of the month with the monthly total for a few stations affected by the westward shift in trough position. It shows that nearly all of the monthly precipitation for these stations took place during the last half of the month when the trough was in the central part of the country. The amplitude of this trough and the anomalous southerly flow to its east were considerably greater in the North than in the South. As a result precipitation amounts, and presumably upward motion, were large in the Great Lakes region but relatively small along the Gulf Coast [3, 4]. Above normal amounts in eastern Nebraska and western Iowa resulted essentially from one cyclone (Feb. 19–20). Omaha, for example, received 2.24 inches, or 87 percent of its monthly precipitation, from this one storm, which

TABLE 1.—*Precipitation at selected stations for February 1954*

	Total for month (in.)	Amount occurring last half of month (in.)	Percent occurring last half of month
Memphis, Tenn.	4.97	4.97	100
Atlanta, Ga.	2.70	2.50	93
Columbus, Ohio	1.78	1.70	96
New Orleans, La.	1.34	1.32	99
Shreveport, La.	.90	.90	100
Omaha, Nebr.	2.59	2.59	100
Grand Rapids, Mich.	2.71	2.27	84

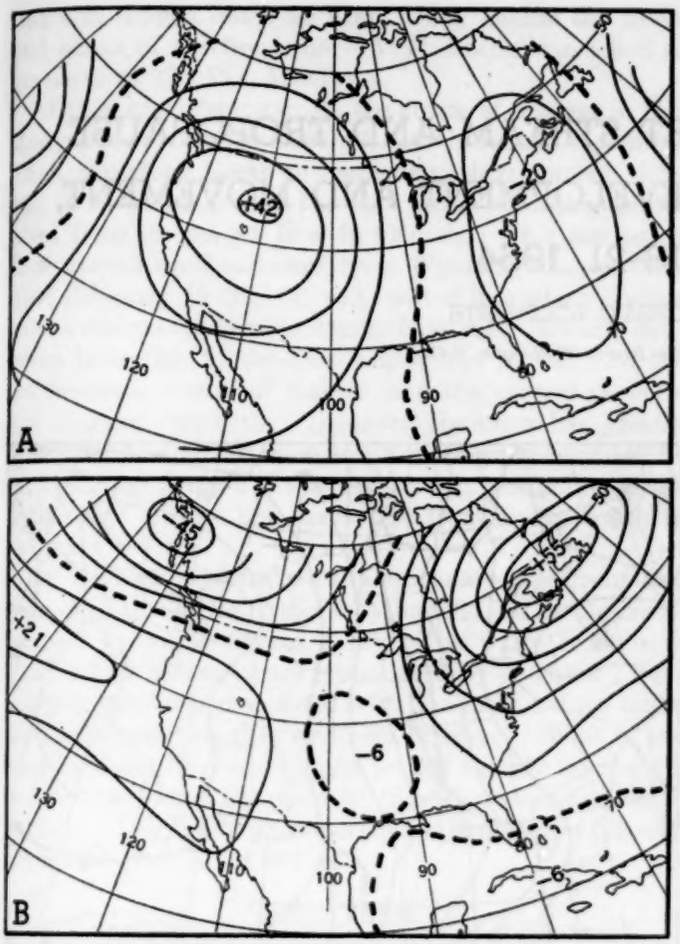

FIGURE 4.—Mean 700-mb. height departures from normal for 15-day periods (A) January 31–February 14, 1954, and (B) February 14–28, 1954. Isopleths are drawn for intervals of 100 ft. with zero line dashed and anomaly centers labeled in tens of feet. Strong anomalous northerly flow prevailed in the East during the first half of the month followed by a reversal to southerly the last half of the month.

was the greatest amount for any 24-hour period for any winter month on record. Furthermore, this made February 1954 the third wettest on record at Omaha.

BLOCKING ACTIVITY

Blocking was an important factor in determining this month's circulation pattern, but to a lesser extent than during January [5]. Again there was a progressive diminution in the speed of the westerlies, originating in the eastern Atlantic and spreading westward to the western Pacific. Concurrent with the weakening of the westerlies in the eastern Pacific, strong anticyclogenesis occurred over Alaska around February 12. The resulting 5-day mean High retrograded during the following week into northeastern Siberia, where it remained for another week and slowly weakened. The mean position of the blocking High for the month as a whole was in northeastern Siberia (fig. 1), compared to a location in the Bering Sea during January [5].

Over Europe, blocking was present in varying strengths throughout the month and was well reflected in the monthly pattern (fig. 1), where anomalies of +480 ft. occurred over Scandinavia and −280 ft. in the Mediterranean. This block was particularly striking in its resemblance to the typical picture in which blocking is considered as a split in the westerlies, with one branch flowing north and the other flowing south (fig. 2A) [6].

REFERENCES

1. D. E. Martin and H. F. Hawkins, Jr., "Forecasting the Weather, The Relationship of Temperature and Precipitation over the United States to the Circulation Aloft," *Weatherwise*, vol. 3, No. 1, Feb. 1950, pp. 16–19.
2. J. Namias and P. F. Clapp, "Confluence Theory of the High Tropospheric Jet Stream," *Journal of Meteorology*, vol. 6, No. 5, Oct. 1949, pp. 330–336.
3. W. H. Klein, "An Objective Method of Forecasting Five-Day Precipitation for the Tennessee Valley," U. S. Weather Bureau *Research Paper* No. 29, Apr. 1949, 60 pp.
4. J. E. Miller, "Studies of Large Scale Vertical Motions of the Atmosphere," *Meteorological Papers*, vol. 1, No. 1, New York University College of Engineering, July 1948, 48 pp.
5. A. F. Krueger, "The Weather and Circulation of January 1954—A Low Index Month with a Pronounced Blocking Wave," *Monthly Weather Review*, vol. 82, No. 1, Jan. 1954, pp. 29–34.
6. R. Berggren, B. Bolin, and C.-G. Rossby, "An Aerological Study of Zonal Motion, Its Perturbations and Break-Down," *Tellus*, vol. 1, No. 2, May 1949, pp. 14–37.

SOME FLUCTUATIONS IN THE JET STREAM AND TROPOPAUSE ASSOCIATED WITH CYCLONIC DEVELOPMENT AND MOVEMENT, FEBRUARY 18-21, 1954

RALPH P. JAMES AND GEORGE C. HOLZWORTH

WBAN Analysis Center, U. S. Weather Bureau, Washington, D. C.

INTRODUCTION

The purpose of this paper is to study the behavior of the jet stream and the tropopause associated with a deep moving cyclone, and especially to study carefully irregularities in winds aloft and temperature reports that do not seem to conform logically to currently envisioned models of jet stream mechanisms and analysis. The emphasis of the paper thus is on such problems as are encountered in day-to-day analysis operations. One of the more widely accepted notions is inferred from the thermal wind equation; that is, winds should increase with height so long as there is a horizontal temperature gradient with colder air to the left of the observed winds. Thus, in a simple idealized case, over the leading edge of a deep cold dome one would expect the wind speeds to increase with height up to the tropopause where the temperature gradient suddenly reverses. Such a case will be described here.

The storm chosen for this study developed in central Wyoming at 1830 GMT, February 18, 1954 along a cold frontal boundary between cold, maritime air to the northwest and warm, highly modified, continental air to the southeast. This storm moved southeastward into Kansas and then recurved to the northeast, passing just to the west of Lake Michigan. With the track of the surface Low center passing through the central part of the United States, the associated jet stream also remained within the States, providing sufficient data for accurate analyses of conditions aloft. This storm will be studied primarily along a fixed cross-section.

SURFACE SYNOPTIC CONDITIONS

At 1830 GMT, February 18, 1954 a cold front extended south-southwestward from a 992-mb. Low located in southern Saskatchewan. This front was the leading edge of a well-defined surge of maritime polar air which moved eastward into the United States from the Pacific and contributed to the formation of a strong Basin High. Some idea of the intensity of this cold front was indicated by the fact that the thermal wind gradient in the 1000–500-mb. layer averaged about 50 knots behind the front. Also, on the corresponding 700-mb. chart the −15° C.

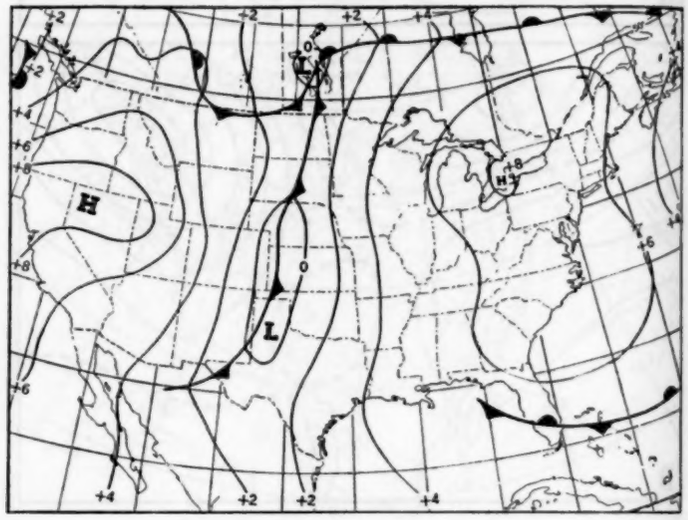

FIGURE 1.—1,000-mb. chart at 0300 GMT on February 19, 1954. Contours are in hundreds of geopotential feet.

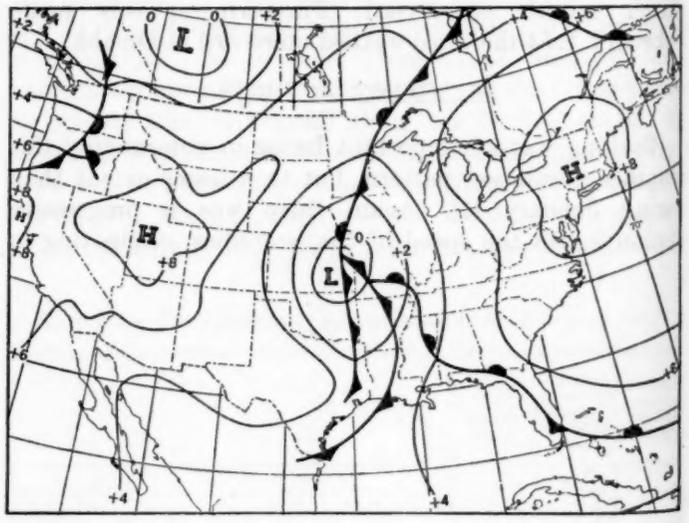

FIGURE 2.—1,000-mb. chart at 0300 GMT on February 20, 1954.

isotherm dipped down to Elko, Nev., behind the front, and ahead of the front the −5° C. isotherm reached as far north as The Pas, Manitoba.

At 1830 GMT, February 18, the storm of interest in this study first appeared as a 996-mb. Low in central Wyoming. Thus, this storm began as a secondary development along and in association with the cold front extending southward from its parent Low in Canada. This secondary Low moved southeastward from Wyoming and at 0300 GMT, February 19 (fig. 1), was located in western Kansas with a central sea level pressure of 994 mb. Twenty-four hours later (fig. 2) the Low center had moved into the northeastern corner of Kansas, and the central pressure had changed very little. However, the storm had greatly intensified and at this time had become a primary center. As seen from figure 2 the intensification resulted from the building of a ridge line across the front to the north of this Low center.

By 1500 GMT, February 19, a secondary cold front had formed in the cold air (this may be followed in the cross-sections shown in figures 9–12). The warm front over Florida had become more pronounced by 0300 GMT, February 20, and was associated with the main storm, intersecting the cold front in southern Missouri. West of the Appalachians this warm front moved rapidly northward and by 0300 GMT, February 21 (fig. 3), was just north of Buffalo. The Low center was located in northern Wisconsin with a pressure of 993 mb.

JET STREAM

The 200-mb. trough associated with this surface Low may be seen in figures 4–6. It may also be noted that the jet stream entering the west coast near latitude 40° N. curved south of the surface position of the Low. This relationship between the jet stream and extratropical cyclones has been found favorable for the deepening of storms [1]. Although this storm did not deepen, the intensity, as measured by the pressure gradient around it, did increase very markedly. With regard to an example by Alaka, Jordan, and Renard [2] it was stated that a deepening Low is generally associated with a well, defined jet maximum and that throughout the period of intensification the Low is located to the left and forward of the jet maximum. In figures 5 and 6 the surface Low is found to the left and slightly behind the jet maximum. This might have been taken as an indication that the Low would not deepen any further.

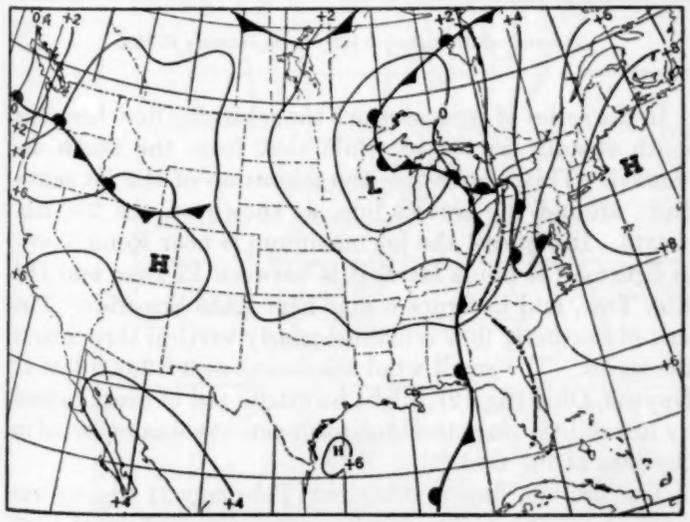

FIGURE 3.—1,000-mb. chart at 0300 GMT on February 21, 1954.

Jet stream analysis can often become a problem when viewing constant pressure surfaces only. To avoid this difficulty, cross-sections were constructed along the same baseline for every 12 hours that the storm was in the United States. Six of these are reproduced in figures 7 through 12. Figures 8, 10, and 12 are synoptic with figures 4, 5, and 6.

The jet axis near Las Vegas, Nev., in figure 7, seemed to conform very well to the usual model; i. e., its axis sloped poleward with height below the 500-mb. level, remained almost vertical to the level of strongest winds, just below the tropopause, and sloped equatorward above that.

The jet maximum was very close to the 200-mb. level, while in the returning flow near Denver it was at a lower elevation. The axes of both flows appeared to be nearly vertical above the 500-mb. level. Twelve hours later (fig. 8) the northwesterly jet had the same slope, but the northwesterly winds had decreased while the southerlies had increased. Both axes were still nearly vertical above the 500-mb. level and both maxima were near 230 mb. However, by 1500 GMT, February 19 (fig. 9), the cross-section of the northwesterly jet had changed considerably. Below the 250-mb. level the axis had continued to move to the northeast and had weakened still further, but above the 250-mb. level the wind maximum still existed near Las Vegas, Nev. A maximum wind of 131 knots (normal to the cross-section) at the station was reported about two thousand feet *above* the tropopause, 22 knots greater than the reported wind at the tropopause. In view of the existing temperature field this report seemed highly unreliable. As a matter of fact the coexistence of such a wind and temperature field is a virtual impossibility, and for this reason the report was discarded as being erroneous. This was the only case in the series where the wind maximum was reported above the tropopause. With this wind discarded the jet followed a logical continuity, both in time and space, which is one of the fundamental principles of good analysis.

At this time, however, the northwesterly jet axis no longer retained a vertical slope above the 500-mb. level. The maximum wind was at Grand Junction, Colo., at 500 mb.; about half-way between Milford, Utah, and Grand Junction at 300 mb.; and northeast of Las Vegas at 200 mb. An inspection of the isotach charts at the three levels breaks down this seemingly single jet stream into two.

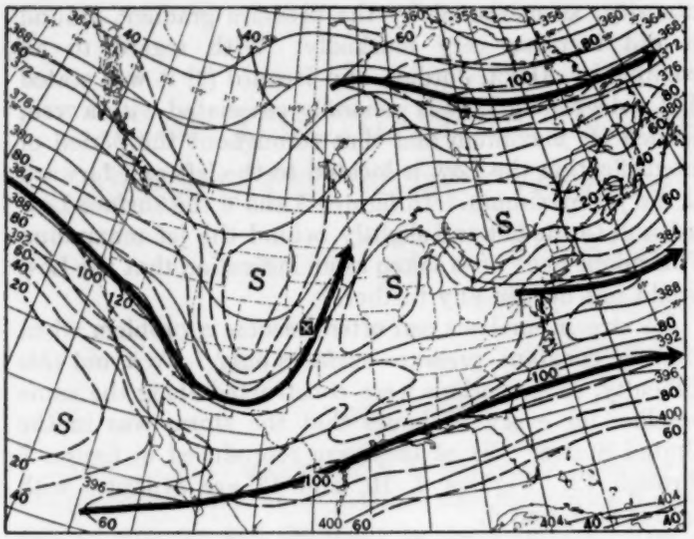

FIGURE 4.—200-mb. chart at 0300 GMT on February 19, 1954. Contours, continuous lines, are in hundreds of geopotential feet. The jet streams are indicated by the wide black lines with arrow heads. Isotachs, dashed lines, are in knots. For clarity the isotherms have been omitted. The small "x" denotes the surface Low center.

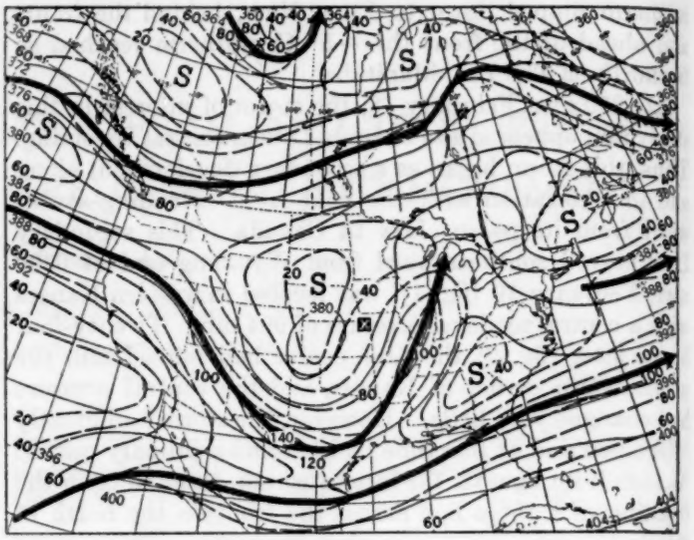

FIGURE 5.—200-mb. chart at 0300 GMT on February 20, 1954.

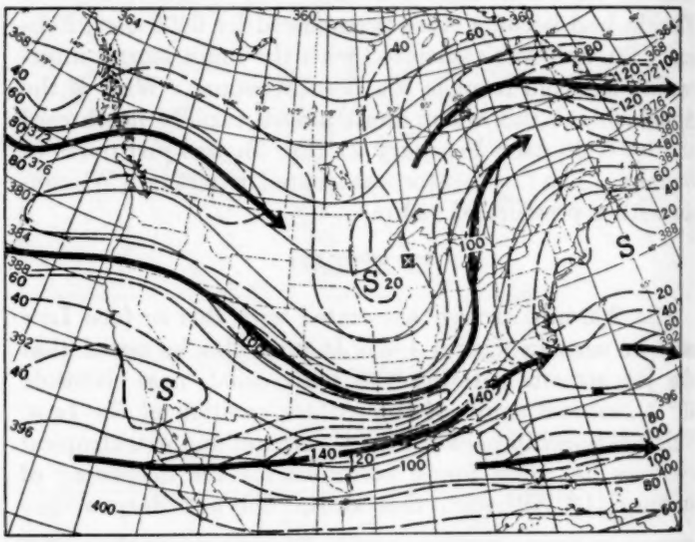

FIGURE 6.—200-mb. chart at 0300 GMT on February 21, 1954.

The lower one, in evidence on the 500-mb. and 300-mb. charts, entered the west coast near latitude 45° N., crossed southern Idaho, and then turned southward across eastern Utah to El Paso, Tex. This was the weaker of the two where it crossed the cross-section. The main jet stream, or core, was the one shown in figure 9 at about 200 mb. near Las Vegas. This is the one carried on the 200-mb. charts in figure, 4–6, and seems to be the main jet.

Figure 10, 0300 GMT, February 20, 12 hours later, shows this double jet a little more clearly. The lower level jet axis sloped from Denver at 500 mb. to a maximum near 300 mb. at Grand Junction. Associated with the main jet, which had a maximum near Milford at 200 mb., was a nearly vertical axis near Las Vegas. After another 12 hours (fig. 11) the maximum wind of the lower jet had increased to 100 knots, and both axes of the northwesterly jets were still very much in evidence. The relationship between the two jets was still the same as when they were first noticed in figure 9, but the maximum wind by this time had lowered to 300 mb. and was associated with the lower jet. The wind data for 400 and 500 mb. reported from Denver at this time seemed to be erroneous. After comparing them with the winds reported at 0900 and 2100 GMT and with the constant pressure charts for 1500 GMT, estimates of the true values were made and incorporated into the cross-section. By 0300 GMT, February 21 (fig. 12) the northwesterly flow normal to the cross-section had become rather flat and diffuse, but the two axes were still identifiable. One reason for this apparent flatness and diffuseness was the angle made by the cross-section surface through the flow pattern. At this time the cross-section cut through the northwesterly jet at a rather oblique angle thereby spreading the isotachs. In viewing all the cross-sections this relative orientation should be kept in mind.

In the series of cross-sections the returning flow from the south steadily increased while that from the north decreased. This emphasizes the migration of the jet maximum around the trough line, as shown on the 200-mb. charts. In figure 4 the jet maximum is near Reno, Nev.; in figure 5 (24 hours later) it is between El Paso and Del Rio, Tex., and in figure 6 it is near Lake Superior. The axis of southerly flow remained nearly vertical throughout the series. The small wind maximum near 12,000 feet at Dayton, Ohio (fig. 12), might be attributed to gusts caused by instability, since thunderstorm activity was reported in the area at the tine.

The 200-mb. flow at 0300 GMT, February 21 (fig. 6) was marked by the rather sudden appearance of a jet over southern Florida. Although the geostrophic winds do not support such strong winds, the existence of this jet was borne out by the observed winds. The use of inter-

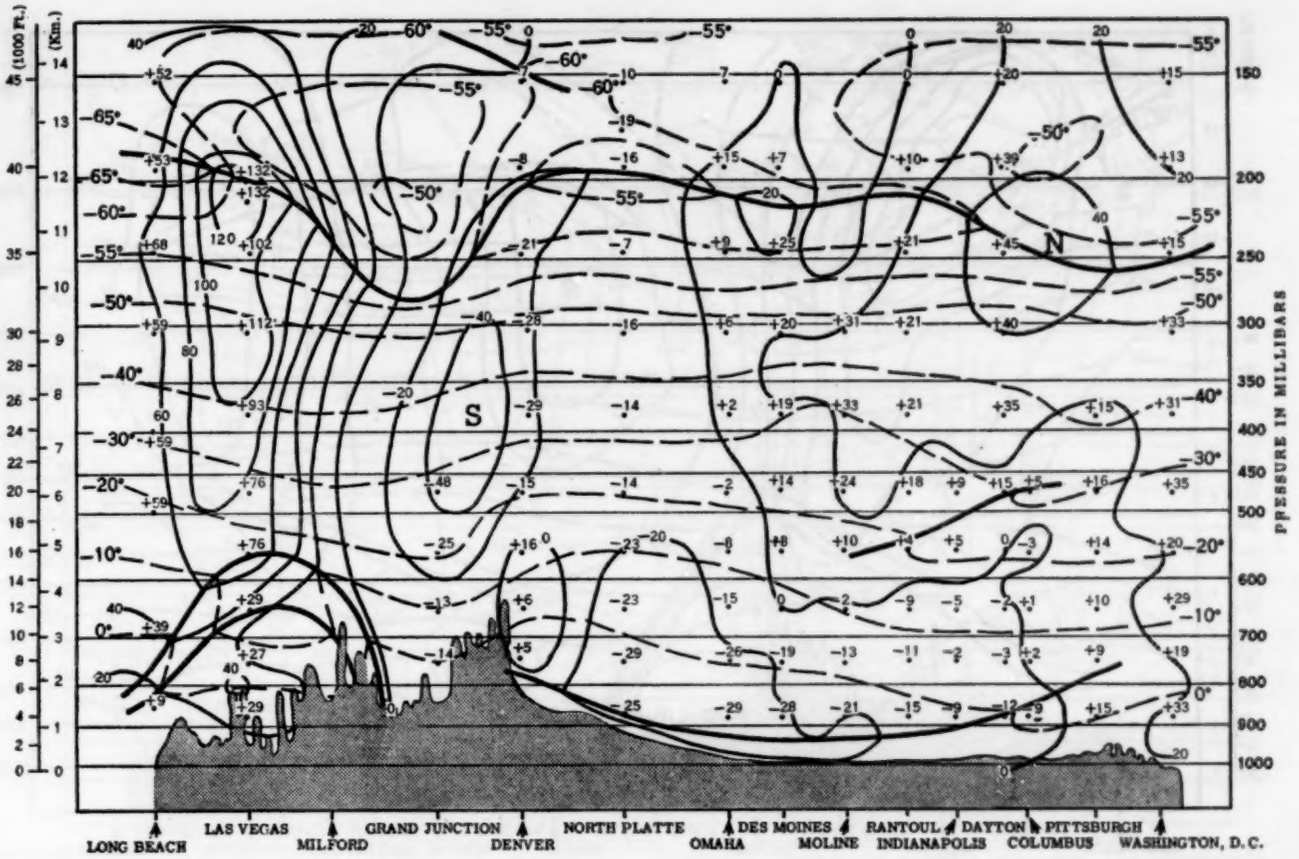

FIGURE 7.—Cross-section, roughly west-east, at 1500 GMT on February 18, 1954. Heavy lines indicate fronts, frontal zones, inversions, and tropopauses. Isotherms in ° C. are shown as dashed lines. Isotachs, shown as thin solid lines, give components of wind (knots) normal to cross-section; positive values are winds blowing out of the diagrams (i. e. from the north) and negative into the diagram.

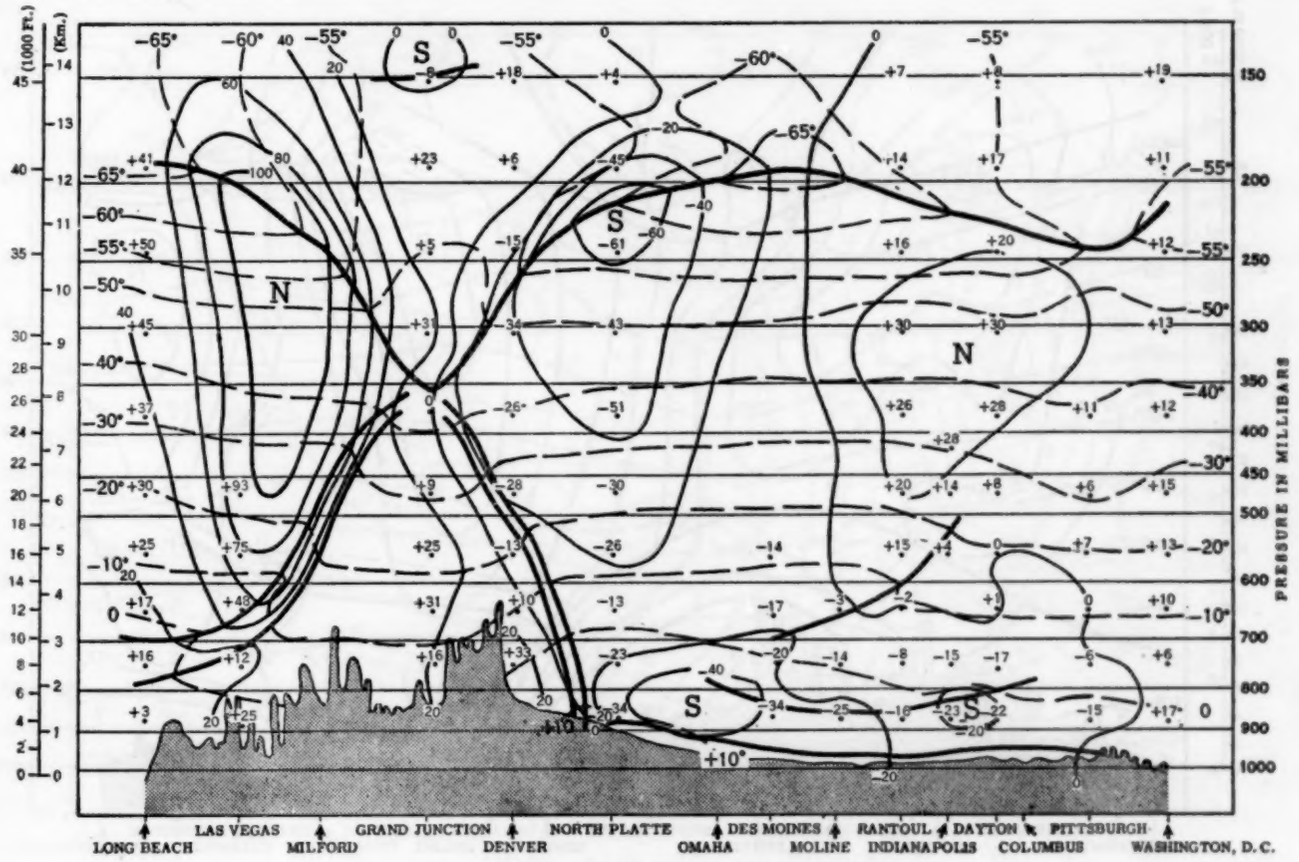

FIGURE 8.—Cross-section at 0300 GMT on February 19, 1954.

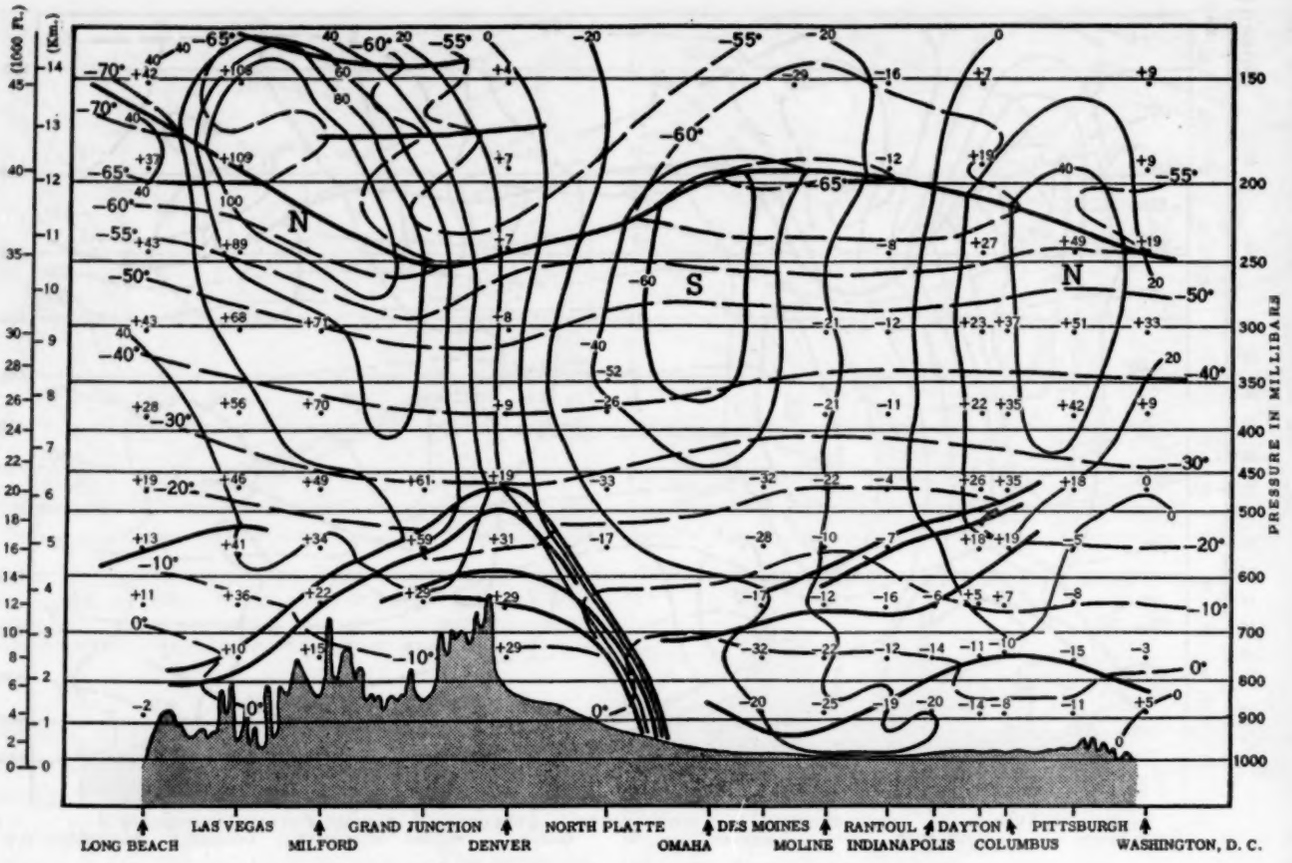

FIGURE 9.—Cross-section at 1500 GMT on February 19, 1954.

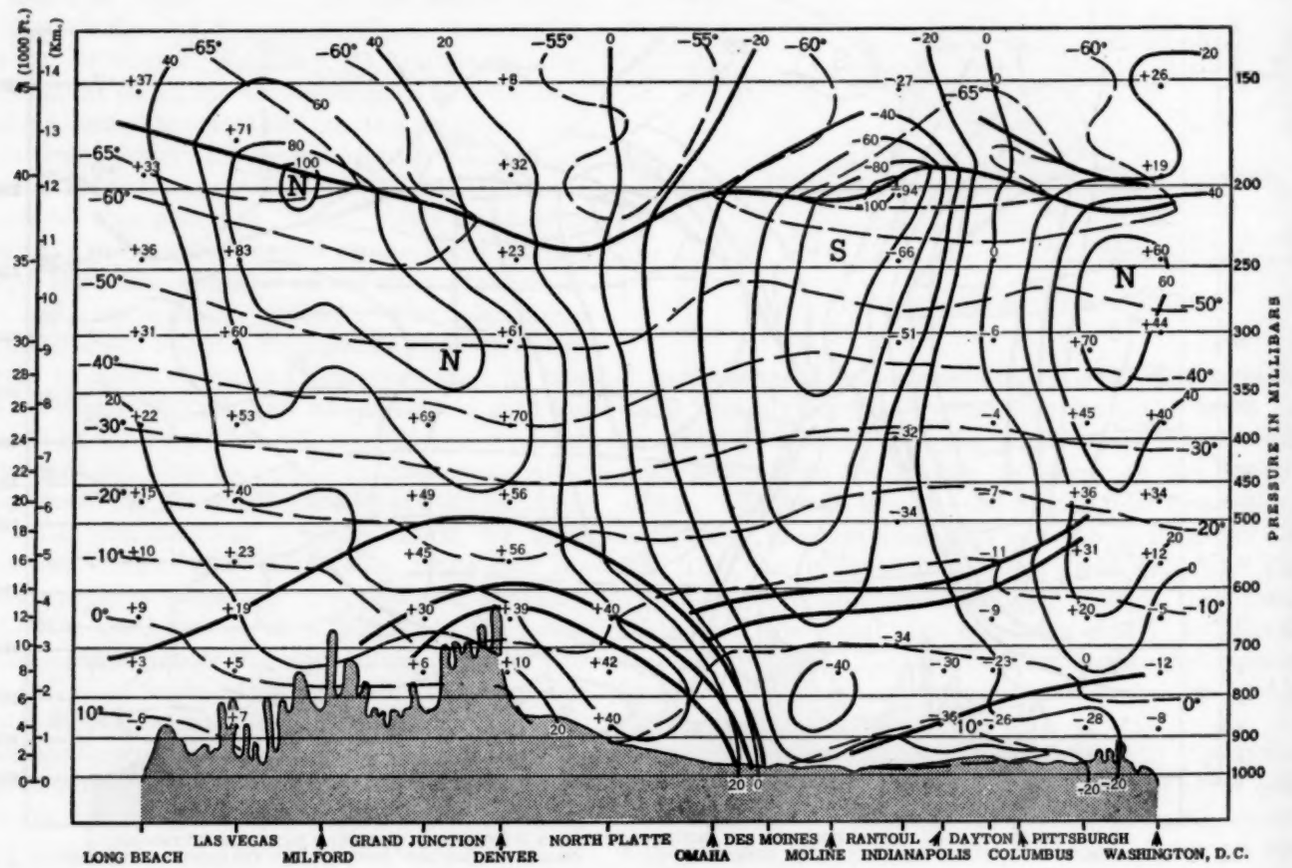

FIGURE 10.—Cross-section at 0300 GMT on February 20, 1954.

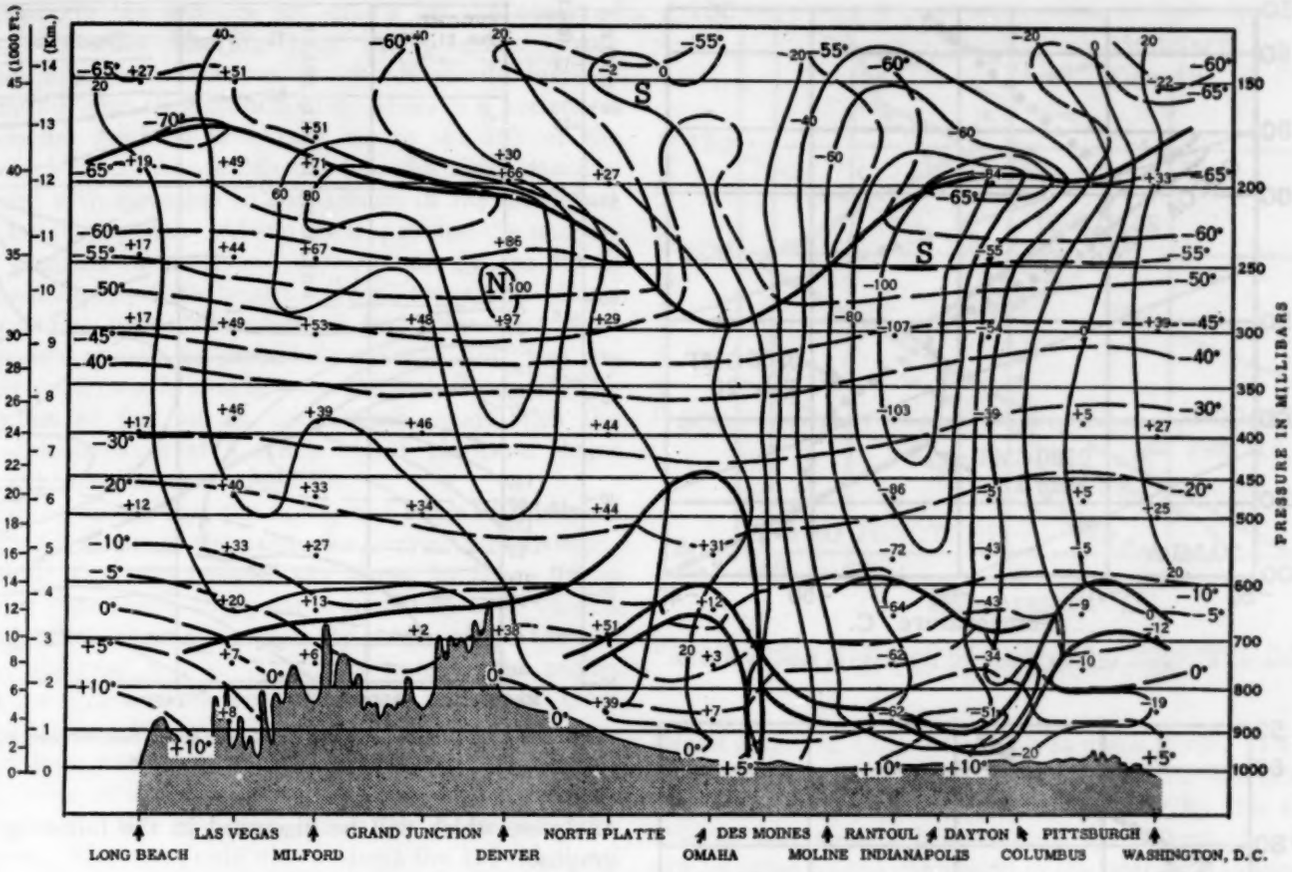

FIGURE 11.—Cross-section at 1500 GMT on February 20, 1954.

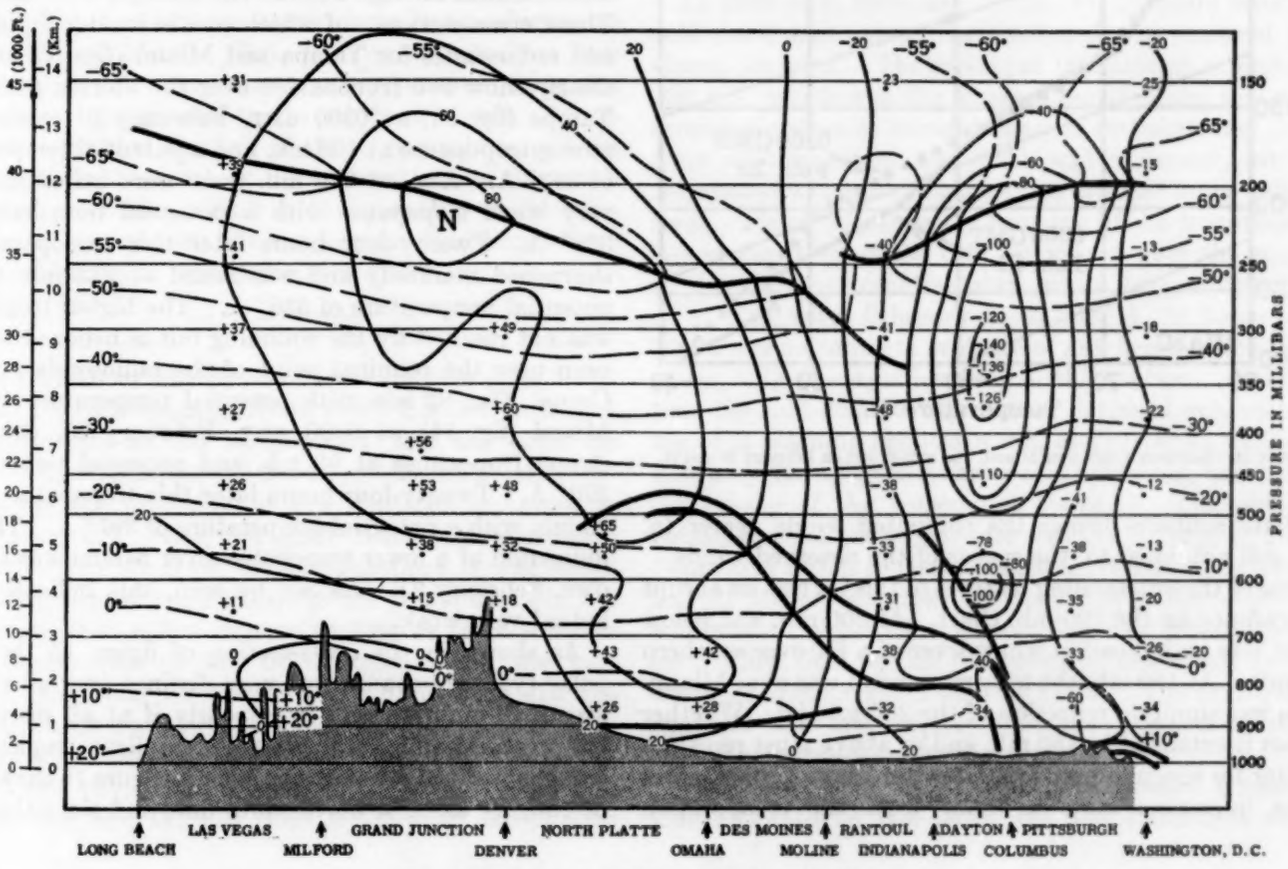

FIGURE 12.—Cross-section at 0300 GMT on February 21, 1954.

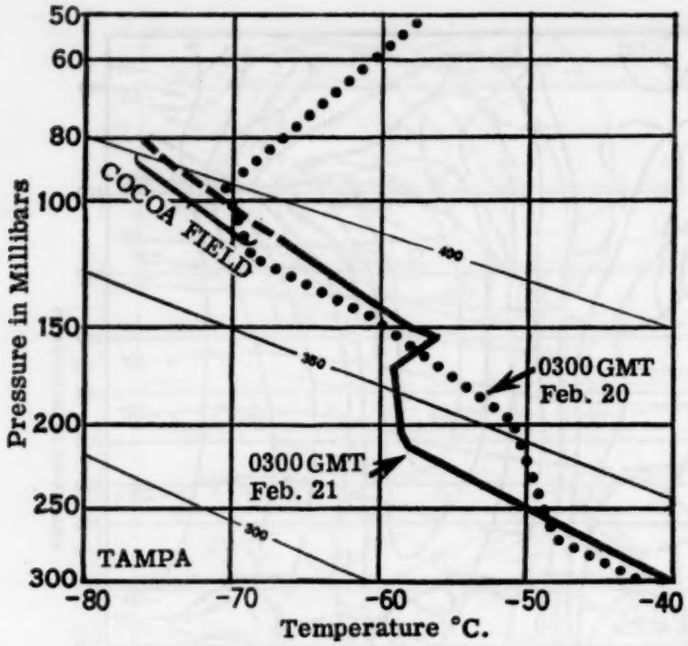

FIGURE 13.—Radiosonde data over Tampa, Fla. at 0300 GMT on February 20 and 21.

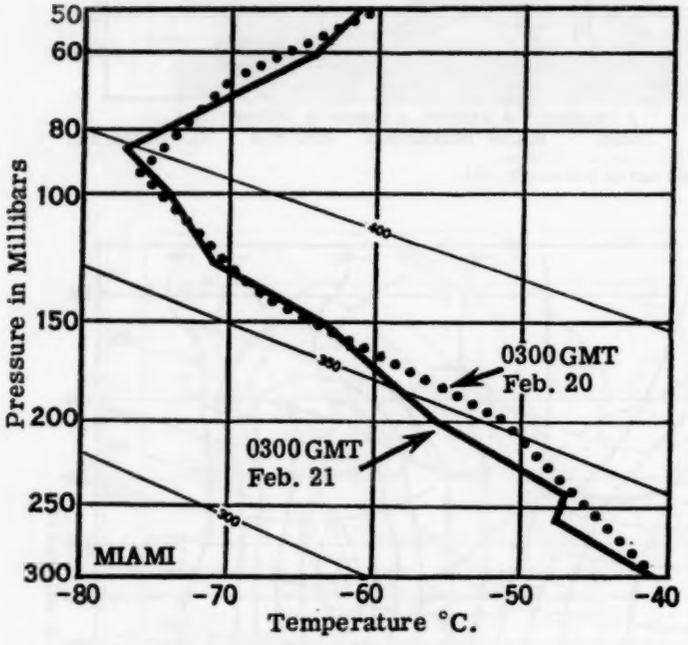

FIGURE 14.—Radiosonde data over Miami, Fla. at 0300 GMT on February 20 and 21.

mediate contours brings the computed winds nearer to, but still not equal to, the speeds of the observed winds.

One of the outstanding features of this jet was its abrupt appearance on the 200-mb. chart. At 300 mb. and below there was no indication whatsoever of a jet over southern Florida. At 150 mb. the maximum wind was over Miami. This was simply a reflection of the 200-mb. jet. Whether or not it extended to 150 mb. and/or above must remain a matter for speculation due to the sparseness of data. Yet some inferences may be made from the cross-section

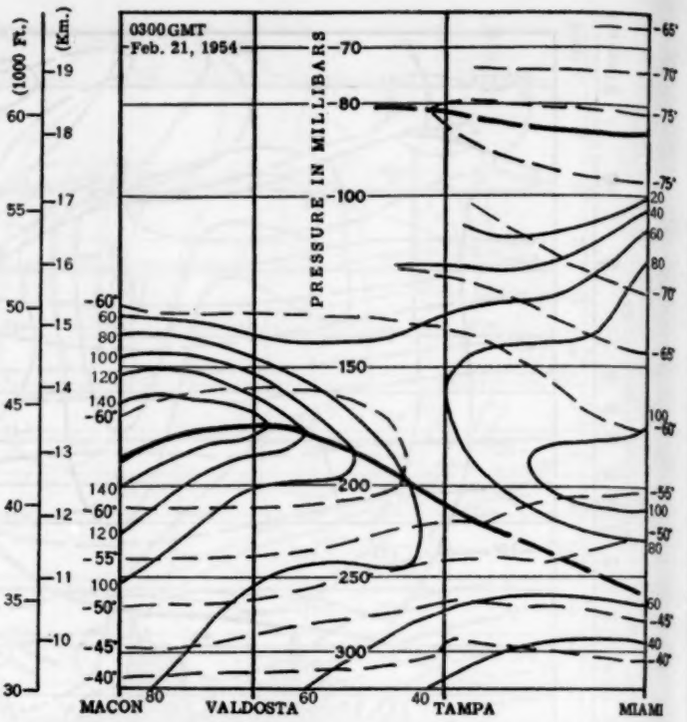

FIGURE 15.—Cross-section over Florida and Georgia at 0300 GMT, February 21, showing tropical and polar type tropopauses.

analyses, which will be discussed in the following paragraphs.

In the search for a logical explanation of this jet several cross-sections through Florida and Georgia were analyzed. These cross-sections (of which one is included (fig. 15)) and radiosondes for Tampa and Miami (figs. 13 and 14) clearly show two tropopauses over the Florida peninsula. Tampa (fig. 13) at 0300 GMT, February 20 exhibited a strong tropopause at 100 mb. and a potential temperature of 393° A. Also, at 270 mb. there were indications of a very weak tropopause with a potential temperature of 328° A. Twenty-four hours later this tropopause had sharpened markedly and was found at 210 mb. with a potential temperature of 336° A. The higher tropopause was not reached by the sounding but is believed to have been near the terminal point of the radiosonde taken at Cocoa, Fla., 82 mb. with potential temperature 405° A. Miami (fig. 14) at 0300 GMT, February 20, showed a strong tropopause at 95 mb. and potential temperature 390° A. Twenty-four hours later this tropopause was at 85 mb. with a potential temperature of 397° A. The first indication of a lower tropopause over Miami was at 0300 GMT, February 21. As can be seen, this indication was indeed very weak.

As shown in the cross-section of figure 15 the lower polar type tropopause was very distinct over all stations except Miami, where it was poorly if at all discernible. However, Miami did exhibit an excellent tropical type tropopause at 85 mb. (see fig. 14). In figure 15 the stations lie roughly along a north-south line, and since the winds

were westerly the isotachs are drawn for the observed winds, westerlies blowing into the diagram. From thermal wind considerations the winds should increase with height over the stations where there is a horizontal temperature gradient with cold air to the left of the observed winds. Above Macon, Ga. the winds steadily increased with elevation to a maximum of 158 knots just below the tropopause. Above the tropopause the temperature gradient reversed and correspondingly the winds decreased rapidly with height. Over Tampa and Miami the strongest winds were located just above the polar tropopause, which, as previously pointed out, was extremely weak over Miami but marked over Tampa. The association of this jet on the 200-mb. chart with the tropical tropopause at a much higher elevation seems likely at a more southerly latitude.

It can be shown that the northward bulge of this wind maximum was due to the particular temperature distribution along the tropopauses. As shown in figure 15 at 200 mb., just above the polar tropopause, over Tampa and Miami there was considerably colder air to the left of the observed winds. This was roughly the region where the bulge in the wind maximum occurred. Over Tampa between 200 and 150 mb. the horizontal temperature gradient was very flat and the maximum maintained itself. Over Miami the horizontal temperature gradient reversed near 180 mb. and the winds decreased with elevation. However, only above about the 115-mb. level did the winds begin to fall off very rapidly with height. The reason for this lag in wind decrease from 180 to 115 mb. is difficult to explain, particularly in the absence of data south of Miami. But, it does appear from this cross-section that there was another jet core along the high tropical tropopause to the south of Miami. Moreover, it seems that the axis of this core would have been oriented from the north at lower elevations to the south at higher elevations. Such a configuration would have been in agreement with the temperature field imposed by a high cold tropical tropopause.

TROPOPAUSE

The analysis of this series of cross-sections (figs. 7–12) presented a good opportunity to study the fluctuations of the tropopause as the surface Low and the polar air behind it moved across the country. As the polar tropopause was the predominant one over the cross-section throughout this series, we shall center the discussion around it. In studying the cross-sections it was found that the potential temperature of the tropopause did not vary more than a few degrees as long as there were no large fluctuations of the tropopause. When the cold dome of the polar air mass became quite deep and the tropopause lowered above this dome, the potential temperature of the tropopause decreased as much as 25° C.

At 1500 GMT, February 18 (fig. 7) the tropopause west of Rantoul, Ill. was close to 200 mb. except over

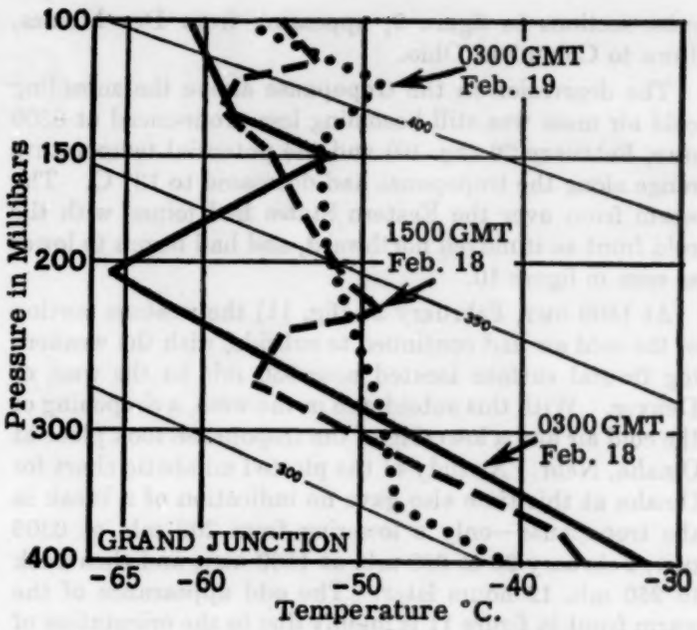

FIGURE 16.—Radiosonde data from Grand Junction, Colo. at 0300 and 1500 GMT on February 18 and 0300 GMT on February 19, 1954.

Grand Junction, Colo. where it was much lower. Twelve hours previous (see fig. 16) it had been near 200 mb. at that station also, but had begun to lower by this time. Cooling had already begun above the 750-mb. level, as can be noted by the depression in the isotherms in figure 7 at Grand Junction.

At 0300 GMT, February 19 (fig. 8), 12 hours later, the cold dome had moved eastward and was centered near Grand Junction. The cooling at that station extended to 320 mb., which was the greatest height along this cross-section in the series to which the cold air penetrated. The front at this height was weak and indistinct, but the tropopause was quite sharp, having lowered to the 350-mb. level. Figure 16 shows the lowering of the tropopause at Grand Junction as the cold air moved over the station. In this case the potential temperature dropped from 325° A. at 0300 GMT, February 18 to 303° A. 24 hours later. There was no concrete evidence of any break in the tropopause, only the rapid lowering of this surface. After this time the cold dome at the surface flattened out, with the top of it reaching about 470 mb. at Denver at 1500 GMT, February 19. Figure 9 shows this flattening, and with it the raising of the tropopause above it. The potential temperature of the tropopause still had a range of 25° C. from Long Beach to Grand Junction, but over the eastern half of the cross-section the potential temperature was within 5° C. of 330° A. A secondary cold front appeared for the first time on this cross-section, and slowly became the more pronounced of the two fronts. The isotherms in figure 12 bear this out, and show that the first front had almost completely frontolized by this time.

The warm front which moved northward across the Eastern States in this series was first discernible on the

cross-sections in figure 9, appearing from Des Moines, Iowa to Columbus, Ohio.

The depression in the tropopause above the subsiding cold air mass was still becoming less pronounced at 0300 GMT, February 20 (fig. 10) and the potential temperature range along the tropopause had decreased to 13° C. The warm front over the Eastern States had joined with the cold front as it moved northward, and had begun to lower as seen in figure 10.

At 1500 GMT, February 20 (fig. 11) the western portion of the cold air had continued to subside, with the weakening frontal surface located near 650 mb. to the west of Denver. With this subsidence in the west, a deepening of the cold air and a lowering of the tropopause took place at Omaha, Nebr. A study of the plotted adiabatic chart for Omaha at this time also gave no indication of a break in the tropopause—only a lowering from 200 mb. at 0300 GMT, February 20 to 300 mb. at 1500 GMT, and then back to 250 mb. 12 hours later. The odd appearance of the warm front in figure 11 is mainly due to the orientation of the cross-section with respect to the warm front. The front was roughly parallel to and just south of the cross-section from Illinois to southeastern Ohio, where it turned southward to the Atlanta, Ga. area and then northeastward to Norfolk, Va.; that is, the front was retarded in its northward movement by the Appalachians. By 0300 GMT, February 21 (fig. 12) the warm front had almost moved off the cross-section, with only Washington, D. C. remaining in the cold air (see fig. 3).

The only tropopause break in the series was found over Rantoul, Ill. at 0300 GMT, February 21 where the upper air sounding indicated a double break in the lapse rate. In itself, this sounding was not a clear-cut case, but the ones taken 12 hours later at Rantoul and Dayton, Ohio did indicate an overlapping of the tropopause.

When analyzing tropopause charts, quite often there is a tendency to draw too many break-lines*, where two tropopauses overlap each other. In figure 8 the tropopause had a steep slope on each side of Grand Junction, where the cold dome was centered, and a potential temperature decrease of about 30° C. from Long Beach to Grand Junction. This was a lowering in the tropopause of 12,000 feet in 24 hours at Grand Junction, and presented a temptation to encircle the latter station with a break-line. It is the opinion of the authors and others after careful study of the plotted adiabatic charts, that there was no break in the tropopause, but only the steep slope as pictured. Figure 11 shows this same dip in the tropopause, but to a lesser degree. This phenomenon can evidently be expected over deep cold domes. Careful study should be given to individual raobs, the polar front, and the high level isotach analyses before break-lines are entered on a tropopause analysis.

*For an explanation of "break-lines" the reader is referred to [4].

SUMMARY

As the storm moved across the country the incoming or northwesterly core of the jet stream slowly weakened from about 140 knots to about 70 knots and lowered from 200 mb. in figure 7 to about 350 mb. in figure 12. The new jet core which appeared at 175 mb. over Las Vegas, Nev. in figure 9 also lowered and weakened slowly during the series. After the surface Low became organized, the returning southerly core of the jet also lowered in height from 230 mb. in figure 8 to about 320 mb. in figure 12. The increase of the southerly wind speed normal to the cross-section was approximately equal to the decrease of the northerly wind speed during the series; i. e., from about 70 to 140 knots. This shows the jet maximum moving along the jet stream and around the upper air trough.

The smallest variation in space of the height of the polar tropopause was 8,000 feet at 0300 GMT, February 20 (fig. 10) when it was at 43,000 feet over Long Beach, Calif. and 35,000 feet over North Platte, Nebr. The greatest variation occurred in association with the deep cold dome 24 hours earlier (fig. 8) when the tropopause had lowered to 40,000 feet at Long Beach and to 26,000 feet at Grand Junction, a variation of 14,000 feet.

While the jet stream, tropopause, and general synoptic conditions may at times appear to be at wide variance with generally accepted models, a careful analysis of the data in this study leads to the conclusion that the current popular models [2, 3] suffice very nicely to explain situations that may at first glance appear to be inconsistent. This is not to imply that all present ideas are in agreement or that all or any one may be taken as the ultimate answer. Undoubtedly, as the science of meteorology progresses, refinements and revisions will be incorporated into the various models, and at times some models will best fit one type of situation, while at other times another model will be more applicable.

ACKNOWLEDGMENTS

The authors wish to thank Mr. F. W. Burnett and Mr. J. Vederman for their many helpful suggestions and review of this article.

REFERENCES

1. H. Riehl and S. Teweles, Jr., "A Further Study of the Relation between the Jet Stream and Cyclone Formation," *Tellus*, vol. 5, No. 1, Feb. 1953, pp. 66–79.
2. N. A. Alaka, C. L. Jordan, and R. J. Renard, "The Jet Stream," *NAVAER* 50-IR-249, June 1, 1953, pp. 40–41.
3. E. Palmén, "The Aerology of Extratropical Disturbances," *Compendium of Meteorology*, American Meteorology Society, Boston, 1951, pp. 599–620.
4. Air Weather Service, "Tropopause Analysis and Forecasting," *Air Weather Service Technical Report* 105-86, March 1952, 31 pp.

U. S. GOVERNMENT PRINTING OFFICE: 1954

Chart I. A. Average Temperature (°F.) at Surface, February 1954.

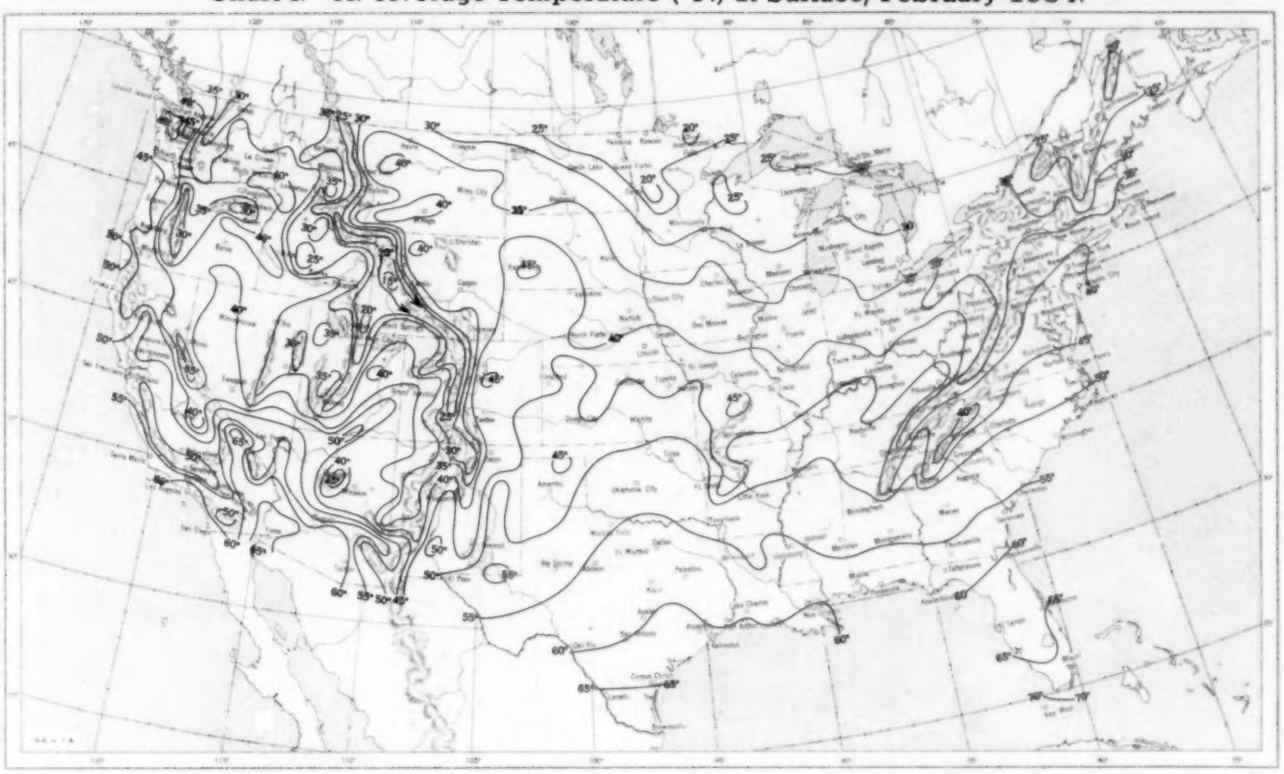

B. Departure of Average Temperature from Normal (°F.), February 1954.

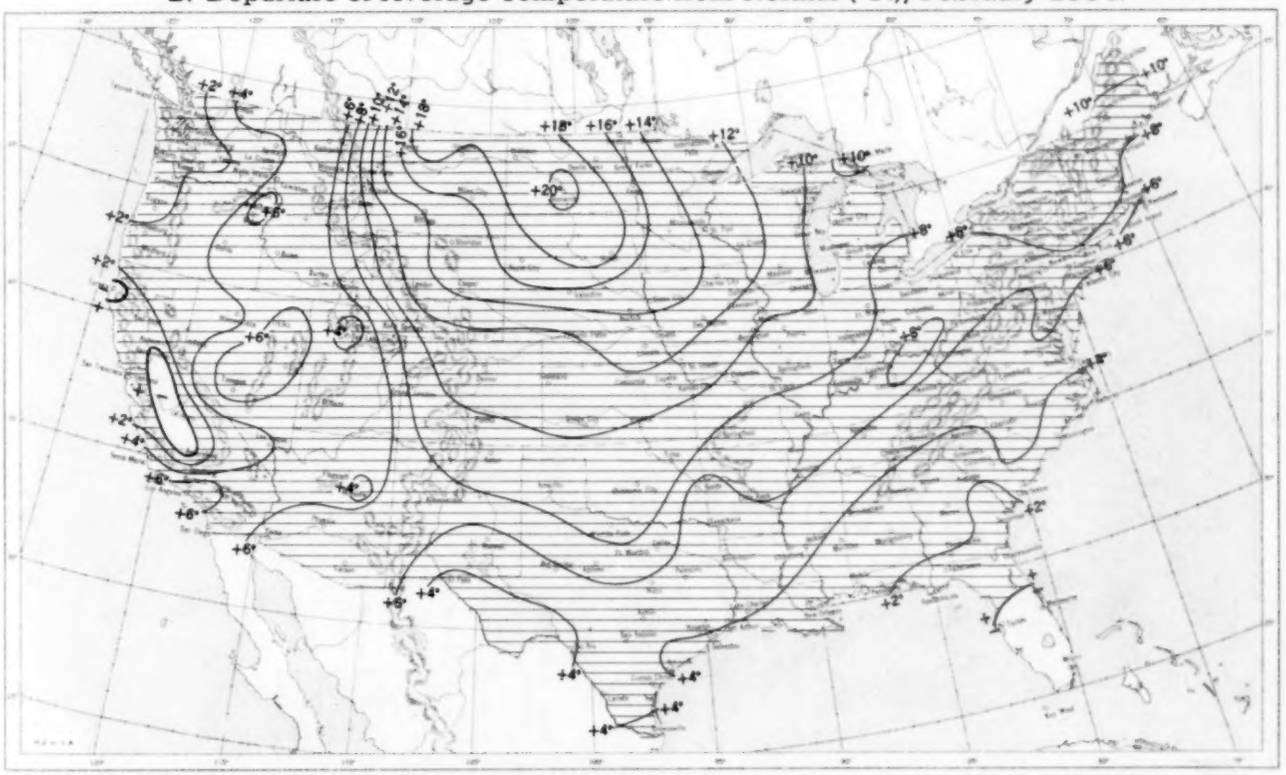

A. Based on reports from 800 Weather Bureau and cooperative stations. The monthly average is half the sum of the monthly average maximum and monthly average minimum, which are the average of the daily maxima and daily minima, respectively.
B. Normal average monthly temperatures are computed for Weather Bureau stations having at least 10 years of record.

Chart II. Total Precipitation (Inches), February 1954.

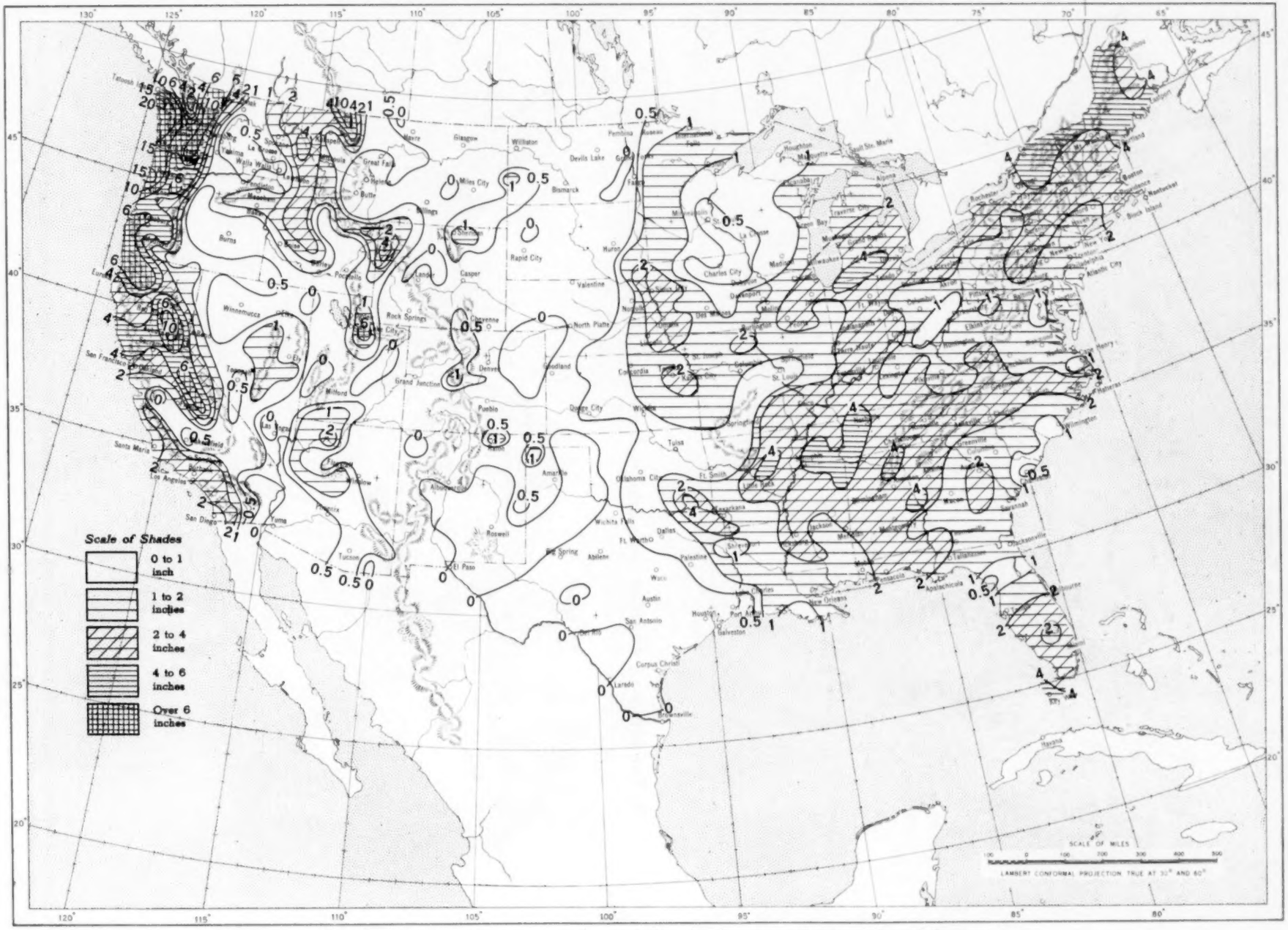

Based on daily precipitation records at 800 Weather Bureau and cooperative stations.

Chart III. A. Departure of Precipitation from Normal (Inches), February 1954.

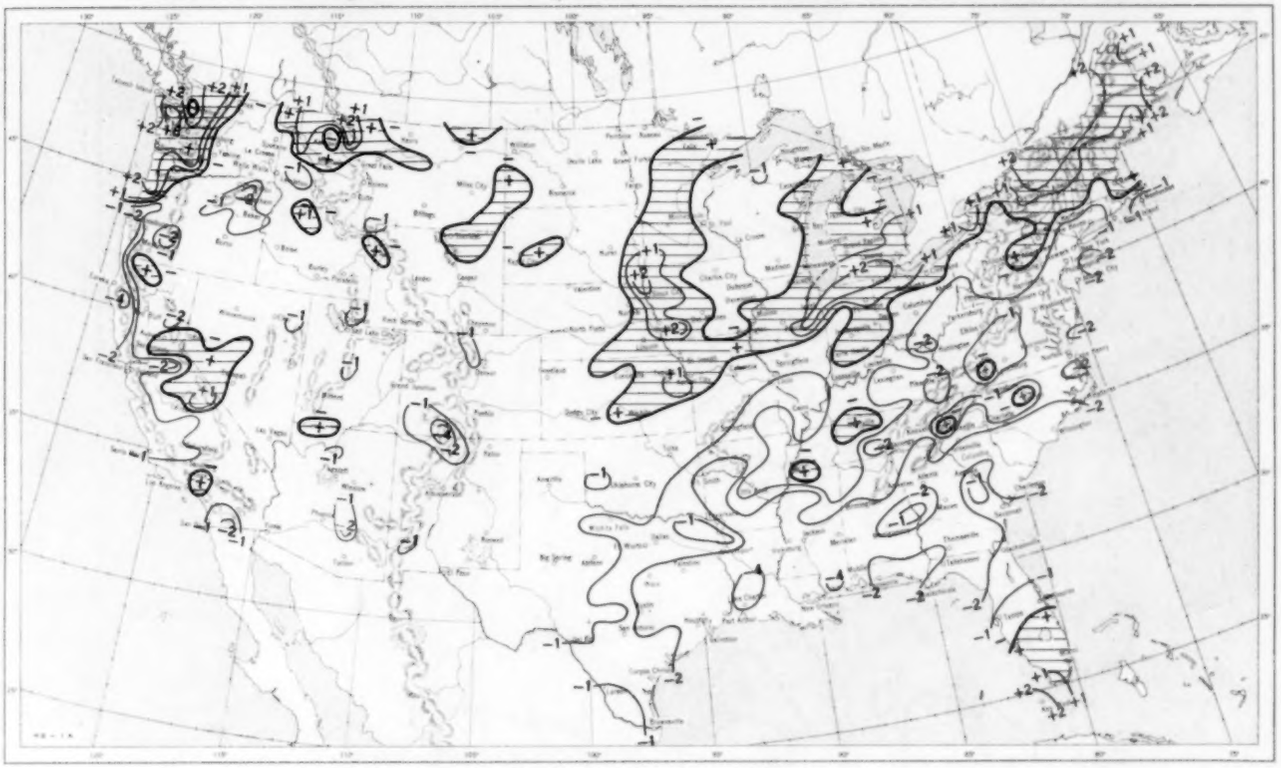

B. Percentage of Normal Precipitation, February 1954.

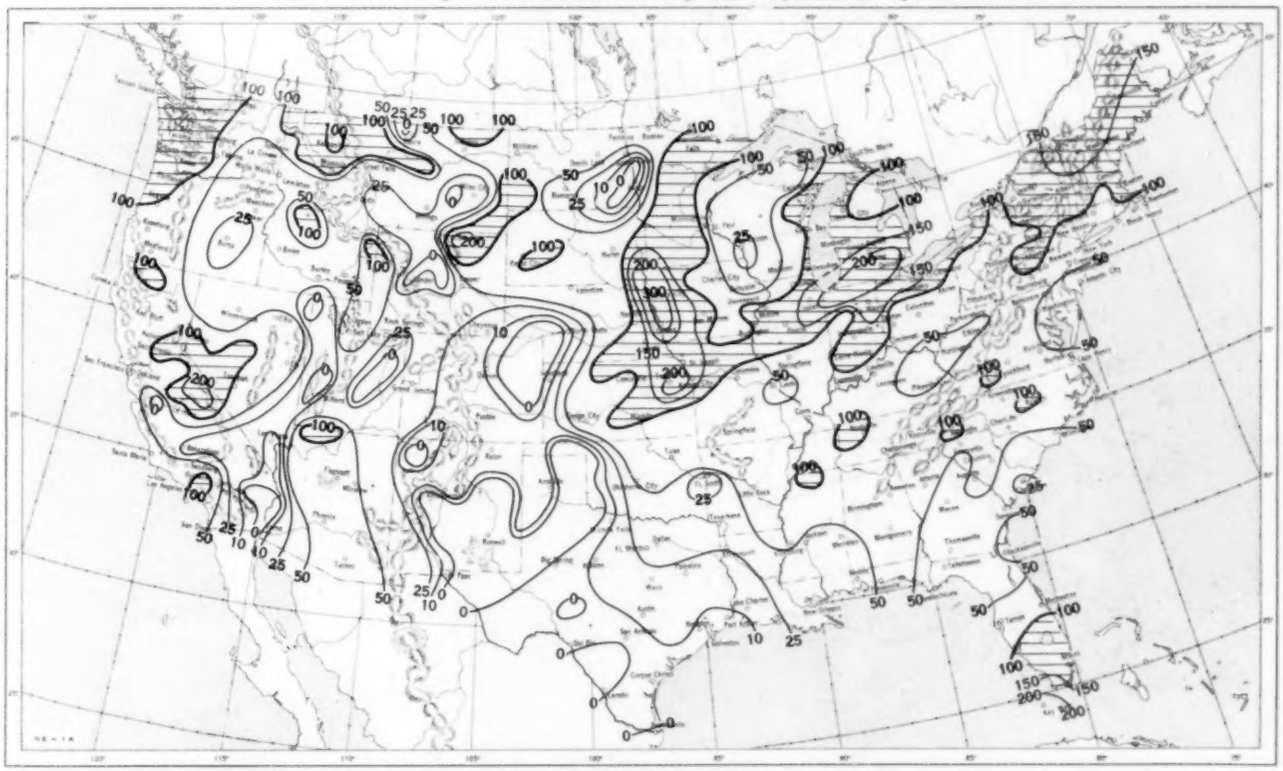

Normal monthly precipitation amounts are computed for stations having at least 10 years of record.

Chart IV. Total Snowfall (Inches), February 1954.

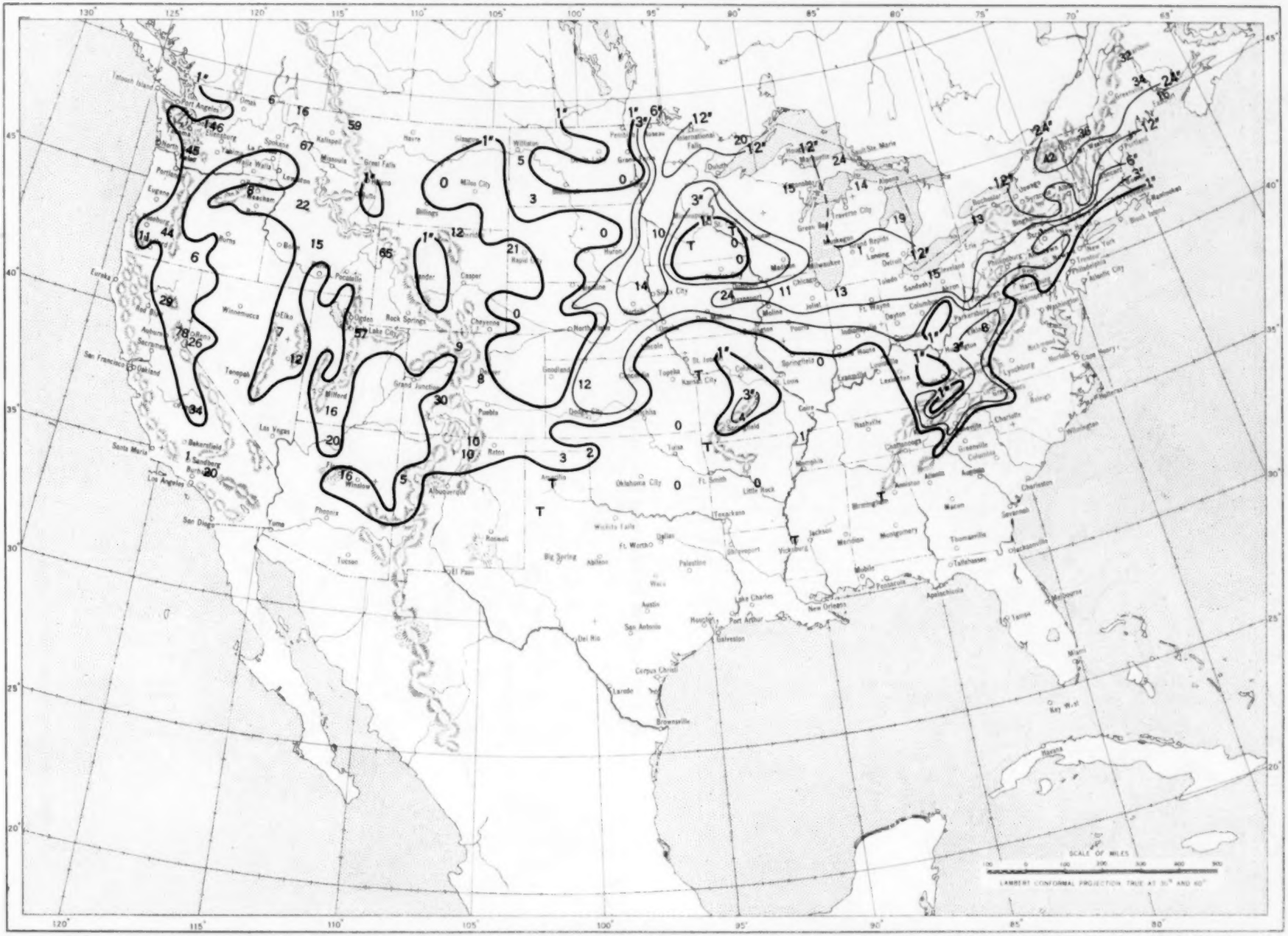

This is the total of unmelted snowfall recorded during the month at Weather Bureau and cooperative stations. This chart and Chart V are published only for the months of November through April although of course there is some snow at higher elevations, particularly in the far West, earlier and later in the year.

Chart V. A. Percentage of Normal Snowfall, February 1954.

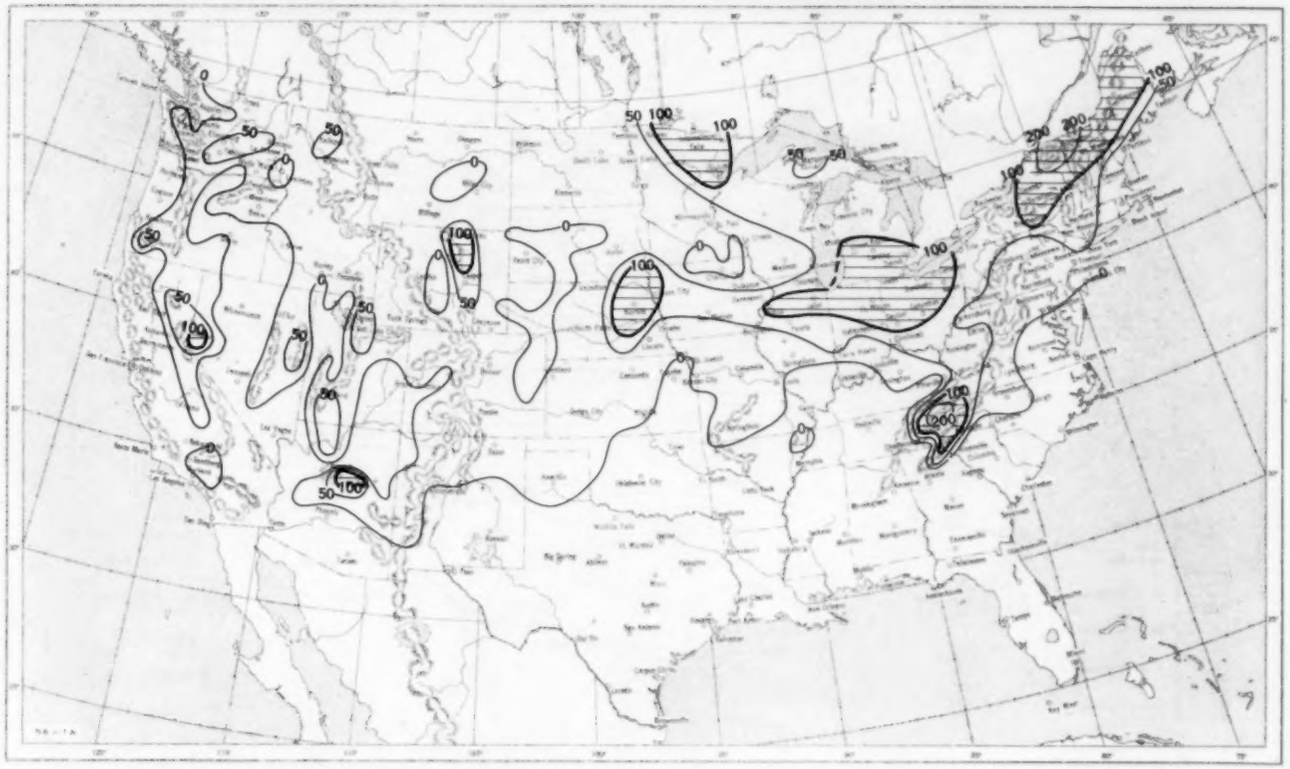

B. Depth of Snow on Ground (Inches), 7:30 a. m. E.S.T., February 23, 1954.

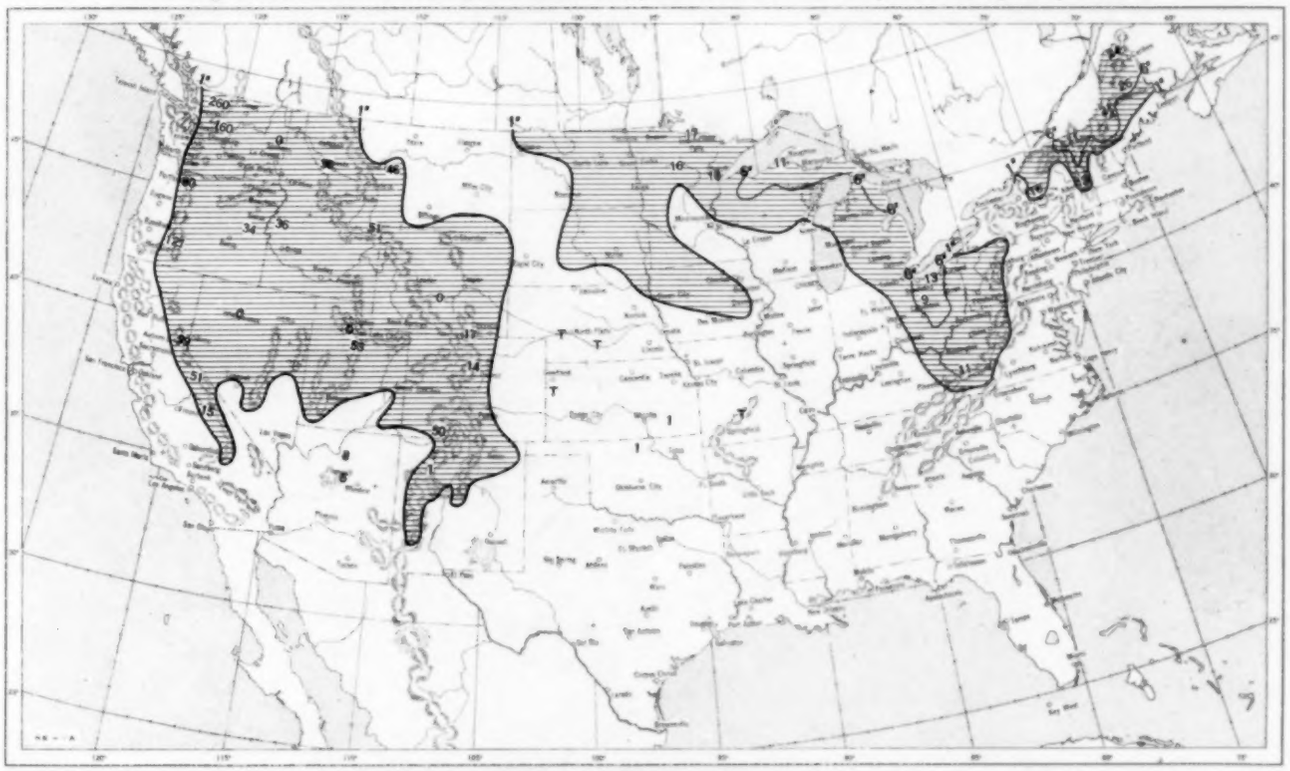

A. Amount of normal monthly snowfall is computed for Weather Bureau stations having at least 10 years of record. B. Shows depth currently on ground at 7:30 a.m. E.S.T., of the Tuesday nearest the end of the month. It is based on reports from Weather Bureau and cooperative stations. Dashed line shows greatest southern extent of snowcover during month.

Chart VI. A. Percentage of Sky Cover Between Sunrise and Sunset, February 1954.

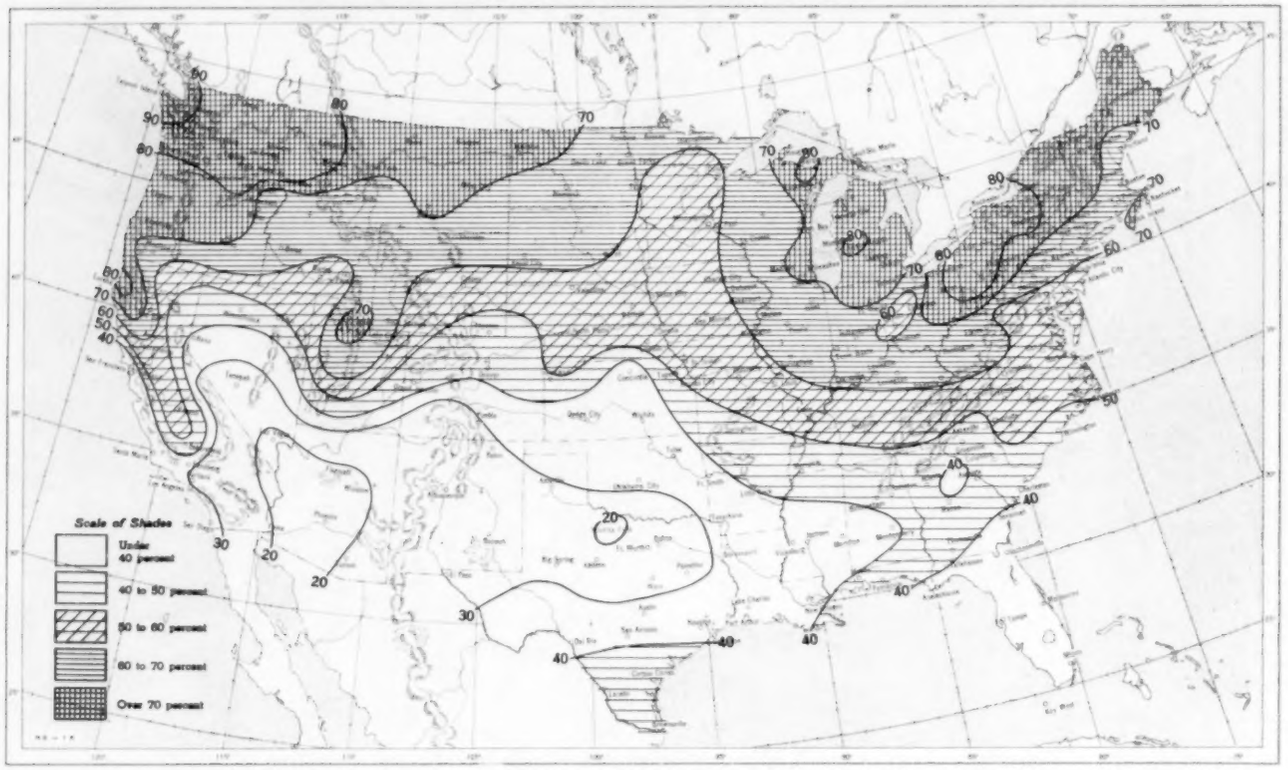

B. Percentage of Normal Sky Cover Between Sunrise and Sunset, February 1954.

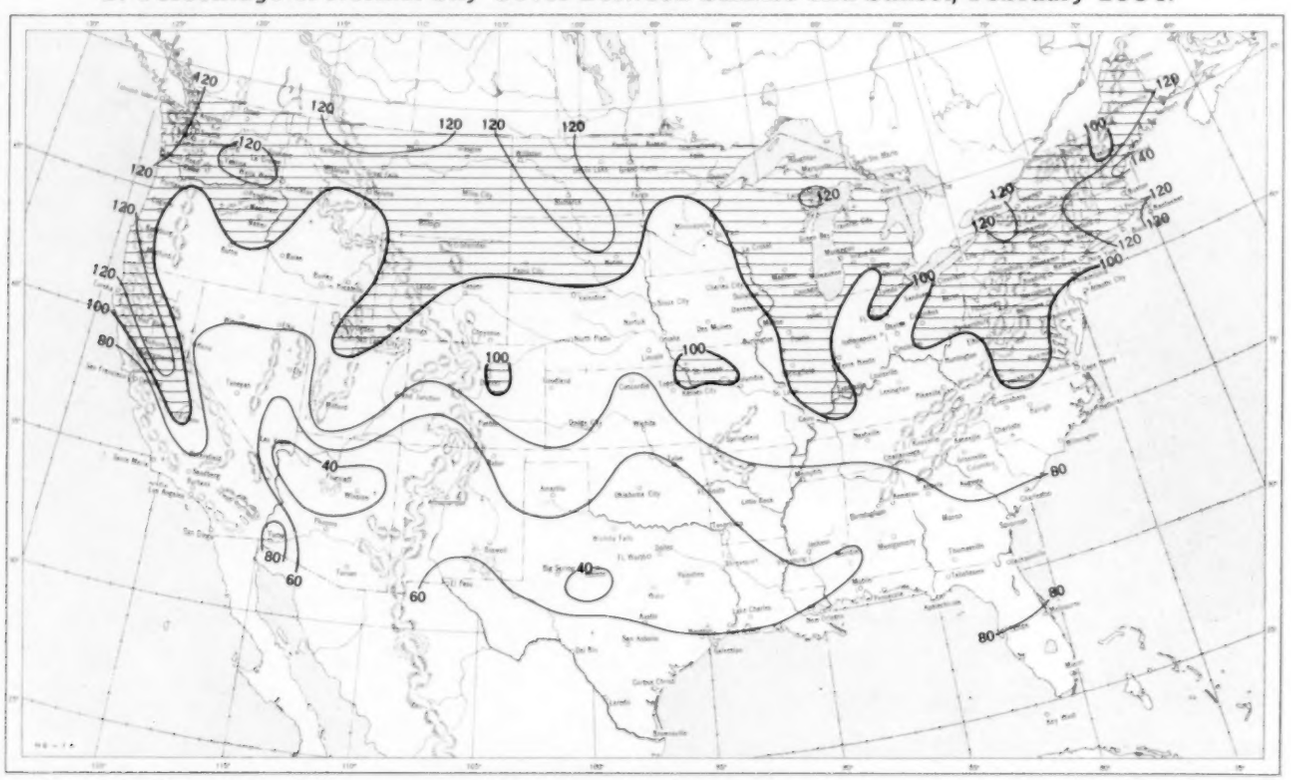

A. In addition to cloudiness, sky cover includes obscuration of the sky by fog, smoke, snow, etc. Chart based on visual observations made hourly at Weather Bureau stations and averaged over the month. B. Computations of normal amount of sky cover are made for stations having at least 10 years of record.

Chart VII. A. Percentage of Possible Sunshine, February 1954.

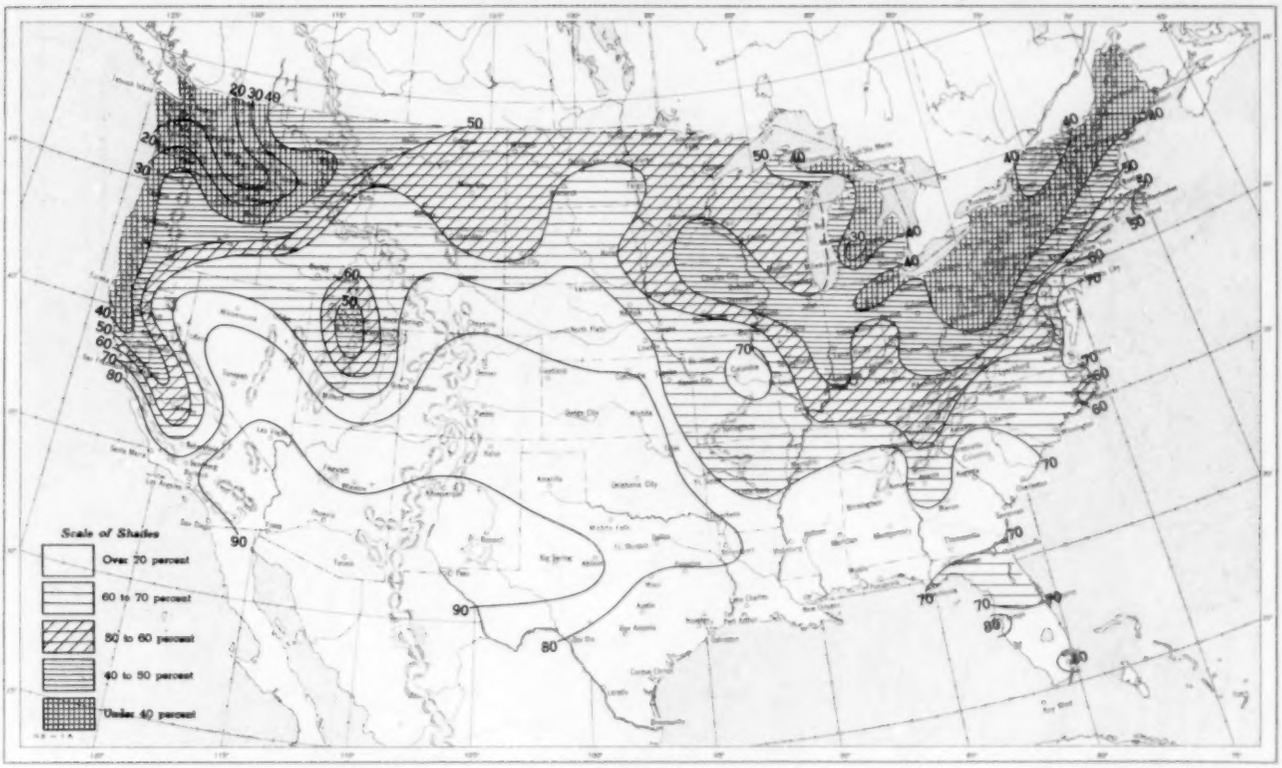

B. Percentage of Normal Sunshine, February 1954.

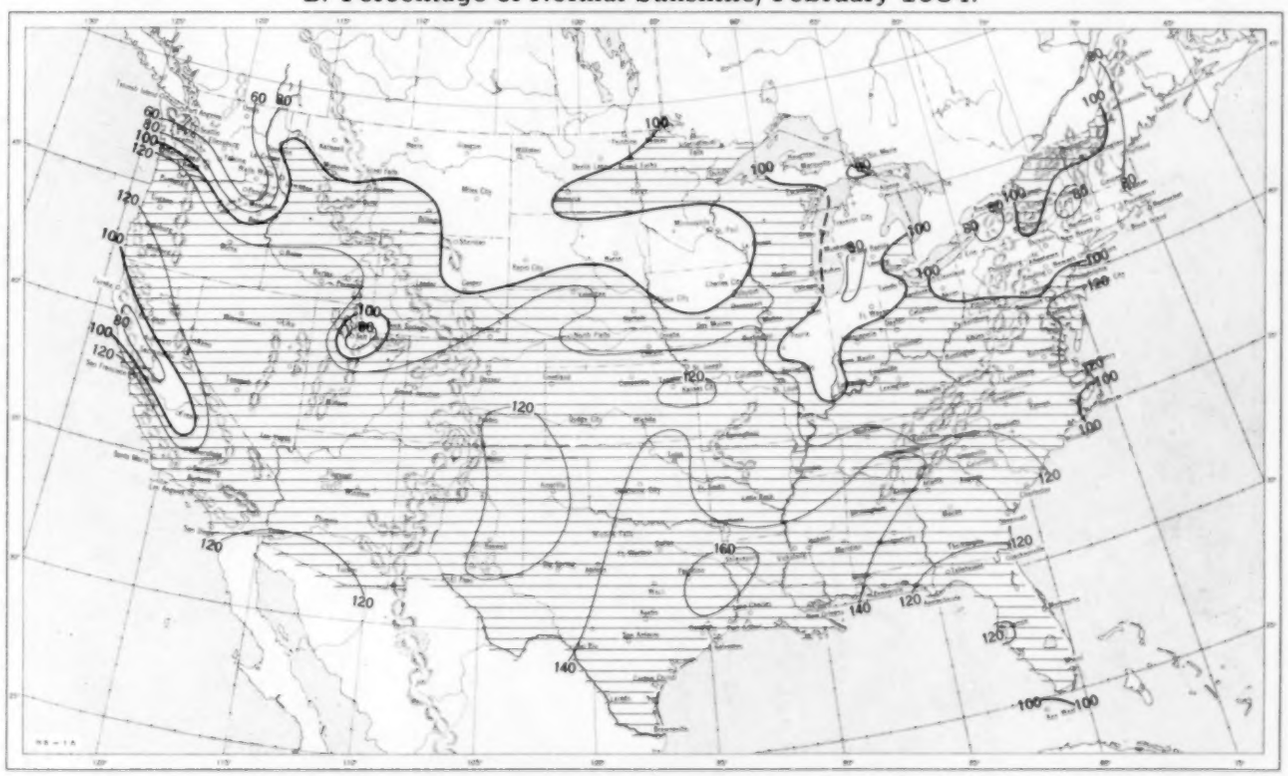

A. Computed from total number of hours of observed sunshine in relation to total number of possible hours of sunshine during month. B. Normals are computed for stations having at least 10 years of record.

Chart VIII. Average Daily Values of Solar Radiation, Direct + Diffuse, February 1954. Inset: Percentage of Normal Average Daily Solar Radiation, February 1954.

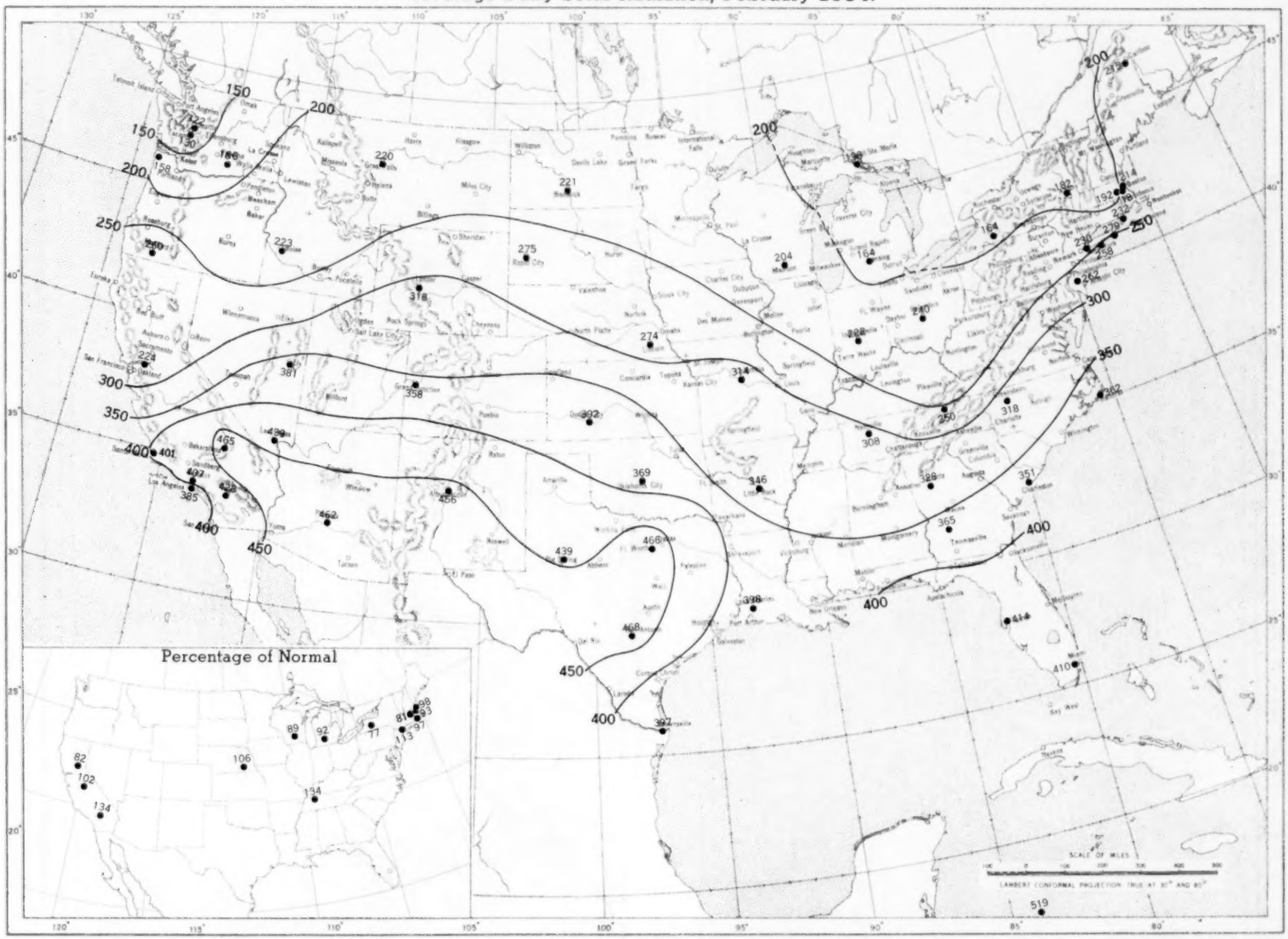

Chart shows mean daily solar radiation, direct + diffuse, received on a horizontal surface in langleys (1 langley = 1 gm. cal. cm. $^{-2}$). Basic data for isolines are shown on chart. Further estimates are obtained from supplementary data for which limits of accuracy are wider than for those data shown. Normals are computed for stations having at least 9 years of record.

Chart IX. Tracks of Centers of Anticyclones at Sea Level, February 1954.

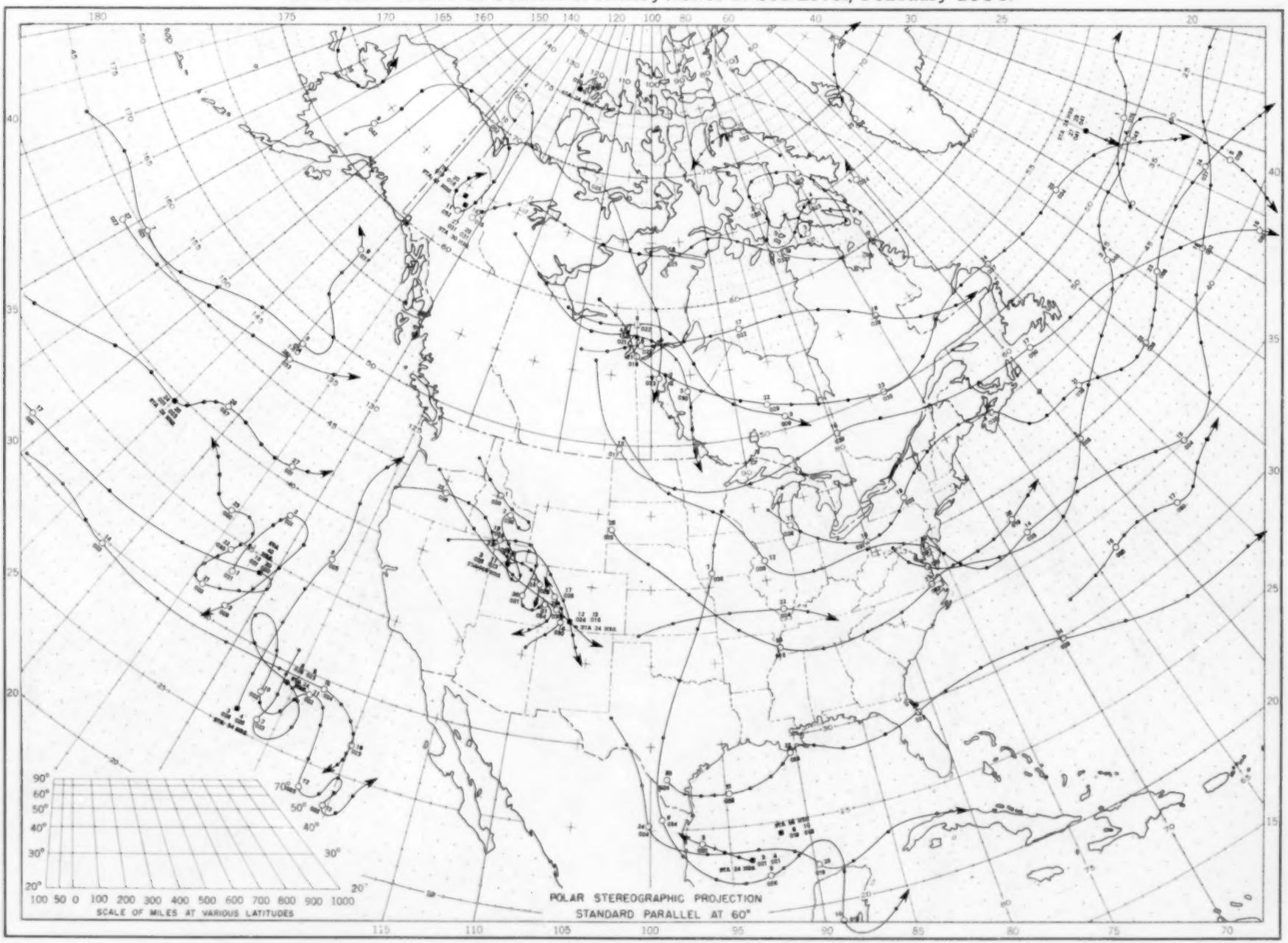

Circle indicates position of center at 7:30 a. m. E. S. T. Figure above circle indicates date, figure below, pressure to nearest millibar. Dots indicate intervening 6-hourly positions. Squares indicate position of stationary center for period shown. Dashed line in track indicates reformation at new position. Only those centers which could be identified for 24 hours or more are included.

Chart X. Tracks of Centers of Cyclones at Sea Level, February 1954.

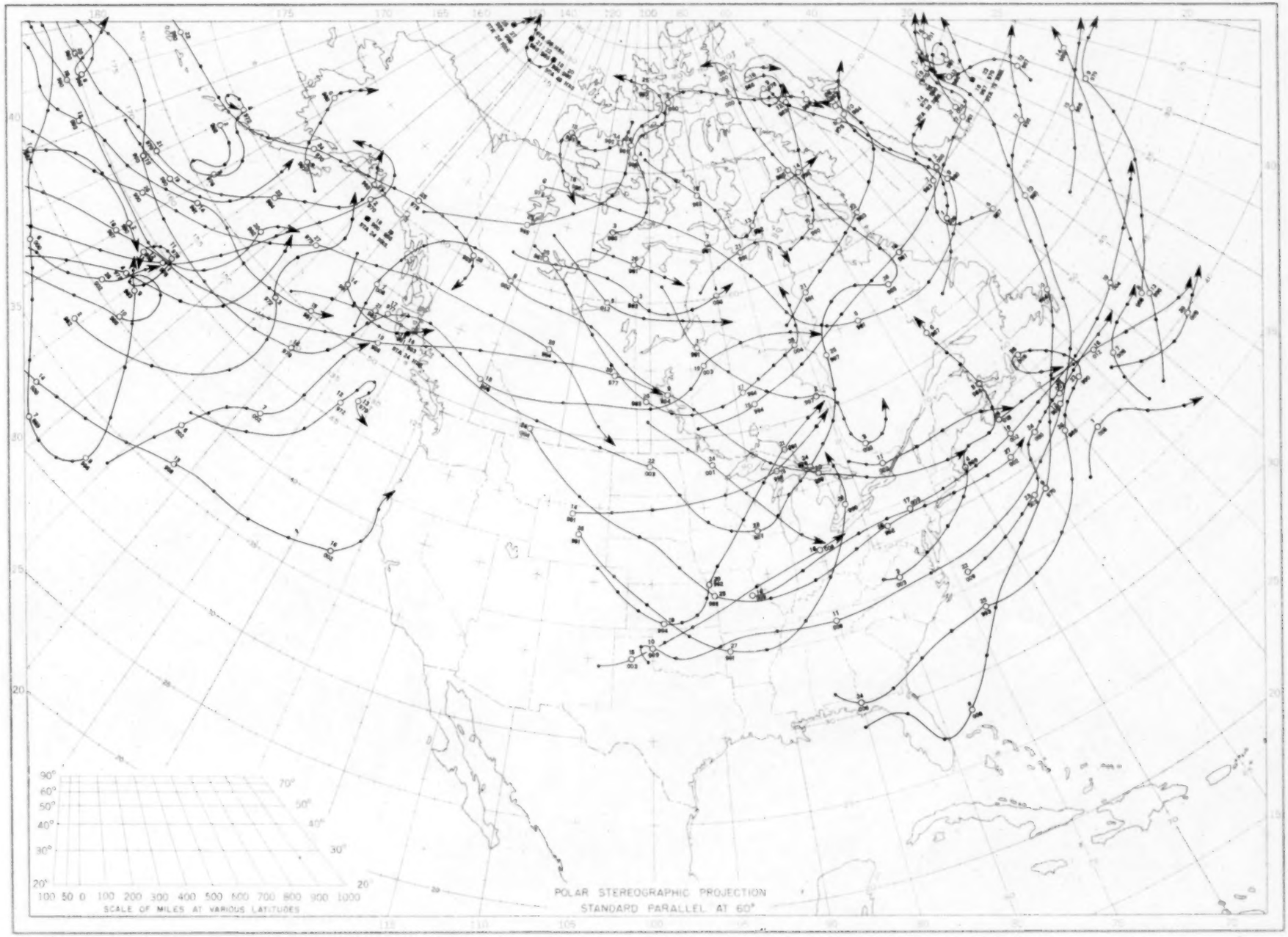

Circle indicates position of center at 7:30 a. m. E. S. T. See Chart IX for explanation of symbols.

Chart XI. Average Sea Level Pressure (mb.) and Surface Windroses, February 1954. Inset: Departure of Average Pressure (mb.) from Normal, February 1954.

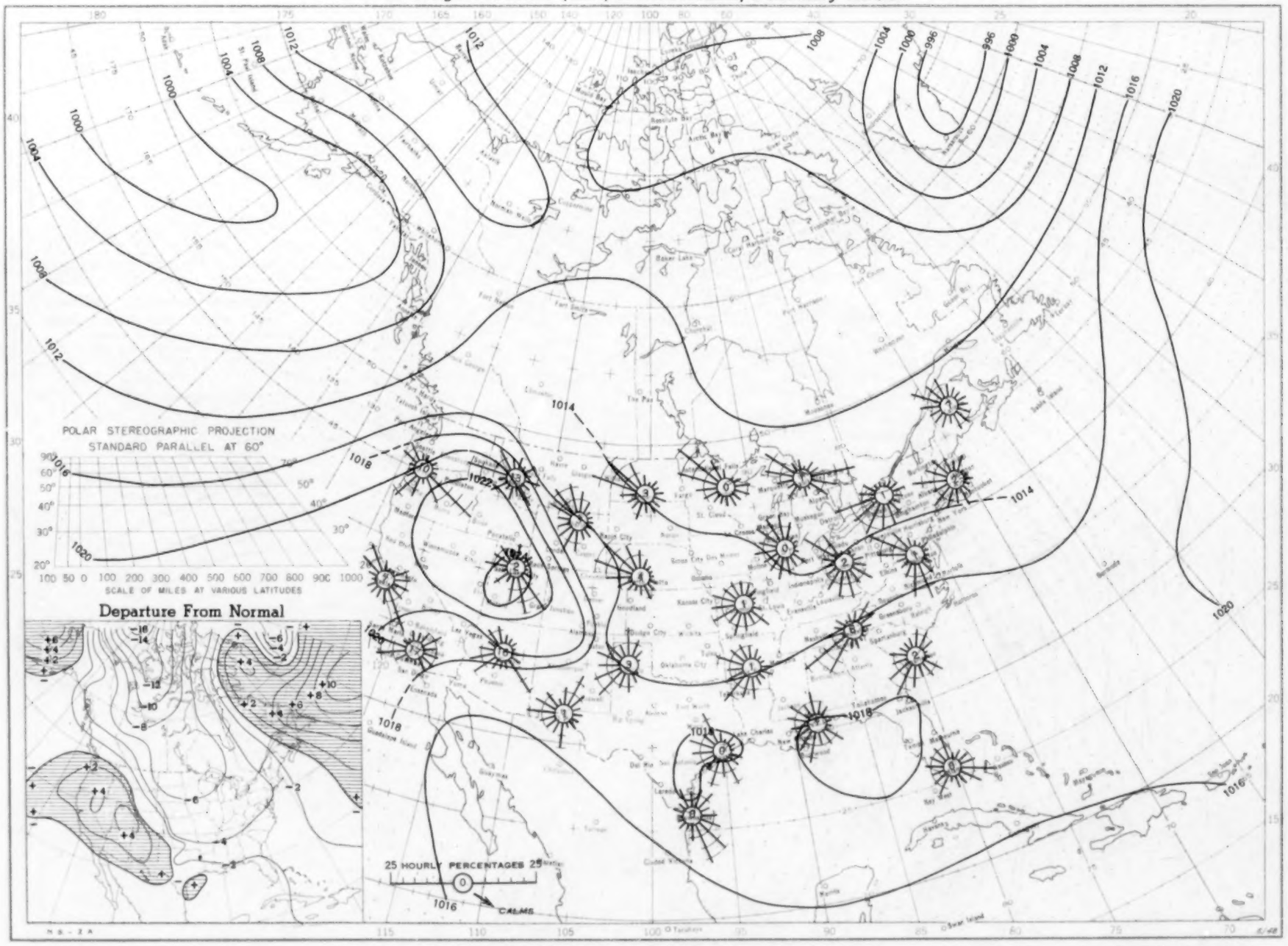

Average sea level pressures are obtained from the averages of the 7:30 a. m. and 7:30 p. m. E. S. T. readings. Windroses show percentage of time wind blew from 16 compass points or was calm during the month. Pressure normals are computed for stations having at least 10 years of record and for 10° intersections in a diamond grid based on readings from the Historical Weather Maps (1899-1939) for the 20 years of most complete data coverage prior to 1940.

Chart XII. Average Dynamic Height in Geopotential Meters (1 g.p.m. = 0.98 dynamic meters) of the 850-mb. Pressure Surface, Average Temperature in °C. at 850 mb., and Resultant Winds at 1500 Meters (m.s.l.), February 1954.

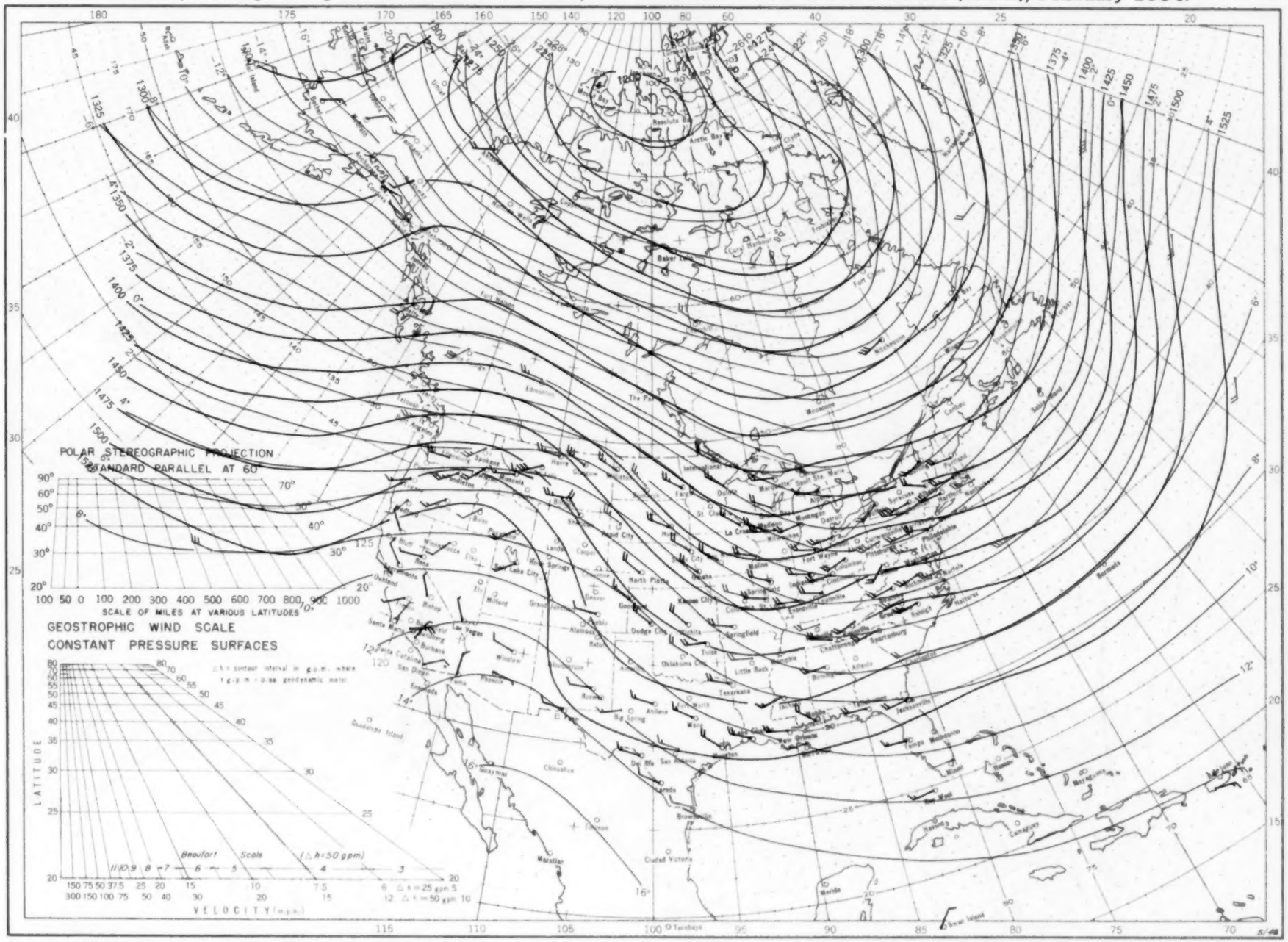

Contour lines and isotherms based on radiosonde observations at 0300 G. M. T. Winds shown in black are based on pilot balloon observations at 2100 G. M. T.; those shown in red are based on rawins taken at 0300 G. M. T. Wind barbs indicate wind speed on the Beaufort scale.

Chart XIII. Average Dynamic Height in Geopotential Meters (1 g.p.m.. = 0.98 dynamic meters) of the 700-mb. Pressure Surface, Average Temperature in °C. at 700 mb., and Resultant Winds at 3000 Meters (m.s.l.), February 1954.

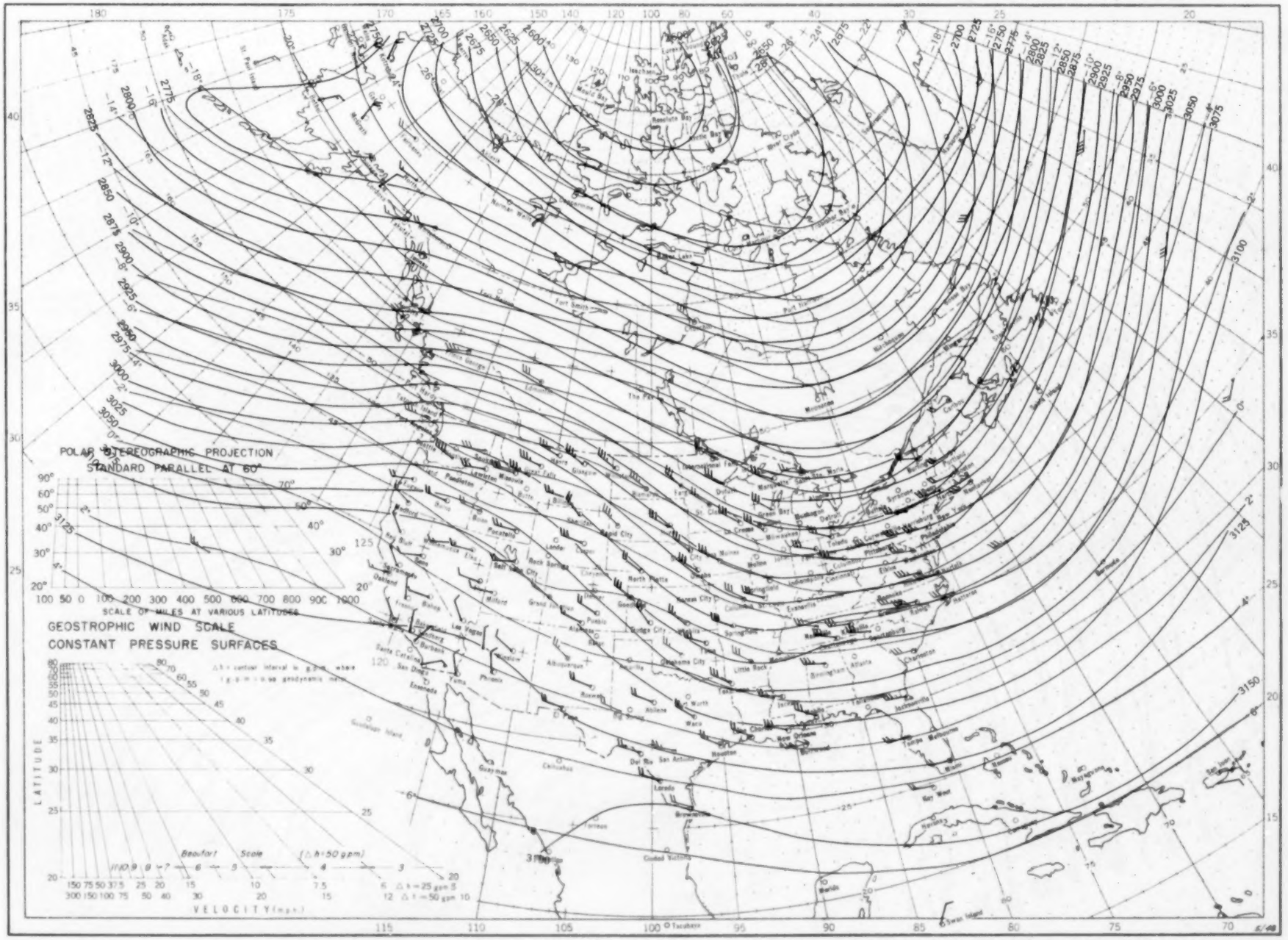

Contour lines and isotherms based on radiosonde observations at 0300 G. M. T. Winds shown in black are based on pilot balloon observations at 2100 G. M. T.; those shown in red are based on rawins taken at 0300 G. M. T. Wind barbs indicate wind speed on the Beaufort scale.

Chart XIV. Average Dynamic Height in Geopotential Meters (1 g.p.m. = 0.98 dynamic meters) of the 500-mb. Pressure Surface, Average Temperature in °C. at 500 mb., and Resultant Winds at 5000 Meters (m.s.l.), February 1954.

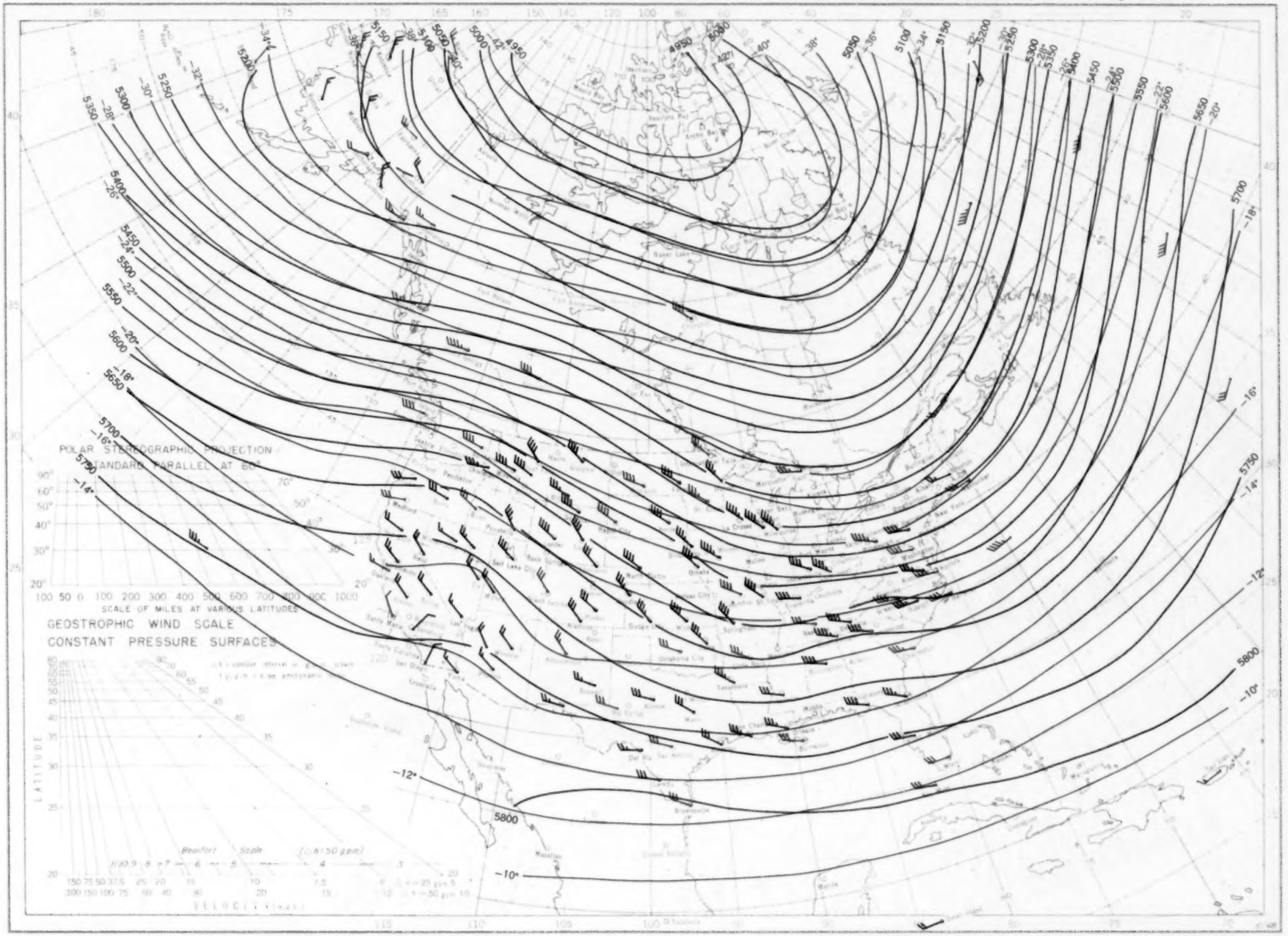

Contour lines and isotherms based on radiosonde observations at 0300 G. M. T. Winds shown in black are based on pilot balloon observations at 2100 G. M. T.; those shown in red are based on rawins at 0300 G. M. T. Wind barbs indicate wind speed on the Beaufort scale.

Chart XV. Average Dynamic Height in Geopotential Meters (1 g.p.m. = 0.98 dynamic meters) of the 300-mb. Pressure Surface, Average Temperature in °C. at 300 mb., and Resultant Winds at 10,000 Meters (m.s.l.), February 1954.

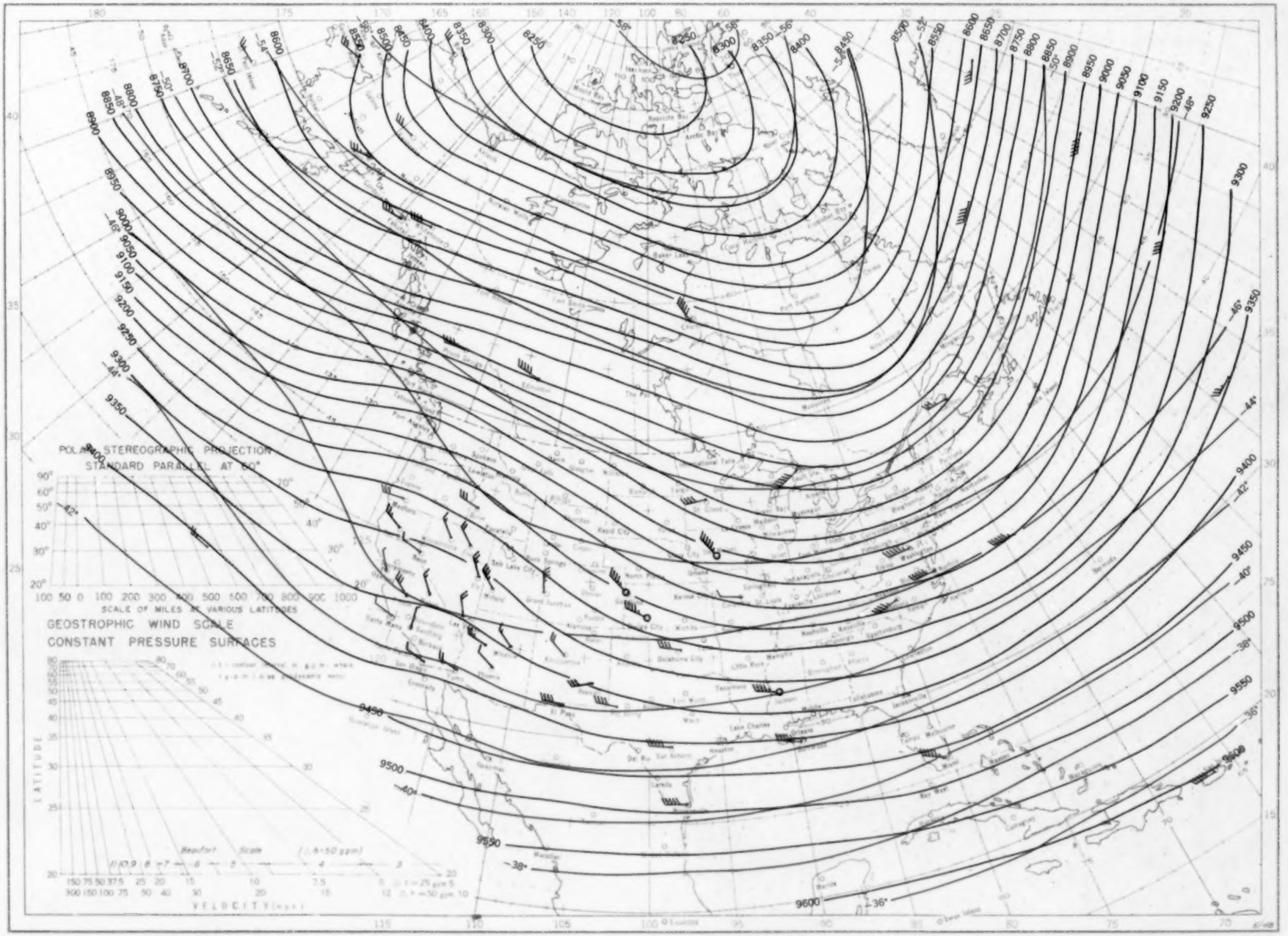

Contour lines and isotherms based on radiosonde observations at 0300 G. M. T. Winds shown in black are based on pilot balloon observations at 2100 G. M. T.; those shown in red are based on rawins at 0300 G. M. T. Wind barbs indicate wind speed on the Beaufort scale.